Cairo University/Massachusetts Institute of Technology
Technological Planning Program

A Derived Flood Frequency Distribution Based on the Density Function of Rainfall Excess

by
Mario A. Diaz-Granados
Juan B. Valdes
Rafael L. Bras

Prepared by
Technology Adaptation Program
Massachusetts Institute
of Technology
Cambridge, Massachusetts
02139

Sponsored by
United States Agency for
International Development

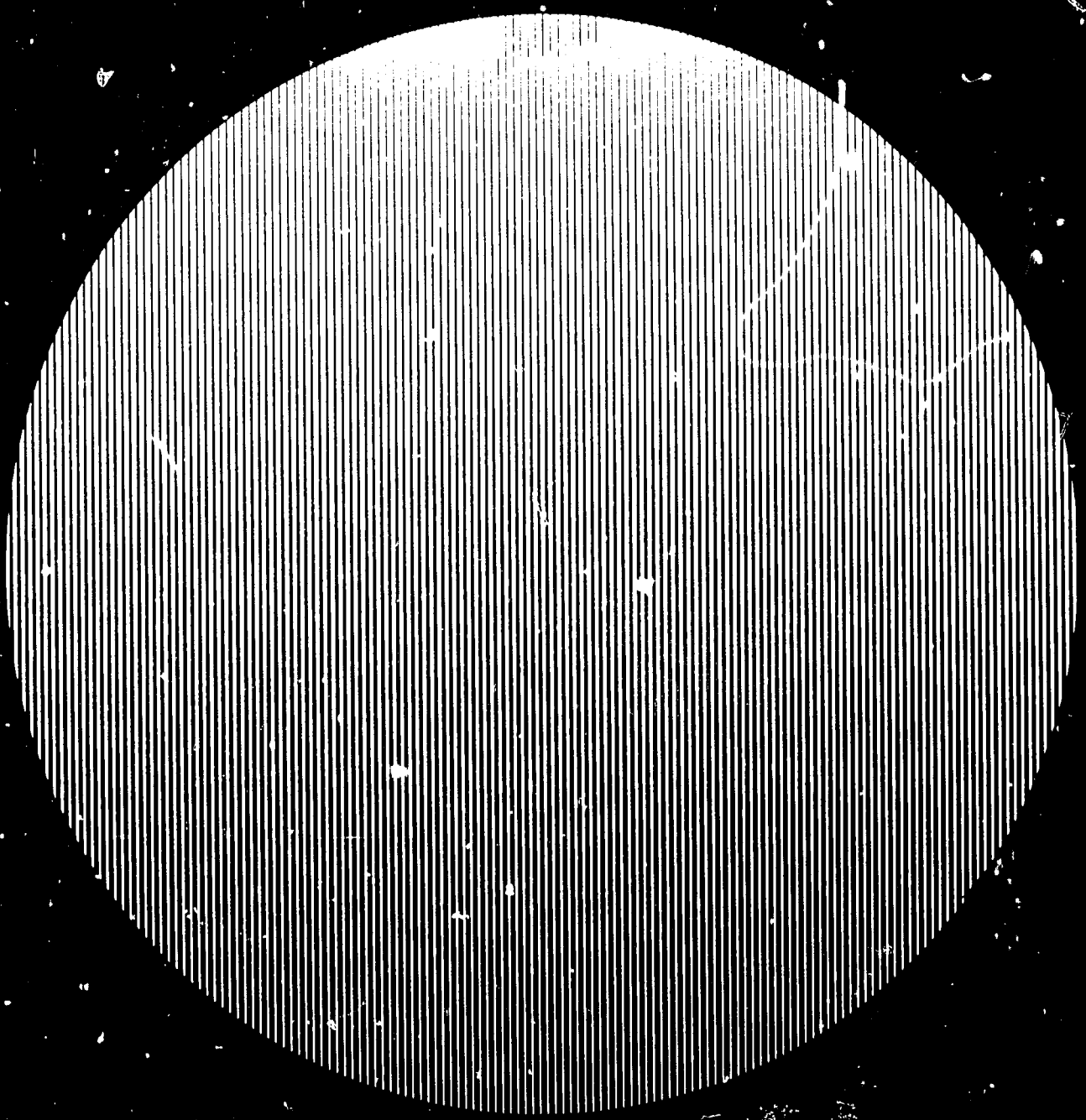

TAP Report 83-14
July 1983

A DERIVED FLOOD FREQUENCY DISTRIBUTION BASED ON THE GEOMORPHOCLIMATIC IUH AND THE DENSITY FUNCTION OF RAINFALL EXCESS

by

Mario A. Diaz-Granados
Juan B. Valdes
and
Rafael L. Bras

Massachusetts Institute of Technology

July 1983

PREFACE

This report is one of a series of publications which describe various studies undertaken under the sponsorship of the Technology Adaptation Program at the Massachusetts Institute of Technology.

The United States Deapartment of State, through the Agency for International Development, awarded the Massachusetts Institute of Technology a contract to provide support at MIT for the development, in conjunction with institutions in selected developing countries, of capabilities useful in the adaptation of technologies and problem-solving techniques to the needs of those countries. This particular study describes research conducted in conjunction with Cairo University, Cairo, Egypt.

In the process of making this TAP supported study some insight has been gained into how appropriate technologies can be identified and adapted to the needs of developing countries per se, and it is expected that the recommendations developed will serve as a guide to other developing countries for the solution of similar problems which may be encountered there.

Fred Moavenzadeh

Program Director

ABSTRACT

The geomorphoclimatic theory is used, along with the joint probability density function of storm duration and storm intensity and the representation of the infiltration process, to derive the flood frequency distribution for a given catchment. The infiltration process is represented by two different approaches: a simple time averaged potential infiltration rate and a more realistic model based on Philip's infiltration equation. The resulting flood frequency distributions are in analytical form, containing only few climatologic and physiographic parameters of the catchment. These frequency distributions are tested against historic records from arid and wet climates with very satisfactory results. They will be very valuable in the design of flood control systems since they provide a theoretical basis for estimating flood frequencies in the absence of streamflow records.

ACKNOWLEDGEMENTS

This study was sponsored by the MIT Technology Adaptation Program, which is funded through a grant from the Agency for International Development, United States Department of State. The views and opinions in this report, however, are those of the authors and do not necessarily reflect those of the sponsors.

The authors would like to acknowledge the complete staff of The Technology Adaptation Program, which includes personnel at both MIT and Cairo University. Their administrative support over the entire period of this study has been most helpful.

The very productive meetings and suggestions of Professor Peter S. Eagleson of MIT are gratefully acknowledged. The discussions held with the faculty of Cairo University are also acknowledged.

A thankful word goes to Ms. Antoinette DiRenzo for patiently typing this work.

Work was performed at the Ralph M. Parsons Laboratory, Department of Civil Engineering, MIT.

TABLE OF CONTENTS

		Page
TITLE PAGE		1
PREFACE		2
ABSTRACT		3
ACKNOWLEDGEMENTS		4
TABLE OF CONTENTS		5
LIST OF PRINCIPAL SYMBOLS		7
LIST OF TABLES		10
LIST OF FIGURES		11
Chapter 1	INTRODUCTION	13
	1.1 Motivation	13
	1.2 Objectives	14
Chapter 2	THE GEOMORPHOCLIMATIC IUH	15
	2.1 Introduction	15
	2.2 Derived Distribution Technique	16
	2.3 Probability Density Functions of the Peak and Time to Peak of the GIUH	17
	2.3.1 Derivation of $f_V^{(1)}(v)$	20
	2.3.2 Derivation of $f_V^{(2)}(v)$	21
Chapter 3	JOINT DISTRIBUTION OF THE EFFECTIVE INTENSITY AND DURATION	24
	3.1 Introduction	24
	3.2 Observed Distribution of Storm Properties	25
	3.3 Derivation of the Distribution of i_e and t_e Based on a Conceptual Model for the Infiltration	28
	3.4 Derivation of the Distribution of i_e and t_e using a Physically Based Model for the Infiltraiton Process	31

Page

3.4.1 Infiltration and Surface Runoff 31
3.4.2 Derivation of the Distribution of i_e and t_e 34
3.4.2.1 Evaluation of $f_{T_r}(t_e)$ 38
3.4.2.2 Evaluation of $f_{I_e|T_e}(i_e, t_e)$ 41
3.4.2.3 Evaluation of $f_{I_e, T_r}(i_e, t_e)$ 43
3.5 Summary 44

Chapter 4 DERIVED FLOOD FREQUENCY DISTRIBUTION 45

4.1 Introduction 45
4.2 Probability Distribution of the Peak Discharge 47
4.3 Recurrence Interval 50
4.4 Flood Frequency Distribution Derived from the Conceptual Infiltration Model 52
4.4.1 Flood Frequency Distribution: A Particular Case 53
4.5 Flood Frequency Distribution Derived from the Physically Based Infiltration Model 57
4.5.1 Santa Paula Creek and Nashua River Basins 76
4.5.2 Ecological Optimality in Water-Limited Natural Soil-Vegetation Systems 82
4.5.3 Flood Frequency Distributions for Santa Paula and Nashua using Climatic Climax Soil Parameters 85

Chapter 5 SUMMARY AND CONCLUSIONS 88

5.1 Summary and Conclusions 88

REFERENCES 89

APPENDIX A A FITTED PROBABILITY DENSITY FUNCTION FOR THE INITIAL SOIL MOISTURE CONCENTRATION 93

A.1 Conservation of Water Mass Equation 93
A.2 Rainfall Event Case 94
A.3 Exfiltration Event Case 95
A.4 The Distribution of s_o 96

APPENDIX B COMPUTER PROGRAM 117

LIST OF PRINCIPAL SYMBOLS

a	gravitational infiltration rate, [L/T]
a_e	asymptotic exfiltration capacity rate, [L/T]
$\bar{A}_i$	average area of a stream of order i.
c	pore disconnectedness index; L_e/L_o
d	diffusivity index
D	soil moisture diffusivity, [L^2/T]
D_e	desorption diffusivity, [L^2/T]
D_i	sorption diffusivity, [L^2/T]
$\bar{e}_p$	average rate of potential evaporation, [L/T]
f_e^*	exfiltration capacity, [L/T]
f_i^*	infiltration capacity, [L/T]
$f_\cdot(\cdot)$	probability density function of the argument
$F_\cdot(\cdot)$	cumulative probability distribution of the argument
g	gravitational acceleration, [L/T^2]
$h(t)$	characteristic response of the basin, IUH
i	intensity, [L/T]
i_e	effective intensity
i_r	total rainfall intensity
$I_1[\cdot]$	first order modified Bessel function of the first kind
$J_1[\cdot]$	first order Bessel function of the first kind
$k(1)$	saturated effective intrinsic permeability, [L^2]
k_v	ratio of potential rates of transpiration and soil surface evaporation
$K(1)$	saturated effective conductivity of the soil, [L/T]
$K_o[\cdot]$	modified Bessel function of the second kind
$\bar{L}_i$	average length of a stream of order i, [L]

m	pore size distribution index
m_i	mean storm intensity, [L/T]
m_{t_b}	mean time between storms, [T]
m_{t_r}	mean storm duration, [T]
m_ν	average annual number of independent storm events
m_s	kinematic wave parameter
M	vegetation canopy density
M_o^*	climatic climax vegetation canopy density
n	effective porosity
N_i	number of streams of order i
p_{ij}	transition probability from channels of order i to channels of order j
$P[\cdot]$	probability of the given argument
q	discharge per unit of width, $[L^2/T]$
q_p	peak of th IUH, $[T^{-1}]$
$Q(t)$	streamflow, $[L^3/T]$
Q_p	peak discharge, $[L^3/T]$
R_A	area ratio
R_B	bifurcation ratio
R_L	length ratio
R_s	surface runoff
s_o	initial uniform soil moisture concentration
S_e	exfiltration sorptivity
S_i	infiltration sorptivity
t	time
t_b	time bewteen storms
t_c	concentration time

t_e	duration of the effective rainfall
t_o	time at which surface reaches saturation during precipitation
t_p	peak time of the IUH
t_r	storm duration
T_B	travel time to the outlet of the basin
$u(t)$	upstream channel inflow response
$u(\cdot)$	unit step function
v	velocity
w	apparent velocity of capillary rise from water table [L/T]
$w(x,t)$	surrogate variable of $q(x,t)$
y	flow depth
Z	penetration depth
α_s	stream kinematic wave parameter
β	reciprocal of average storm intensity
δ	reciprocal of average storm duration
γ	reciprocal of mean interarrival time
$\delta(\cdot)$	delta function
λ	parameter of the linear reservoir assumption
λ_Ω^*	parameter of the modified linear reservoir assumption
$\phi_i(d,s_o)$	dimesionless sorption diffusivity of soil
Θ	effective volume soil moisture content
Θ_i	initial probability in the GIUH
$\Psi(1)$	saturated soil matrix potential, [L]
ϕ	average potential rate of infiltration
Ω	basin order
$\mathcal{L}(\cdot)$	Laplace Transform

LIST OF TABLES

Table No.		Page
4.1	Geomorphologic and Climatic Characteristics of Davidson River Catchment	54
4.2	Coefficients of J_i	65
4.3	Mean Annual Discharge for the Southern and Northern Branches of the Nashua River	80
4.4	Climatic Climax Soil Parameters for Santa Paula and Nashua Catchments	84

LIST OF FIGURES

Figure No.		Page
3.1	Representation of the Infiltration Process	33
3.2	Storm Characteristics vs. Infiltration Capacity	36
3.3	Surface Runoff Generating Areas in the i_r-t_r Plane	37
3.4	Integration Area for Evaluating the CDF of t_e	39
3.5	Approximation of K(c)	42
4.1	Regions where Equation 4.5 is Valid	49
4.2	Integration Region for Evaluating the CDF of Q_p	49
4.3	Flood Frequency Curve, Davidson River	55
4.4	Flood Frequency Curve, Davidson River	56
4.5	Approximation of $f(A\ i_e/Q_p)$	61
4.6	Integration Region for Evaluating the 4th Term of Equation 4.15	63
4.7	Flood Frequency Curve for Different Values of m	69
4.8	Flood Frequency Curve for Different Values of α	70
4.9	Flood Frequency Curve for two Different Types of Soil	71
4.10	Flood Frequency Curve Changing i_r and t_r	72
4.11	Flood Frequency Curve for Different Values of the Initial Soil Moisture Concentration	73
4.12	Flood Frequency Curve for Santa Paula Creek	77
4.13	Flood Frequency Curve for Nashua River	81
4.14	Flood Frequency Curve for Santa Paula Creek with Climax Soil Parameters	86
4.15	Flood Frequency Curve for Nashua River with Climax Soil Parameters	87

Page

A.1 Representation of the Exfiltration Process 99

A.2 Initial Soil Moisture Distribution from Simulation 102

Chapter 1

INTRODUCTION

1.1 Motivation

Quantification of hydrologic behavior in regions of sparse data is one of the most challenging problems in the field. Lack of data is common in the majority of the river systems of the world, particularly those in inaccessible or underdeveloped regions. Ideally, it should be possible to estimate basin response using information available through field observations, climatic records and or remote sensing. Methodologies have been suggested to relate river response to basin geomorphology (Rodriguez-Iturbe and Valdes, 1979), in which the Instantaneous Unit Hydrograph is interpreted as the probability density function of the travel time that a drop of water, landing anywhere in the basin, takes to reach the outlet. Geomorphology is quantified by basic parameters like the Horton numbers, which are easily obtained from generally available topographic information. This basin response is called the Geomorphologic Instantaneous Unit Hydrograph (GIUH). Recently, Rodriguez-Iturbe et al., (1982) introduced the Geomorphoclimatic Instantaneous Unit Hydrograph, GcIUH which is a stochastic reinterpretation of the latter, implied by the stochasticity of the effective rainfall. Hebson and Wood (1982) derived a flood frequency distribution from the joint probability density function of the intensity and duration of the effective precipitation proposed by Eagleson (1972), and the GIUH as the catchment rainfall-runoff relationship, with good results. Kirshen and Bras (1982) worried about the exponential travel time distribution for channels assumed in the GIUH, and proposed a time distribution based on the linearized equations

of motion. Finally, Cordova and Rodriguez-Iturbe (1982) used the Geomorphoclimatic Instantaneous Unit Hydrograph and the direct runoff given by the U.S. Soil Conservation Service method to calculate flood frequencies from registered maximum annual depths of total rainfall for different durations.

1.2 Objectives

In this report, two theoretical flood frequency distributions will be derived. They will be based on parameters representing the effective precipitation and the Geomorphoclimatic Instantaneous Unit Hydrograph, (GcIUH). The GcIUH is a stochastic reinterpretation of the hydrogeomorphologic response, of Rodriguez-Iturbe and Valdes (1979). Stochasticity is introduced through effective rainfall of the region. The first flood frequency result corresponds to a conceptual model of the infiltration given by an average potential rate. The second approach uses a physically based model of the infiltration process. The resulting frequency curves are a function of the basin's climatic and geomorphologic parameters as well as estimates of vegetative canopy density and effective soil porosity. This means that in principle all regions of the world could be "hydrologically" mapped with reasonable efforts.

Chapter 2

THE GEOMORPHOCLIMATIC IUH

2.1 Introduction

Rodriguez-Iturbe and Valdes (1979), linked in an analytical manner the geomorphologic parameters of a given catchment with its hydrologic response. The result is the Geomorphologic Instantaneous Unit Hydrograph, GIUH. In their work expressions for the main characteristics of the GIUH, namely the peak and time to peak, were presented; both of them are functions of v, the peak velocity of the response.

According to Rodriguez-Iturbe et al., (1982), if an effective rainfall, represented by an intensity (i_e), constant throughout the duration t_e, is assumed to occur over the basin, then the parameters i_e, and t_e must be reflected in the velocity v. This velocity may then be analytically expressed as a function of them. Besides, since i_e and t_e are random variables, whose joint distribution represents the influence of climate on the GIUH, then q_p and t_p are also random variables, whose distributions depend on the geomorphology of the basin and on the joint distribution of i_e and t_e. Consequently, through its parameterization in terms of q_p and t_p, the IUH can be interpreted as a stochastic unit impulse response function, called the Geomorphoclimatic IUH by Rodriguez-Iturbe et al., (1982). In this chapter some relevant aspects of the geomorphoclimatic theory which will be useful in Chapter 4 will be presented.

2.2 Derived Distribution Technique

The derived distribution technique is well established in probability theory (e.g., Freeman, 1963, and Benjamin and Cornell, 1970). It provides a tool to derive the density function of a dependent variable(s) from random variables whose joint density function is known. The following is the conceptual framework. Suppose that a variable y is related to a vector of parameters, Θ, by a function g:

$$y = g(\Theta) \tag{2.1}$$

The elements of vector Θ are random variables with a given joint probability density function $f(\Theta)$ and a corresponding cumulative distribution $F(\Theta)$. Due to the randomness of Θ, y is also a random variable with cumulative distribution given by

$$F_Y(y) = \text{Prob}[y' \leq y] = \int_{R_Y} f_\Theta(\Theta) d\Theta \tag{2.2}$$

in which R_y represents the region, within the possible values of Θ, where $y' \leq y$. Obviously, the PDF of y is

$$f_Y(y) = \frac{d}{dy} F_Y(y) \tag{2.3}$$

In some cases interest is centered in deriving the joint distribution of n random variables that have a one-to-one relationship with respect to other n random variables with a known joint distribution. That joint distribution may be found by using the method of Jacobians (Freeman, 1963). When n is two, the method is as follows: assume that x_1 and x_2 are random variables whose joint distribution $f_{X_1, X_2}(x_1, x_2)$ is known, and that they are related to y_1 and y_2, by one-to-one functions:

$$x_1 = g_1^{-1}(y_1, y_2)$$

$$x_2 = g_2^{-1}(y_1, y_2)$$

then, the joint distribution of y_1 and y_2 is given by:

$$f_{Y_1,Y_2}(y_1,y_2) = f_{X_1,X_2}\left\{g_1^{-1}(y_1,y_2),\ g_2^{-1}(y_1,y_2)\right\}\left|\frac{\partial(x_1,x_2)}{\partial(y_1,y_2)}\right| \qquad (2.4)$$

where the last term of the right hand side is the absolute value of the Jacobian. In the simplest case in which n is equal to one, the distribution of y is:

$$f_Y(y) = \left|\frac{dg^{-1}(y)}{dy}\right| f_X[g^{-1}(y)] \qquad (2.5)$$

2.3 Probability Density Functions of the Peak and Time to Peak of the GIUH

The expressions for the peak and time to peak of the GIUH (Rodriguez-Iturbe and Valdes, 1979) are:

$$q_p = \frac{1.31}{L_\Omega} R_L^{0.43} v \qquad (2.6)$$

$$t_p = \frac{0.44 L_\Omega}{v}\left(\frac{R_B}{R_A}\right)^{0.55} R_L^{-0.38} \qquad (2.7)$$

where L_Ω is the length in km of the highest order stream, R_B, R_A and R_L are the Horton's numbers and v is the peak velocity in m/s. Using g as given by Equation 2.6 in Equation 2.5, the PDF of q_p is:

$$f_Q(q_p) = \frac{L_\Omega}{1.31\ R_L^{0.43}}\ f_V\left[\frac{L_\Omega}{1.31\ R_L^{0.43}}\ q_p\right] \tag{2.8}$$

In order to complete the derivation of $f_Q(q_p)$, the distribution of v needs to be determined. It can be derived from the joint distribution of i_e and t_e, since these variables are related to v through the kinematic wave approximation of the equations of motion. Note that v at a given time during the storm has been assumed constant throughout the basin (Rodriguez-Iturbe and Valdes, 1979). Notice that the kinematic wave is an approximation and this is just one way of doing it.

According to this approximation, the average first order subcatchment has a concentration time given by Eagleson (1970):

$$t_c = \left[\frac{\bar{L}_1\ i_*^{1-m_s}}{\alpha_s}\right]^{1/m_s}$$

where

$$i_* = \frac{\bar{A}_1}{\bar{L}_1}\ i_e\ ,$$

α_s and m_s are the kinematic wave parameters of the average first order channel (m_s=5/3 for rectangular channels), and $\bar{A}_1$ and $\bar{L}_1$ represent the average area and average stream length of the first order subcatchments.

Since the velocity is assumed constant throughout the basin then, a first order subcatchment may be exclusively used throughout the analysis. The expression of the peak velocity depends on the relative duration of the effective rainfall with respect to the concentration time. Specifically,

$$v = \alpha_s(\bar{A}_1 i_e t_e/\bar{L}_1)^{m_s-1} \qquad \text{if } t_e \leq t_c \tag{2.9}$$

$$v = \alpha_s^{1/m_s}(\bar{A}_1 i_e)^{1-1/m_s} \qquad \text{otherwise} \tag{2.10}$$

Accordingly, $f_V(v)$ is composed of two terms, i.e.,

$$f_V(v) = w f_V^{(1)}(v) + (1-w) f_V^{(2)}(v) \tag{2.11}$$

where $w = \text{Prob}[t_e \leq t_c]$, $f_V^{(1)}(v)$ stands for the case $t_e \leq t_c$ and $f_V^{(2)}(v)$ for the case $t_e > t_c$. From Equations 2.9 and 2.10, it can be seen that $f_V^{(1)}(v)$ may be derived from the joint distribution of i_e and t_e, whereas $f_V^{(2)}(v)$ can be obtained from the marginal distribution of i_e only.

Rodriguez-Iturbe et al., (1982) assume that i_e and t_e are independent random variables with exponential distributions. This assumption is acceptable at least for events beyond a certain threshold, and is more adequate for describing total precipitation. Then,

$$f_{I_e}(i_e) = \beta_e e^{-\beta_e i_e} \tag{2.12}$$

$$f_{T_e}(t_e) = \delta_e e^{-\delta_e t_e} \tag{2.13}$$

and therefore,

$$F_{I_e,\,T_e}(i_e,t_e) = \beta_e\,\delta_e \exp(-\beta_e i_e - \delta_e t_e) \tag{2.14}$$

From the above equation, Eagleson (1981) obtained the PDF of the effective storm depth, h, which is defined as the product of i_e and t_e:

$$h = i_e t_e \tag{2.15}$$

$$f_H(h) = 2\beta_e \delta_e K_o[2(\beta_e \delta_e h)^{\frac{1}{2}}] \tag{2.16}$$

where $K_o[\cdot]$ is the modified Bessel function of the second kind and zero order

2.3.1 Derivation of $f_V^{(1)}(v)$

Replacing Equation 2.15 in Equation 2.9, the expression of the peak velocity becomes:

$$v = \alpha_s(\bar{A}_1 h/\bar{L}_1)^{m_s-1}$$

Using this relation in Equation 2.5, the PDF of v may be written as:

$$f_V^{(1)}(v) = \frac{\bar{L}_1}{\alpha_s(m_s-1)\bar{A}_1}\left(\frac{v}{\alpha_s}\right)^{(2-m_s)/(m_s-1)} f_H\left[\frac{\bar{L}_1}{\bar{A}_1}\left(\frac{v}{\alpha_s}\right)^{1/(m_s-1)}\right]$$

However, $f_H(\cdot)$ has already been defined. Therefore, introducing $f_H(\cdot)$ as given by Equation 2.16, the distribution of v is:

$$f_V^{(1)}(v) = \frac{2\beta_e \delta_e L_\Omega R_L^{1-\Omega}}{(m_s-1)\alpha_s A_\Omega R_A^{1-\Omega}}\left(\frac{v}{\alpha_s}\right)^{(2-m_s)/(m_s-1)} K_o\left[2\left(\frac{\beta_e \delta_e L_\Omega R_L^{1-\Omega}}{A_\Omega R_A^{1-\Omega}}\right)^{\frac{1}{2}}\left(\frac{v}{\alpha_s}\right)^{1/2(m_s-1)}\right] \tag{2.17}$$

where the definitions of R_A and R_L have been used to express $f_V^{(1)}(v)$ in terms of L_Ω and A_Ω.

2.3.2 Derivation of $f_V^{(2)}(v)$

When the peak velocity is given by Equation 2.10, its distribution can also be derived following processes similar to those of the past section:

$$f_V^{(2)}(v) = \frac{m_s}{(m_s-1)\bar{A}_1}\left(\frac{v}{\alpha_s}\right)^{1/(m_s-1)} f_{I_e}\left[\frac{v^{m_s/(m_s-1)}}{\bar{A}_1\alpha_s^{1/(m_s-1)}}\right]$$

or, using Equation 2.12

$$f_V^{(2)}(v) = \frac{\beta_e m_s}{(m_s-1)A_\Omega R_A^{1-\Omega}}\left(\frac{v}{\alpha_s}\right)^{1/(m_s-1)} \exp\left[\frac{-\beta_e v^{m_s/(m_s-1)}}{A_\Omega R_A^{1-\Omega}\alpha_s^{1/(m_s-1)}}\right] \qquad (2.18)$$

In order to completely define the general expression of the distribution of v, the probability that $t_e \leq t_c$ must be evaluated. The expression obtained by Rodriguez-Iturbe et al., (1982) is

$$w = 1 - \frac{e^{-2\sigma}\Gamma(\sigma+1)}{\sigma^\sigma} \qquad (2.19)$$

where

$$\sigma = \beta_e^{2/7}\,(0.4\delta_e)^{5/7}(A_\Omega R_A^{1-\Omega})^{-2/7}(L_\Omega R_L^{1-\Omega})^{5/7}\,\alpha_s^{-3/7}$$

Rodriguez-Iturbe et al., (1982) studied the order of magnitude of w and concluded that it is very small, justifying the following approximation for $f_V(v)$:

$$f_V(v) \simeq f_V^{(2)}(v)$$

Therefore, recalling Equation 2.8, the PDF of q_p, in its final form,

is:

$$f_Q(q_p) = 3.534\ \Pi q_p^{3/2} \exp(-1.412\ \Pi q_p^{5/2}) \tag{2.20}$$

where q_p is given in hr^{-1}, and

$$\Pi = \frac{\beta_e L_\Omega^{5/2}}{A_\Omega R_L \alpha_\Omega^{3/2}} \tag{2.21}$$

In the above equation, the units are as follows: β_e(hr/cm), L_Ω(Km), A_Ω(Km^2) and α_Ω($sec^{-1}\ m^{-1/3}$). The latter is defined as:

$$\alpha_\Omega = \frac{S_\Omega^{\frac{1}{2}}}{n_\Omega b_\Omega^{2/3}} \tag{2.22}$$

where S_Ω, n_Ω and b_Ω are the slope, the Manning roughness coefficient and the width (in m) of the stream of order Ω.

Proceeding in a similar manner as done for q_p, the PDF of t_p can easily be derived. The expression for this:

$$f_T(t_p) = 0.656\Pi\ t_p^{-7/2} \exp(-0.262\Pi\ t_p^{-5/2}) \tag{2.23}$$

where t_p is given in hours, and the ratio R_B/R_A has been replaced by its most probable value of 0.80 as suggested by Rodriguez-Iturbe et al., (1979).

Finally, for a specific effective rainfall with an intensity i_e, the peak and time to peak of the Geomorphoclimatic IUH can be written as:

$$q_p = \frac{0.871}{\Pi_{i_e}^{2/5}} \tag{2.24}$$

$$t_p = 0.585\Pi_{i_e}^{2/5} \tag{2.25}$$

where

$$\Pi_{i_e} = \frac{L_\Omega^{5/2}}{i_e A_\Omega R_L \alpha_\Omega^{3/2}} \tag{2.26}$$

The above equations will be utilized in Chapter 4, when flood frequency distributions for a given basin are derived from the Geomorphoclimatic IUH and two different expressions for the joint probability density function of i_e and t_e, which are developed in the next chapter.

Chapter 3

JOINT DISTRIBUTION OF THE EFFECTIVE INTENSITY AND DURATION

3.1 Introduction

In the preceeding chapter, the derivation of the Geomorphoclimatic IUH was based on the assumption that the joint distribution of the effective intensity and duration of the rainfall events is the result of independent exponential distributions for each variable. Unfortunately, in practice neither the effective intensity, i_e, nor its corresponding duration, t_e, can be measured in the field in order to estimate the parameters of the distributions. Only gross precipitation measurements are available from historical records. However, the joint distribution of i_e and t_e may be derived from the joint PDF of the gross precipitation, represented by an intensity i, and a storm duration t_r, and a model that describes the infiltration process. This model may be conceptual or physically based. In this chapter, the marginal distributions of i and t_r are assumed independent and exponentially distributed. This type of distribution is more adequate for i and t_r than for i_e and t_e, as used by Rodriguez-Iturbe et al., (1982). The joint distribution, which is the product of the marginals, will be coupled to two models of the infiltration process: a conceptual one in which the infiltration is assumed to be constant and equal for all the rainfall events, and a physically based one, in which the infiltration process is described by the Philip equation (Philip, 1960).

3.2 Observed Distributions of Storm Properties

To perform rainfall data analysis, an independent storm event must be defined. Grace and Eagleson (1966) used the rank correlation coefficient to establish the minimum interstorm time above which two successive storms may be considered independent events. Grayman and Eagleson (1969), using five years of hourly rainfall data at Boston, found that the storm intensity and duration, and the time between storms are distributed exponentially. Restrepo and Eagleson (1982) concluded, however, that the rank correlation coefficient assures that storm depths are linearly independent, but it does not necessarily imply that the storms are independent events. Under the assumption that the arrivals of independent storm events are Poisson distributed, it may be shown that the storm interarrival time is exponentially distributed. Using this assumption, Restrepo and Eagleson (1982) proposed, as criterion to define independence, finding the time between storms which yields a coefficient of variation equal to 1, an implicit condition in the exponential distribution. For twelve stations located in different sites in the United States and Colombia, representing different climates, Restrepo and Eagleson (1982) found that, under the above criterion, the exponential distribution provides a good representation of the interarrival time, the time between storms and the storm duration. However, the exponential was not as good a model of storm intensity.

In this work, it will be assumed that the point storm duration, average point storm intensity and interstorm time, denoted t_b, are exponentially distributed. Formally,

$$f_I(i) = \beta^* e^{-\beta^* i}, \quad i \geq 0$$

$$f_{T_r}(t_r) = \delta\, e^{-\delta t_r}, \quad t_r \geq 0 \tag{3.1}$$

$$f_{T_b}(t_b) = \gamma\, e^{-\gamma t_b}, \quad t_b \geq 0 \tag{3.2}$$

where

$$\beta^* = m_i^{-1}$$

$$\delta = m_{t_r}^{-1}$$

$$\gamma = m_{t_b}^{-1}$$

where m_i, m_{t_r}, and m_{t_b} are the mean storm intensity, mean storm duration and mean interarrival time, respectively.

By definition, the total point storm depth, h, is the product of i and t_r. If the conditional distribution of h given t_r is defined as follows (Eagleson, 1972).

$$f_{H|T_r}(h, t_r) = \beta^* t_r^{-1} e^{-\beta^*(h/t_r)}$$

then it can be proven that i and t_r are independent, and therefore, the joint distribution of i and t_r becomes:

$$f_{I,T_r}(i, t_r) = \beta^* \delta \exp(-\beta^* i - \delta t_r)$$

In order to reduce the average point rainfall depth to the average areal rainfall depth, the U. S. Weather Bureau (1957-1960) has proposed the following correction factor:

$$K = 1 - \exp(-1.1\, t_r^{1/4}) + \exp(-1.1\, t_r^{1/4} - 0.003861 A_\Omega)$$

where t_r is given in hours and A_Ω, the catchment area, in km^2. Eagleson (1972) made a simplification of the above equation replacing t_r by its mean value, i.e.,

$$K \simeq 1 - \exp(-1.1\delta^{-1/4}) + \exp(-1.1\delta^{-1/4} - 0.003861 A_\Omega) \tag{3.3}$$

Therefore, assuming that the areal storm duration is equal to the point storm duration the areal storm intensity becomes.

$$i_r = Ki,$$

and then its distribution is defined as

$$f_{I_r}(i_r) = \frac{\beta^*}{K} e^{-\beta^* i_r / K}$$

or

$$f_{I_r}(i_r) = \beta\, e^{-\beta i_r} \tag{3.4}$$

where

$$\beta = \beta^*/K$$

Finally, the joint distribution of the areal storm intensity and storm duration is

$$f_{I_r,\, T_r}(i_r,\, t_r) = \beta\delta \exp(-\beta i_r - \delta t_r) \tag{3.5}$$

3.3 Derivation of the Distribution of i_e and t_e Based on a Conceptual Model of the Infiltration Process

Eagleson (1972) included infiltration effects as a spatially averaged potential loss rate, ϕ, substracted from the average areal rainfall intensity for each storm event:

$$\begin{aligned} i_e &= i_r - \phi \\ t_e &= t_r \end{aligned} \qquad \text{if } i_r > \phi \tag{3.6a}$$

$$\begin{aligned} i_e &= 0 \\ t_e &= 0 \end{aligned} \qquad \text{if } i_r \leq \phi \tag{3.6b}$$

When $i_r > \phi$ there is a one-to-one relationship between pairs of i_e, t_e, and i_r, t_r, and therefore, from the joint PDF of i_r and t_r (Equation 3.5), the distribution of i_e and t_e may be calculated by derived distributions, as explained in Section 3.2. Consequently,

$$i_r = i_e + \phi$$

$$t_r = t_e$$

and applying Equation 2.4, the desired distribution is:

$$f_{I_e,\,T_e}(i_e,\,t_e) = \beta\delta\, e^{-\beta\phi} \exp(-\delta t_e - \beta i_e) \quad i_e,\, t_e > 0 \tag{3.7}$$

When i_r is less than or equal to ϕ, all the rainfall is infiltrated. In terms of the distribution of i_e and t_e, this situation is represented by a spike at $i_e = 0$ and $t_e = 0$, whose value is given by:

$$p(i_e,t_e) = \int_o^\infty \left[\int_o^\phi f_{I_r,T_r}(i_r,t_r)di_r \right] dt_r \qquad i_e = t_e = 0$$

$$= \int_o^\infty \left[\int_o^\phi \beta\delta \exp(-\beta i_r - \delta t_r)di_r \right] dt_r$$

$$p(i_e,\,t_e) = 1 - e^{-\beta\phi}, \quad i_e = t_e = 0 \tag{3.8}$$

Therefore, Equations 3.7 and 3.8 completely define the distribution of i_e and t_e.

According to Eagleson (1972), the infiltration loss rate may be estimated as follows:

Let n = average annual number of rainfall excess events

Θ = average annual number of independent rainfall events

P = average annual point rainfall depth.

R = average annual runoff

R_d = average annual direct runoff

Defining

$$\phi_1 = R/P$$

and

$$\phi_2 = R_d/R$$

Then, on the average,

$$P\phi_1\ \phi_2 = nE[i_e t_e]$$

where $E[\cdot]$ is the expected value of the argument. Assuming that

$$E[i_e t_e] \simeq E[i t_r] = P/O$$

then

$$\frac{n}{\Theta} = \phi_1 \phi_2$$

On the other hand,

$$\frac{n}{\Theta} = \int_{\phi}^{\infty} (f_{i_r}) di_r = e^{-\beta\phi}$$

which gives

$$\phi_1\ \phi_2 = e^{-\beta\phi}$$

and solving for ϕ:

$$\phi = -\frac{1}{\beta} \ln(\phi_1\ \phi_2) \qquad (3.9)$$

Eagleson (1972) presents typical values for ϕ_1 and ϕ_2 for different basins in USA.

In the next section, the derivation of the joint distribution of i_e and t_e using a physically based model of the infiltration process will be presented.

3.4 Derivation of the Distribution of i_e and t_e Using a Physically Based Model for the Infiltration Process

3.4.1 Infiltration and Surface Runoff

The soil infiltration rate is the flux of water which the soil can absorb through its surface when it is maintained in contact with water at atmospheric pressure (Cordoba and Bras, 1979). It depends on the initial moisture conditions and the texture, structure and uniformity of the soil profile. As long as the rate of water supply is smaller than the soil infiltration capacity, water penetrates as fast as it is supplied, and the supply rate determines the actual infiltration rate. On the other hand, when the supply rate exceeds the soil infiltration capacity, the latter determines the actual infiltration rate.

The one-dimensional concentration dependent equation of the diffusion process in unsaturated media is:

$$\frac{\partial \Theta}{\partial t} = \frac{\partial}{\partial z}\left[D(\Theta)\,\frac{\partial \Theta}{\partial z}\right] = \frac{\partial K(\Theta)}{\partial z} \qquad (3.10)$$

where Θ is the effective volumetric moisture content, t is time, $K(\Theta)$ is the effective hydraulic conductivity, $D(\Theta)$ is the diffusivity and z is the vertical direction. Philip (1960) integrated the above equation for the following boundary conditions:

for $t = 0$ and $z > 0$ $\quad \Theta = \Theta_o$

for $t > 0$ and $z = 0$ $\quad \Theta = \Theta_s$

where Θ_o is a initial constant soil moisture content and Θ_s is the soil moisture content at saturation condition.

Using Philip's solution, Eagleson (1978) represented the infiltration capacity f_i^* by

$$f_i^* = \frac{1}{2} S_i t^{-\frac{1}{2}} + a \tag{3.11}$$

where the term a is the gravitational infiltration rate (it takes into account also the water table influence), and S_i is the infiltration sorptivity, embodying capillarity. The expressions for a and S_i are:

$$a = \frac{1}{2} K(1) \ (1 + s_o^c) - w \tag{3.12}$$

$$S_i = 2(1-s_o) \ [5nK(1)\psi(1)\phi_i(d,s_o)]/3m\pi\}^{\frac{1}{2}} \tag{3.13}$$

where

π = 3.14159...

$K(1)$ = saturated effective conductivity of soil

s_o = initial (uniform) soil moisture concentration in the surface boundary layer.

$\psi(1)$ = saturated matrix potential of soil

$\phi_i(d,s_o)$ = dimensionless sorption diffusivity of soil

n = effective porosity of soil

c = pore disconnectedness index

m = pore size distribution index

w = apparent velocity of capillary rise from water table.

For different soil textures, Eagleson (1978) gives typical values of the above parametes.

A typical storm situation over a given catchment is shown in Figure 3.1, in which the several soil types presented in the latter are assumed to be lumped into a single representative soil.

According to Equation 3.11, at the beginning of the storm event, the infiltration capacity of the soil will commonly be greater than the intensity of the rainfall. The surface soil moisture will then adjust itself

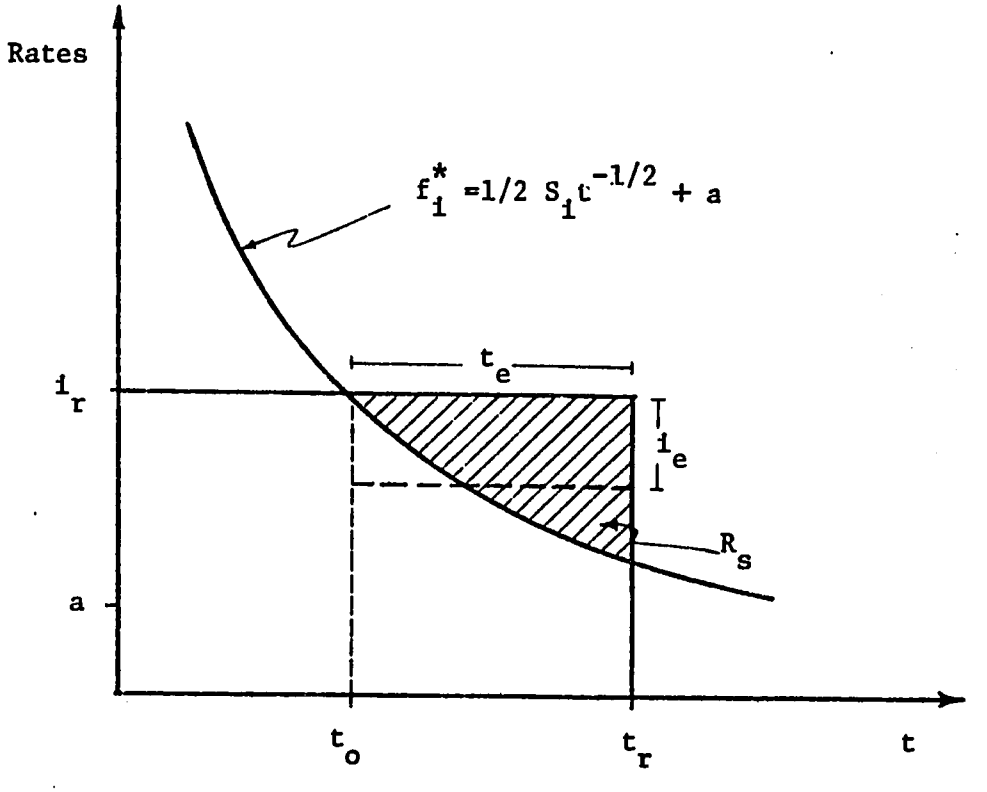

Representation of the infiltration process

Figure 3.1

to this value. The infiltration capacity will decrease with time because the water already infiltrated increases the soil moisture content. The soil moisture content will increase up to some time t_o at which the soil surface may reach saturation and $f_i^* = i_r$. For t between t_o and t_r surface runoff will be generated. This runoff, R_s, is indicated by the shaded area of Figure 3.1, and it represents the effective rainfall.

Eagleson (1978) gives an approximation for t_o, and calculates R_s in a consistent manner with that approximation. The expressions for these two variables are:

$$t_o \simeq \frac{S_i^2}{2(i_r-a)^2} \tag{3.14}$$

$$R_s \approx (i_r-a)t_r - S_i(t_r/2)^{\frac{1}{2}} \tag{3.15}$$

3.4.2 Derivation of the Distribution of i_e an t_e

The effective rainfall will be represented, as before, by an intensity i_e, constant through the duration t_e, as shown in Figure 3.1. Consequently,

$$t_e = t_r - t_o \tag{3.16}$$

$$i_e = R_s/t_e \tag{3.17}$$

The above two equations defined through Equations 3.12 to 3.15 will allow the derivation of f_{I_e}, T_e (i_e,t_e).

Looking at the relation between the storm characteristics and the infiltration capacity, three cases can be defined. They are presented in Figure 3.2. Cases 1 and 2 do not produce surface runoff, case 3 does. In case 1 the duration of the storm event is not enough for the soil surface to reach saturation conditions, and in case 2 the intensity of

the rainfall is less than the gravitational infiltration and therefore, the soil surface will never be saturated. As it is shown in Figure 3.2, the critical parameter in establishing surface runoff is t_r: if t_r is greater than t_o, runoff will be produced. Figure 3.3 shows the runoff producing region in the plane $i_r - t_r$. The shaded areas represent those storms that do not generate surface runoff (cases 1 and 2). Therefore, the integration of $f_{I_r,\ T_r}\ (i_r,t_r)$ over the shaded areas will give the probability of no effective rainfall from storm event. This is

$$\text{Prob}[i_e = 0, t_e = 0] = \int_{R_{1,2}} f_{I_r,T_r}(i_r,t_r)\ di_r dt_r$$

where $R_{1,\ 2}$ is the shaded area of Figure 3.3, or replacing $R_{1,\ 2}$ and using Equation 3.5:

$$\text{Prob}[i_e = 0, t_e = 0] = \int_o^\infty \left[\int_o^{a+S_i(2t_r)^{-\frac{1}{2}}} \beta\delta \exp(-\beta i_r - \delta t_r) di_r \right] dt_r$$

$$= 1 - \delta e^{-\beta a} \int_o^\infty \exp(-\delta t_r - \beta S_i (2t_r)^{-\frac{1}{2}}) dt_r$$

This last integral does not have an exact solution. However, it may be analytically approximated in the same manner as Eagleson (1972). He shows that for

$$I_o = K_1 \int_o^\infty \exp(-K_1 x - K_2 x^{-K_3}) dx$$

a good approximation is:

$$I_o \simeq e^{-\sigma/K_3}\ \sigma^{-\sigma}\ \Gamma(\sigma+1) \qquad (3.18)$$

provided σ is of order unity, where

$$\sigma = K_1 (K_2\ K_3/K_1)^{1/(K_3+1)}$$

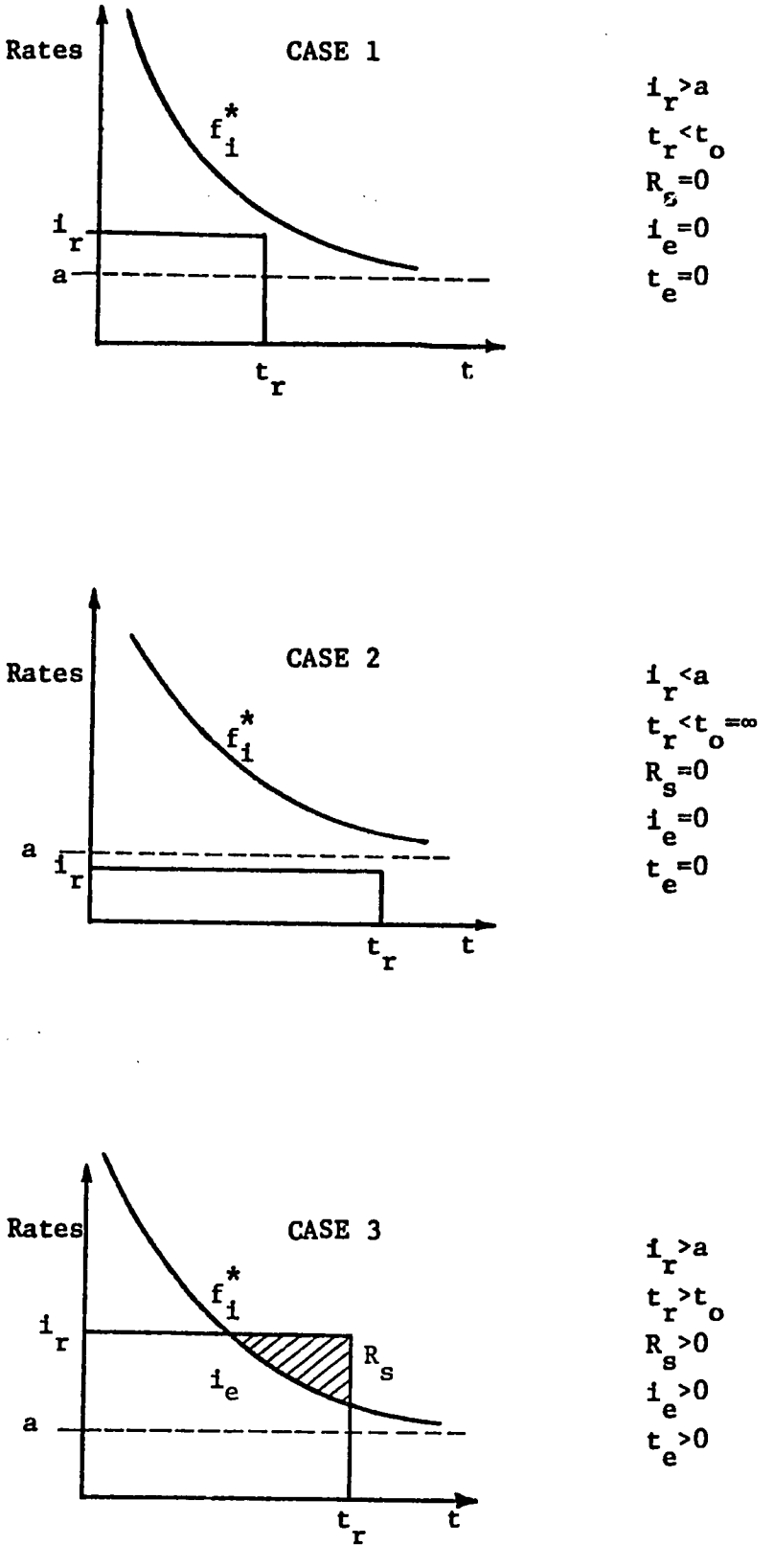

Figure 3.2 Storm characteristics vs infiltration capacity

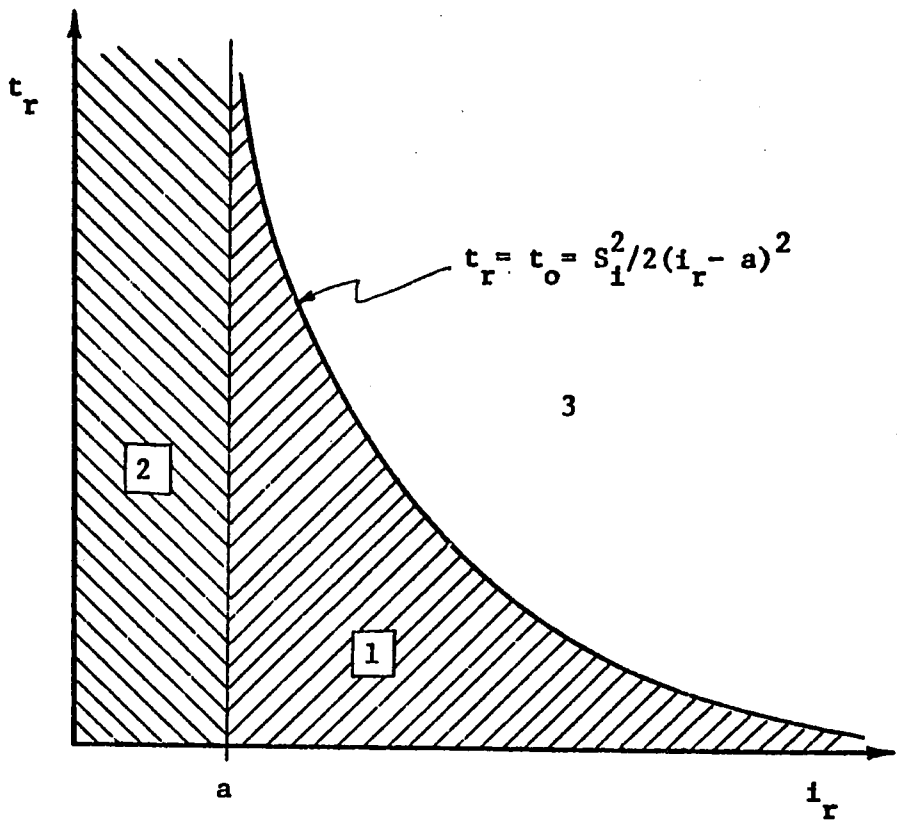

Surface runoff generating areas in the i_r - t_r plane (shaded areas = no runoff)

Figure 3.3

Therefore,

$$\text{Prob}[i_e=0,\ t_e=0] \simeq 1 - \exp(-\beta a-2\sigma)\Gamma(\sigma+1)\sigma^{-\sigma} \tag{3.19}$$

where

$$\sigma = \delta\left(\frac{\beta S_i}{2\sqrt{2\sigma}}\right)^{2/3} \tag{3.20}$$

The above expression represents the discrete part of the joint probability distribution of i_e and t_e. The continuous part will be calculated as:

$$f_{I_e,T_e}(i_e,t_e) = f_{I_e|T_e}(i_e,t_e)\cdot f_{T_e}(t_e) \tag{3.21}$$

3.4.2.1 Evaluation of $f_{T_e}(t_e)$

Figure 3.4 shows the plant i_r-t_r where the dashed lines represent different values of t_e, e.g., t_{e_1} and t_{e_2}. The shaded area corresponds to values of t_e between 0 and t_{e_1}. Therefore, integration of $f_{I_r,T_r}(i_r, t_r)$ over that area will give the probability that t_e is between 0 and t_{e_1}, i.e.,

$$\text{Prob}[0 < t_e \leq t_{e_1}] = \int_a^\infty\left[\int_{t_o}^{t_{e_1}+t_o} \delta\beta\exp(-\delta t_r-\beta i_r)dt_r\right]di_r$$

$$= \beta\int_a^\infty \exp[-\beta i_r-\delta S_i^2/2(i_r-a)^2]\{1-\exp(-\delta t_{e_1})\}di_r$$

Let $y = i_r-a$. Then,

$$\text{Prob}[0 < t_e < t_{e_1}] = \beta\, e^{-\beta a}[1-\exp(-\delta t_{e_1})]\int_o^\infty \exp(-\beta y-\delta S_i^2/2y^2)dy \tag{3.22}$$

where the last integral is a function of β, δ and S_i but not of t_{e_1}. It may be approximated in the same manner as before by using Equation 3.18. However, in order to preserve the properties of any PDF, it is evaluated indirectly as follows. The probability that t_e is equal to zero has been

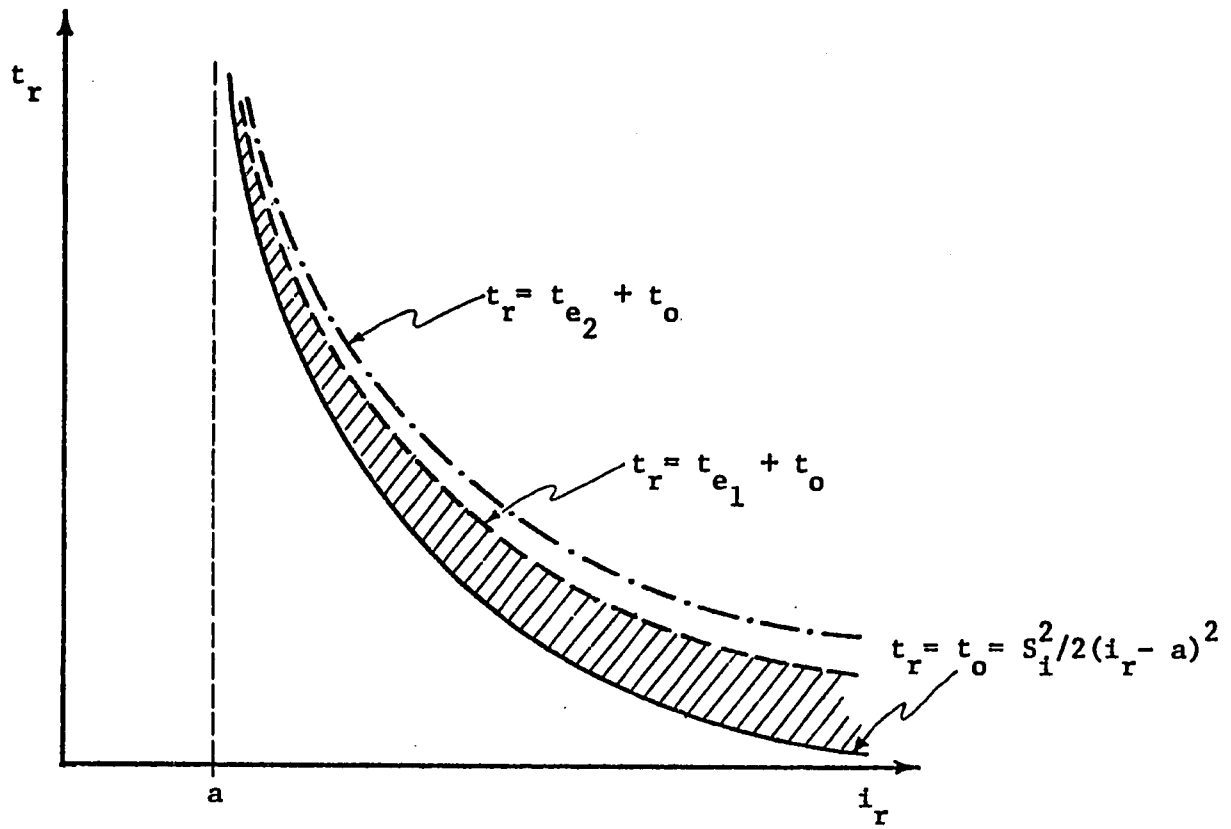

Integration area for evaluating the CDF of t_e

Figure 3.4

already calculated: it is given by Equation 3.19 since t_e is equal to zero if and only if i_e is also equal to zero. Therefore, using Equations 3.19 and 3.22, the cumulative probability density function of t_e can be expressed as:

$$F_{T_e}(t_e) = \text{Prob}[t_e=o] + \beta e^{-\beta a}[1-e^{-\delta t_e}]K(\beta,\delta,S_i)$$

where

$$\text{Prob}[t_e=o] = 1 - \exp(-\beta a-2\sigma)\Gamma(\sigma+1)\sigma^{-\sigma}$$

and

$$K(\beta,\delta,S_i) = \int_o^\infty \exp(-\beta y-\delta S_i^2/2y^2)dy$$

$K(\beta,\delta,S_i)$ is then calculated such that

$$F_{T_e}(t_e) \to 1 \text{ as } t_e \to \infty$$

Consequently,

$$K(\beta,\delta,S_i) = e^{-2\sigma}\Gamma(\sigma+1)\sigma^{-\sigma}/\beta$$

and

$$F_{T_e}(t_e) = 1 - \Gamma(\sigma+1)\sigma^{-\sigma}\exp(-\beta a-2\sigma-\delta t_e); \tag{3.23}$$

which gives

$$f_{T_e}(t_e) = \delta\Gamma(\sigma+1)\sigma^{-\sigma}\exp(-\beta a-2\sigma-\delta t_e); \quad t_e > o$$

with (3.24)

$$P_{T_e}(t_e) = 1 - \Gamma(\sigma+1)\sigma^{-\sigma}\exp(-\beta a-2\sigma) \quad , \quad t_e = o$$

where σ is given by Equation 3.20.

3.4.2.2 Evaluation of $F_{I_e|T_e}(i_e,t_e)$

As noted above, when t_e is zero, i_e is also zero, and the probability that i_e is zero given that t_e is zero may be evaluated by Equation 3.19. For i_e and t_e greater than zero, replacing Equation 3.15 in Equation 3.17:

$$i_e = [(i_r-a)t_r - S_i(t_r/2)^{\frac{1}{2}}]/t_e$$

But $t_r = t_o + t_e$, which replaced in the above equation yields:

$$i_e = (i_r-a)(1+t_o/t_e) - S_i(1/t_e + t_o/t_e^2)^{\frac{1}{2}}/2 \qquad (3.25)$$

Define $c=t_e/t_o$. From Equation 3.14 the following relation holds:

$$(i_r-a) = S_i/(2t_o)^{\frac{1}{2}}$$

Replacing c and the above equation in Equation 3.25, yields

$$i_e = S_i \{(1 + 1/c) - (1/c + 1/c^2)^{\frac{1}{2}}\}/(2t_o)^{\frac{1}{2}}$$

or

$$i_e = K(c)\ (i_r-a) \qquad (3.26)$$

where

$$K(c) = [1+c - (1+c)^{\frac{1}{2}}]/c \qquad (3.27)$$

In order to make Equation 3.26 tractable, K(c) as given by Equation 3.27, has to be approximated by some other function. The approximation chosen here is

$$K(c) \simeq 0.60729c^{0.09229} \qquad (3.28)$$

which is compared to the exact one in Figure 3.5.

Introducing the above function into Equation 3.26:

$$i_e \simeq 0.60729(t_e/t_o)^{0.09229}\ (i_r-a)$$

and recalling the definition of t_o:

$$i_e \simeq 0.6474\ S_i^{-0.1846}\ t_e^{0.09229}\ (i_r-a)^{1.1846} \qquad (3.29)$$

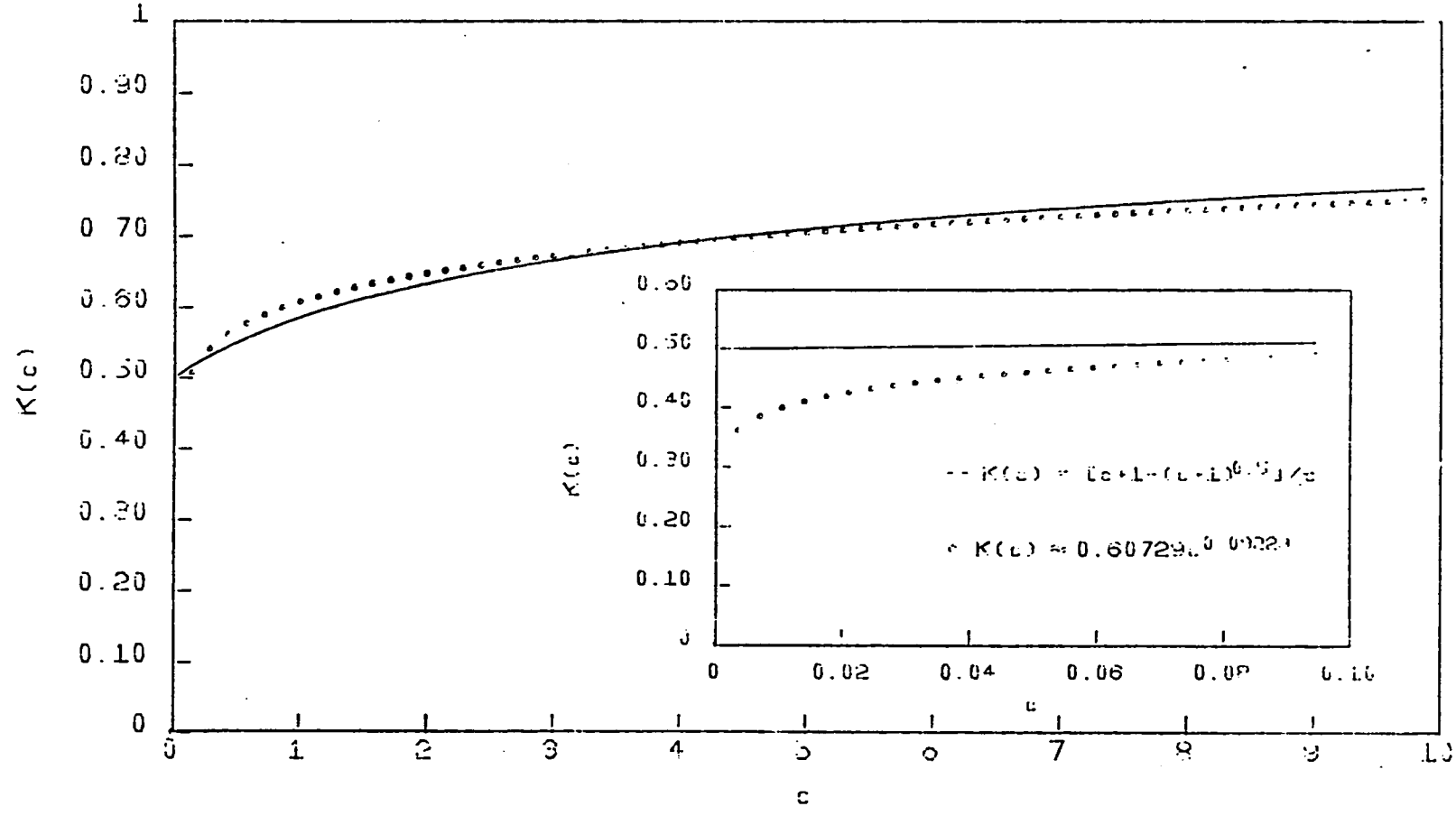

Approximation of K(c)

Figure 3.5

This approximation of i_e allows an explicit solution for i_r

$$i_r \simeq 1.4434\, S_i^{0.1558}\, t_e^{-0.0779}\, i_e^{0.8442} \tag{3.30}$$

which can be used as $g^{-i}(i_e)$ in Equation 2.5 to easily obtain the conditonal distribution of i_e given t_e:

$$f_{I_e|T_e}(i_e,t_e) = 1.2185\beta(S_i/t_e)^{0.1558}\, t_e^{-0.0779} \cdot$$

$$\cdot\exp(-1.4434\beta S_i^{0.1558}\, i_e^{0.8442}\, t_e^{-0.0779}) \tag{3.31}$$

$$i_e,\ t_e > 0$$

3.4.2.3 Evaluation of $f_{I_e,T_e}(i_e,t_e)$

Replacing Equations 3.24 and 3.31 in the expression given by Equation 3.21, the joint distribution of the intensity and duration of the effective rainfall in terms of the parameters of the joint distribution of the intensity and duration of the total precipitation, and the average characteristics of the soils of the basin is

$$f_{I_e,T_e}(i_e,t_e) = 1.2185\beta\delta\exp(-\beta a-2\sigma)\Gamma(\sigma+1)\sigma^{-\sigma}\,(S_i/i_e)^{0.1558}\, t_e^{-0.0779}$$

$$\cdot\exp(-\delta t_e + 1.4434\beta S_i^{0.1558}\, i_e^{0.8442}\, t_e^{-0.0779}) \tag{3.32}$$

$$\text{for } i_e,\ t_e > 0$$

with

$$P_{I_e,T_e}(i_e,t_e) = 1 - \exp(-\beta a-2\sigma)\Gamma(\sigma+1)\sigma^{-\sigma}$$

$$\text{for } i_e = t_e = 0$$

where σ is given by Equation 3.20

3.5 Summary

In this chapter two expressions for the joint probability distribution of the intensity and duration of the effective rainfall have been derived. Both of them use the same joint distribution of the intensity and duration of the total precipitation, which is given as the product of independent exponential distributions; however, the infiltration process has been represented in two different manners. In the first case a simple average potential loss rate was used, whereas the second case is based on a physical model of the infiltration process, the Philip equation.

These expressions of the joint distribution of i_e and t_e will be used in the next chapter to derive the flood frequency distribution for a particular basin.

Chapter 4

DERIVED FLOOD FREQUENCY DISTRIBUTION

4.1 Introduction

The design of water resources systems demands quantification of future events for which no exact time of occurrence can be forecasted (Linsley et al., 1982). Hence, the probability that the event of interest (usually floods or droughts) will equal or exceed a specified value must be given. These probabilites are important for the economic and social evaluation of a project, since they are helpful in determining risks associated with proposed designs or anticipated operating schemes.

The probability of a flood peak of a given magnitude is often described by its return period. The return period or recurrence interval, T_E, of a flood is the expected number of years before the occurrence of a flood of equal or greater magnitude. The probability that a T_E-year flood will be exceeded in any given year is $1/T_E$. Numerous statistical distributions have been suggested to fit data in order to gain information on the magnitude of floods with longer return periods than those associated with the observations. This means that observed floods are required to perform traditional frequency analysis.

Nevertheless, theoretical flood frequency distributions may be derived from appropriate climatic distributions and catchment parameters, using a suitable catchment rainfall-runoff relationship. Eagleson (1972) analytically derived the flood frequency distribution for a V shape plane

assuming exponential distributions for the effective intensity and duration of the rainfall events, and the kinematic wave equations for relating these parameters and the catchment characteristics to the dynamics of overland and streamflow. Distributions for more complex catchment representations were not mathematically tractable. However, his relation agrees well with observations from three Connecticut catchments. Chan and Bras (1978, 1979) derived, based on Eagleson's approach, the frequency distribution for the volume of water above a given threshold discharge, which is applicable in the design of storage devices, flood control systems and storm waters treatment facilities in urban areas. Hebson and Wood (1982) derived a flood frequency distribution from the same distribution of the effective rainfall parameters used by Eagleson (1972) and the Geomorphologic Instantaneous Unit Hydrograph (GIUH) proposed by Rodriguez-Iturbe and Valdes (1979), also with good results.

Derived flood frequency distributions provide a theoretical basis for estimating flood frequency in the absence of streamflow records and for extrapolating empirical estimates based on short records, using only accessible climatic data and catchment parameters.

In this chapter the derivation of two flood frequency distributions are presented. They are based on the Geomorphoclimatic Instantaneous Unit Hydrograph (see Chapter 2) and the distributions of the intensity and duration of the effective rainfall derived in the last chapter. Verification with observed floods in three catchments will also be performed.

Probability Distribution of the Peak Discharge

The main characteristics of the IUH are the peak, q_p, and time to peak, t_p. According to Henderson (1963), if these two parameters are correctly estimated, the real shape of the IUH is not very important, and a triangular approximation is generally adequate for prediction purposes. In the case of triangular IUH, Henderson (1963) gives the following expression for the peak discharge at the outlet of the basin, Q_p

$$Q_p = \frac{2 i_e t_e A_\Omega}{t_b} \left(1 - \frac{t_e}{2t_b}\right) \quad \text{for } t_e < t_b \tag{4.1a}$$

$$Q_p = i_e A_\Omega \quad \text{for } t_e > t_b \tag{4.1b}$$

where i_e is the intensity of the effective rainfall, constant through a duration t_e, A_Ω is the basin area, and t_b is the base time of the IUH. For a triangular IUH:

$$q_p t_b = 2$$

and therefore, Equation 4.1 becomes:

$$Q_p = i_e t_e A_\Omega \; q_p(1 - q_p t_e/4) \quad \text{for } t_e < 2/q_p \tag{4.2a}$$

$$Q_p = i_e A_\Omega \quad \text{for } t_e > 2/q_p \tag{4.2b}$$

In the context of the Geomorphoclimatic theory, Rodriguez-Iturbe et al., (1982) express the peak of the IUH (see Equations 2.24 and 2.26) as:

$$q_p = \frac{0.871}{\Pi_{i_e}^{2/5}} \tag{4.3}$$

where

$$\Pi_{i_e} = \frac{L_\Omega^{5/2}}{i_e A_\Omega R_L \alpha_\Omega^{3/2}} \tag{4.4}$$

where L_Ω is the length of the stream of highest order in Km, α_Ω is kinematic wave parameter of this stream, whose units are $sec^{-1}m^{-1/3}$; i_e is given in cm/hr, A_Ω in Km^2 and q_p in inverse hours.

Consequently, Equation 4.3 may be introduced into Equation 4.2 to obtain the following expression:

$$Q_p = 0.871K_1A_\Omega\, i_e^{7/5}\, t_e(1-0.871K_1 i_e^{2/5}\, t_e/4); \qquad (4.5a)$$

$$\text{for } t_e < \frac{2}{0.871K_1}\, i_e^{-2/5}$$

$$Q_p = i_e A_\Omega; \qquad \text{for } t_e \geq \frac{2}{0.871K_1}\, i_e^{-2/5} \qquad (4.5b)$$

where K_1 is defined as:

$$K_1 = \frac{(A_\Omega R_L)^{2/5}\alpha_\Omega^{3/5}}{L_\Omega} \qquad (4.6)$$

Solving for t_e from Equation 4.5a:

$$t_e = \frac{2}{0.871K_1}\, i_e^{-2/5}\left[1 - \left(1 - \frac{Q_p}{A_\Omega i_e}\right)^{\frac{1}{2}}\right] \qquad (4.7)$$

Note from the above equation that when i_e is equal to Q_p/A_Ω, t_e becomes the limiting value in Equation 4.5

The peak discharge is a random variable. Its random nature arises from the randomness of i_e and t_e. Figure 4.1 presents the i_e-t_e plane with the areas where Equations 4.5a and 4.5b apply. For a particular value of Q_p, Equation 4.7 (or 4.5a) is valid for i_e greater than or equal to Q_p/A_Ω, as Figure 4.2 shows. This equation is plotted with the dashed-dotted line. Besides, the vertical dashed line corresponds to Equation 4.5b for the same value of Q_p. Consequently, the shaded area in Figure 4.2 represents the region of the i_e-t_e plane where the peak discharge is less than or equal to that particular value of Q_p. In other words, it is the inte-

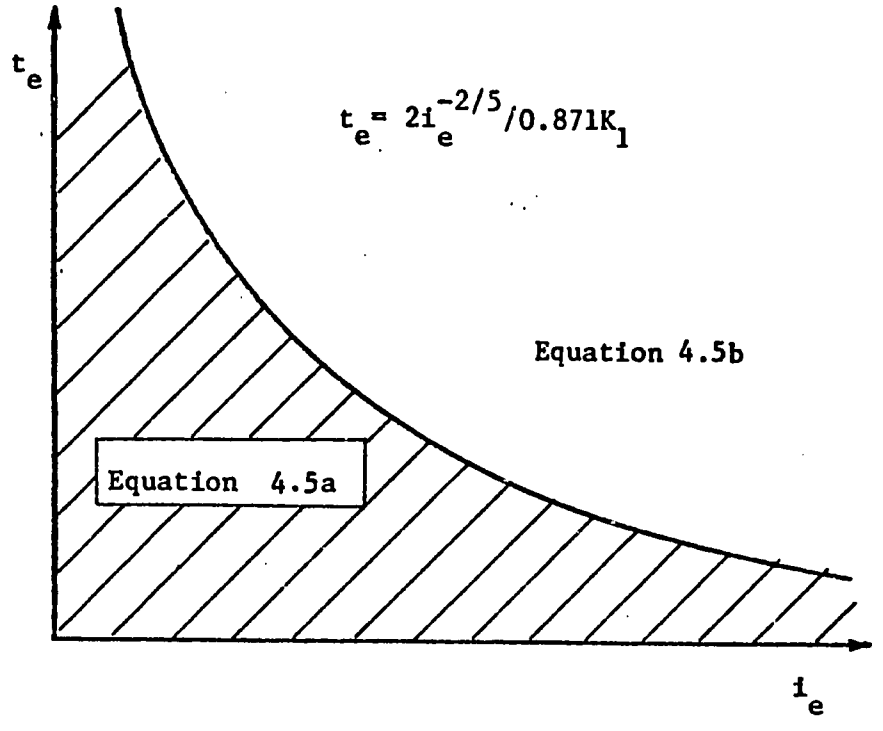

Figure 4.1 Regions where Equation 4.5 is valid

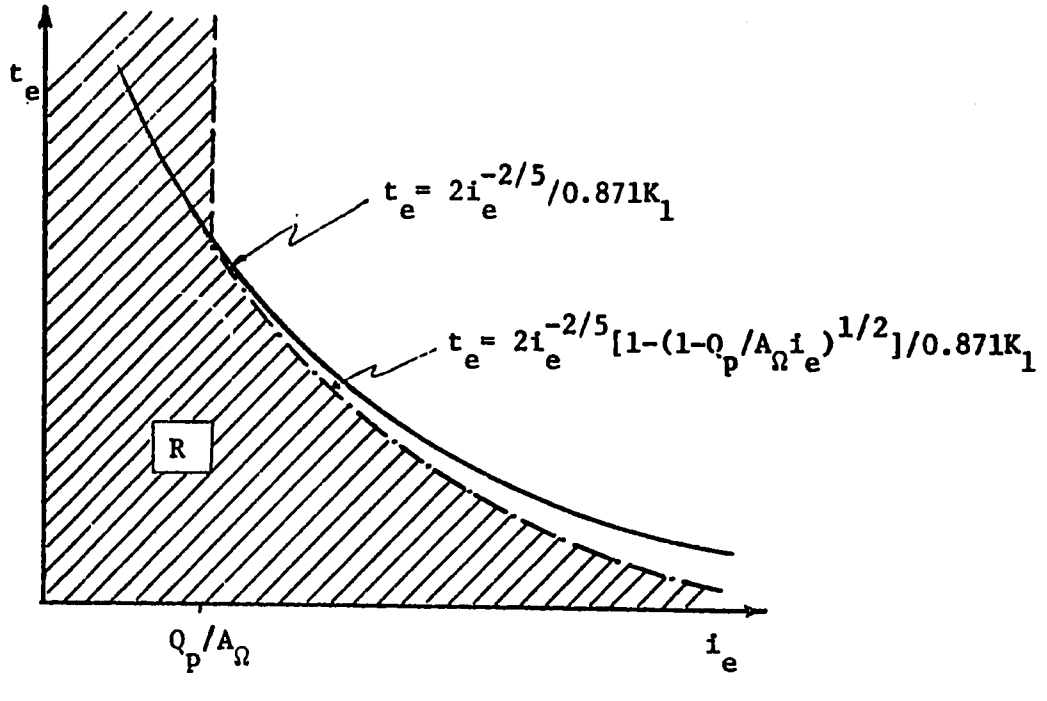

Figure 4.2 Integration region for evaluating the CDF of Q_p

gration area for evaluating the cumulative probability distribution of Q_p, i.e.;

$$F_Q(Q_p) = \int_R f_{I_e,T_e}(i_e,t_e)di_e dt_e$$

or defining R:

$$F_Q(Q_p) = \int_o^{Q_p^*}\left[\int_o^{\infty} f_{I_e,T_e}(i_e,t_e)dt_e\right]di_e + \int_{Q_p^*}^{\infty}\left[\int_o^{t_e^*} f_{I_e,T_e}(i_e,t_e)dt_e\right]di_e \qquad (4.8)$$

where t_e^* is given by Equation 4.7 and $Q_p^* = Q_p/A_\Omega$

Before using the joint distributions of i_e and t_e derived in the previous chapter, the next section presents a manner to evaluate the recurence interval of the floods from $F_Q(Q_p)$.

4.3 Recurrence Interval

$F_Q(Q_p)$ represents the probability of occurrence of a flood event for all times. Commonly, in engineering practice, extreme value distributions of floods are obtained from annual exceedance series, which are expressed as a function of the recurrence interval, i.e., the interval measured in years during which an event of specified magnitude will be equalled or exceeded once on the average.

According to Eagleson (1972), and following the presentation of Chan and Bras (1979), the exceedance probability of a flood with a magnitude Q_E is:

$$F_E(Q_E) \equiv \text{Prob}[Q_p > Q_E] = 1-F_Q(Q_E) \tag{4.9}$$

Define

N = number of years of observations of an event (peak flow in this case).

n = average number of observations per year

nN = total number of observations

If the values of the observations of the event are arranged in decreasing order of magnitude, with order number m=1 for the maximum value, and m=nN for the minimum one, an ordered series may be conformed with expected probability of exceedance given approximately by:

$$F_E(Q_{E_m}) = \text{Prob}[Q_p \geq Q_{E_m}] = \frac{m}{nN+1} \tag{4.10}$$

For an annual exceedance series, only the N highest values from the nN values have to be considered, i.e.,

$$P_E(Q_{E_m}) \equiv \text{Prob}[Q_p \geq Q_{E_m}]\Big|_{\substack{\text{annual} \\ \text{basis}}} = \frac{m}{N+1} = \frac{1}{T_E} \tag{4.11}$$

where T_E is the recurrence interval or return period in years. Dividing Equation 4.11 by Equation 4.10:

$$\frac{P_E(Q_{E_m})}{F_E(Q_{E_m})} = \frac{nN+1}{N+1} = \left(\frac{1}{T_E}\right)\left[\frac{1}{F_E(Q_{E_m})}\right]$$

Frequently, N>>1, then the above equation becomes

$$\left(\frac{1}{T_E}\right)\left[\frac{1}{F_E(Q_{E_m})}\right] \simeq \frac{nN}{N} = n$$

or

$$\frac{1}{T_E} = nF_E(Q_{E_m}) = n[1-F_Q(Q_{E_m}] \tag{4.12}$$

where, in the case considered here, $F_Q(\cdot)$ is given by Equation 4.8.

4.4 Flood Frequency Distribution derived from the Conceptual Infiltration Model

The joint distribution of the intensity and duration of the effective rainfall, derived from the representation of the infiltration as an average potential rate (see Section 3.3) may be used in Equation 4.8 in order to obtain the CDF of the peak discharge, $F_Q(Q_p)$. Using Equations 3.7 and 3.8, which define the distribution of the effective rainfall, with Equation 4.8, results, after some calculations, in

$$F_Q(Q_p) = 1 - \beta e^{-\beta\phi} \int_{Q_p^*}^{\infty} \exp-\left\{\beta i_e + \frac{2}{0.871K_1} i_e^{-2/5}\left[1-(1-Q_p^*/i_e\right]^{\frac{1}{2}}\right\} di_e \qquad (4.13)$$

where Q_p^* is equal to Q_p/A_Ω.

The above integral cannot be calculated analytically and numerical methods must be invoked to solve it. The asymptotic behavior of $F_Q(Q_p)$ can be checked easily: as Q_p tends to infinity, the lower and upper limits of the integral become the same and the integral tends to zero; it follows that:

$$F_Q(Q_p) = 1 \quad \text{as} \quad Q_p \to \infty,$$

fulfilling the CDF's property. On the other extreme, when Q_p is equal to zero, the integral analytically collapses to $1/\beta$ so:

$$F_Q(0) = 1 - e^{-\beta\phi}$$

which is the value of the spike at the origin ($i_e=t_e=0$), as given by Equation 3.8.

Futhermore, the return period is given by:

$$\frac{1}{T_E} = m_\nu \beta e^{-\beta\phi} \int_{Q_p^*}^{\infty} \exp-\left\{\beta i_e + \frac{2}{0.871 K_1} i_e^{-2/5} \left[1-(1-Q_p^*/i_e)^{\frac{1}{2}}\right]\right\} di_e \qquad (4.14)$$

where m_ν is the average annual number of independent rainfall events.

In the next subsection, the flood frequency distribution for a particular basin, based on the above equation, will be evaluated and compared with a frequency distribution based on streamflow records.

4.4.1 Flood Frequency Distribution: A Particular Case.

The flood frequency distribution derived above will be compared with observations from a particular catchment. The one chosen in this work is the Davidson River catchment located in the rugged Appalachian Mountains of western North Carolina. It is one of the catchments reported by Hebson and Wood (1982), Table 4.1 summarizes pertinent geomorphologic and climatic characteristics. Figure 4.3 shows the resulting flood frequency distribution. As it can be seen, the derived distribution does not have the same slope as the observed data (plotted according to the Weibull's plotting position formula), for small floods it overestimates a given recurrence interval, while for large floods, the tendency is the opposite. It is important to note that the value of the area used in the calculations, unlike Hebson and Wood (1982), is the total catchment area; this should correspond to the contributing area producing runoff, and therefore, the implicit assumption by Hebson and Wood is that the contributing area follows the law of stream areas, which is calculated using total drainage areas. This assumption is not an obvious extension of the mentioned law. Figure 4.4, uses half the area, as Hebson and Wood, and a ϕ of 0.72,

TABLE 4.1

Geomorphologic and Climatic Characteristics of Davidson River Catchment (from Hebson and Wood, 1982)

Basin Order: $\Omega = 3$

$A_\Omega = 104.6\ Km^2$

$R_A = 4.80$

$R_B = 3.96$

$R_L = 2.41$

$L_\Omega = 8.8\ Km$

$\beta = 2.46\ hr/cm$

$\delta = 0.19/hr$

$m_\upsilon = 24$

$\phi_1 = 0.61$

$\phi_2 = 0.103$

$\phi = 1.05\ cm/hr$

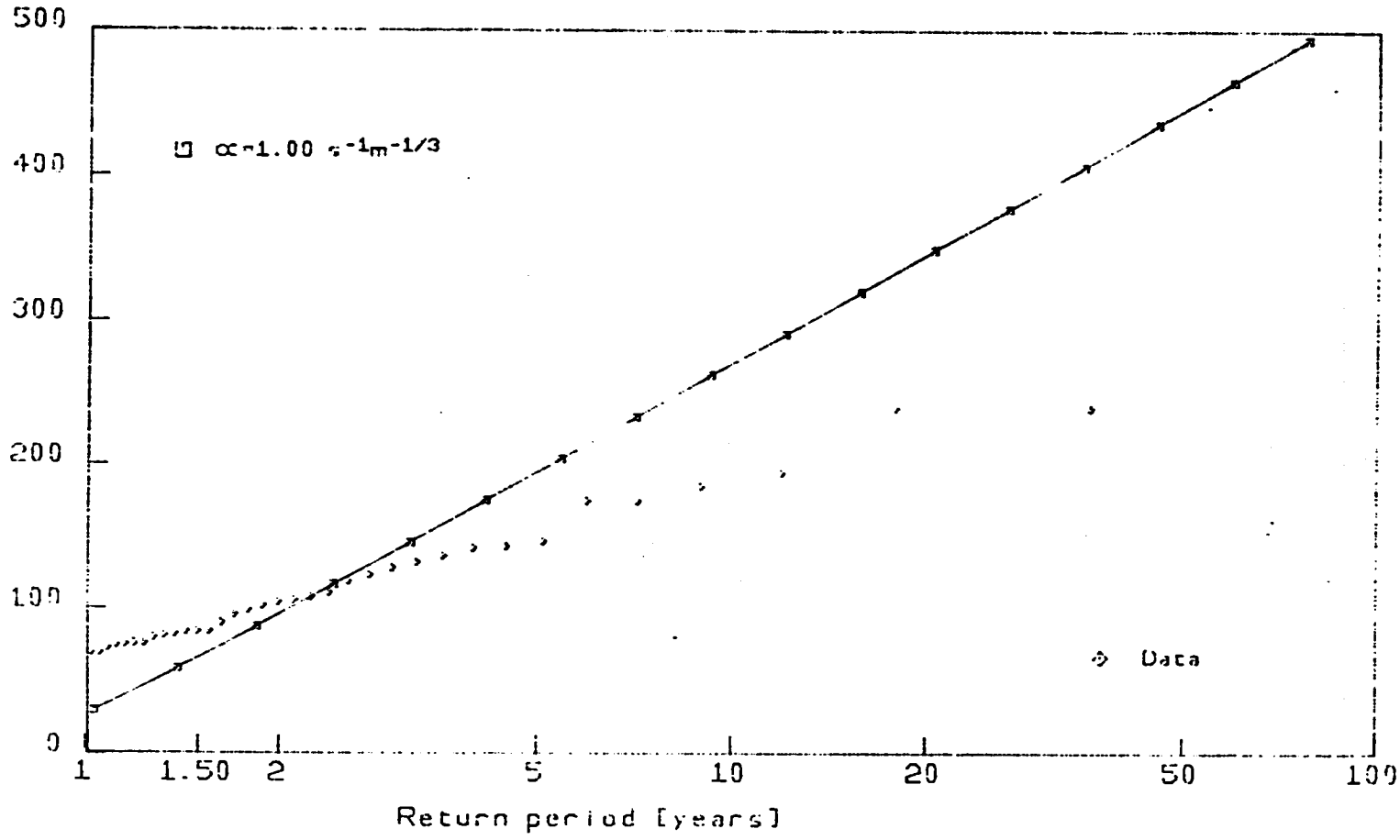

Flood frequency curve

i_p=0.4 cm/hr t_p=5.3 hr A=104.6 km² R_L=2.4 L=8.8 km Φ=1.1 cm/hr m_s=24.

Davidson Basin

Figure 4.3

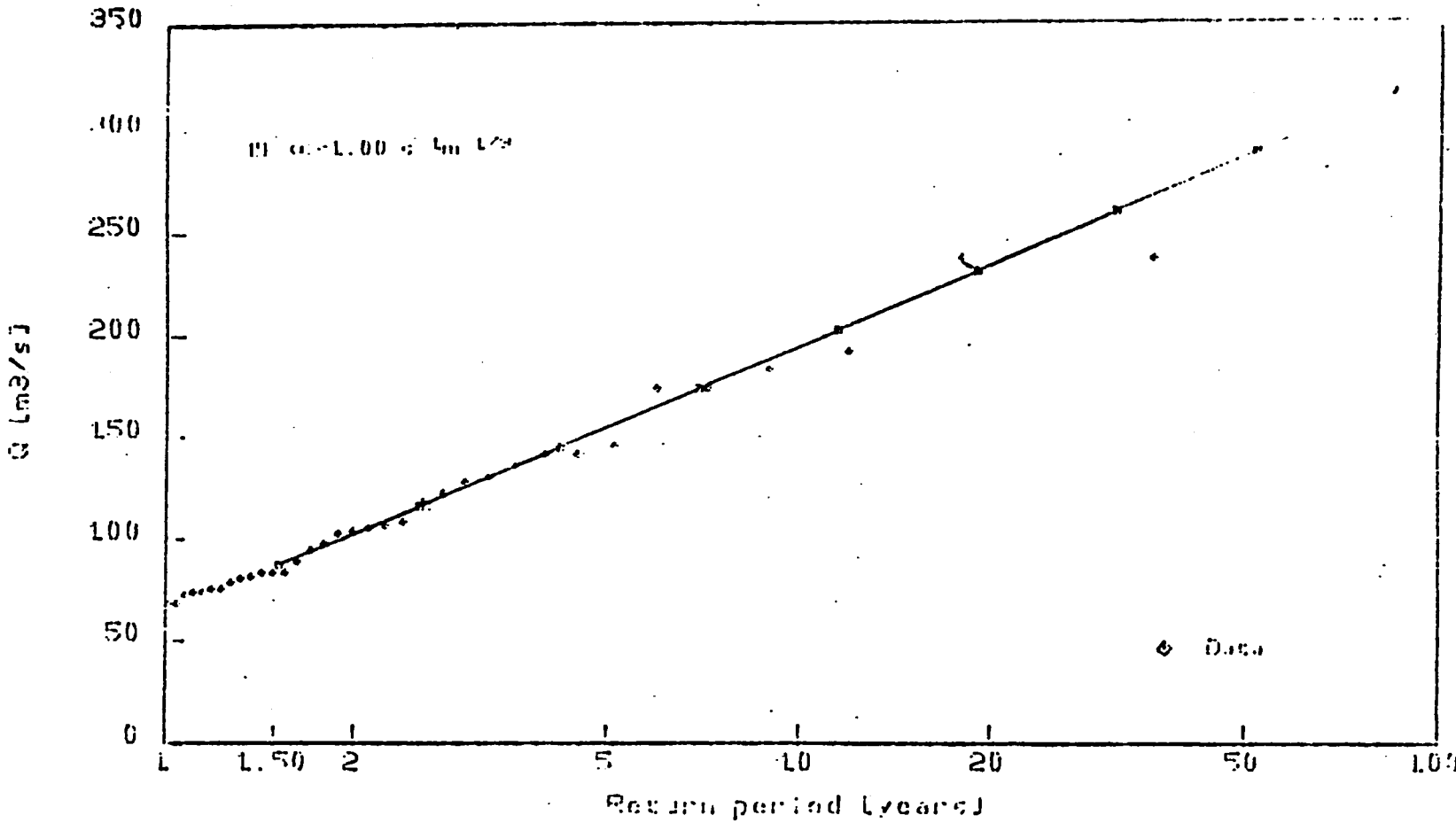

Flood frequency curve

i_p=0.4 cm/hr t_p=5.2 hr A=62.3 km² R_L=2.4 L=8.8 km Φ=0.7 cm/hr n_s=24

Davidson Basin

Figure 4.4

which gives a much better agreement between the derived distribution and the observations. Apparently the flood frequency distribution resulting from the conceptual infiltration model can reproduce the Davidson data only after considerable calibration. Further research is needed in this area.

4.5 Flood Frequency Distribution Derived from the Physically Based Infiltration Model

The flood frequency distribution may also be obtained from the joint probability density function of the intensity and duration of the effective rainfall, already derived in Chapter 3 from a physically based model of the infiltration process.

In this case, Equation 4.8 is:

$$F_Q(Q_p) = 1 - \exp(-\beta a - 2\sigma)\Gamma(\sigma+1)\sigma^{-\sigma} + \int_0^{Q_p^*} \left[\int_0^{\infty} f_{I_e,T_e}(i_e,t_e)dt_e\right]di_e + \int_{Q_p^*}^{\infty} \left[\int_0^{t_e^*} f_{I_e,T_e}(i_e,t_e)dt_e\right]di_e \tag{4.15}$$

where $f_{I_e,T_e}(i_e,t_e)$ is given by Equation 3.32. The first two terms of the above equation represent the value of the spike at Q_p equal to zero. Introducing Equation 3.32, the third term of Equation 3.15 becomes:

$$\int_0^{Q_p^*} \left[\int_0^{\infty} f_{I_e,T_e}(i_e,t_e)dt_e\right]di_e$$

$$A^* \int_0^{\infty} e^{-\delta t_e} t_e^j \left[\int_0^{Q_p^*} i_e^{-k} \exp(-1.4434\beta S_i^k i_e^{\ell} t_e^j)di_e\right]dt_e$$

where

$$A^* = 1.2185\,\delta\beta\,\exp(-\beta a-2\alpha)\Gamma(\sigma+1)\sigma^{-\sigma}\,S_i^k$$

$$j = -0.0779$$

$$k = 0.1558$$

$$\ell = 0.8442$$

Letting $y=i_e^{\ell}$, the inner integral can be evaluated, and after some calculations, the final result of the above integration exercise is:

$$\exp(-\beta a-2\sigma)\Gamma(\sigma+1)\sigma^{-\sigma}\left\{1-\delta\int_o^{\infty}\exp-\left[1.4434\beta S_i^k\,Q_p^{*k}\,t_e^j+\delta t_e\right]dt_e\right\} \qquad (4.16)$$

Similarly, the fourth term of Equation 4.15 becomes:

$$\int_{Q_p^*}^{\infty}\left[\int_o^{t_e^*} f_{I_e,T_e}(i_e,t_e)dt_e\right]di_e =$$

$$A^*\int_{Q_p^*}^{\infty} i_e^{-k}\left[\int_o^{t_e^*} t_e^j\exp-\left[\delta t_e+1.4434\beta S_i^k\,i_e^{\ell}\,t_s^j\right]dt_e\right]di_e \qquad (4.17)$$

The inner integral cannot be evaluated analytically, and since its upper integration limit is function of i_e, it is not possible to change the integration order as done in the evaluation of the third term of Equation 4.15. Therefore, there are two possibilities for dealing with the above expression: one is to evaluate it numerically (a double integral), or to approximate t_e^* with a more tractable function that allows the evaluation of the inner integral analytically (in this way, computer time will be reduced in the calculation of $F_Q(Q_p)$). The latter was chosen here. The expression for t_e^* is (Equation 4.7):

$$t_e^* = \frac{2}{0.871K_1}\,i_e^{-2/5}\left[1-(1-Q_p^*/i_e)^{\frac{1}{2}}\right] \qquad (4.18)$$

with the condition that i_e must be greater than or equal to Q_p. The approximation adopted affects only the last factor of the above equation, i.e.,

$$
\begin{aligned}
[1 - (1-Q_p^*/i_e^*)^{\frac{1}{2}}] &\simeq (Q_p^*/i_e^*)^{3.1358} && Q_p^* < i_e < 1.2Q_p^* \\
&\simeq (0.80482Q_p^*/i_e^*)^{1.36396} && 1.2Q_p^* < i_e < 2Q_p^* \\
&\simeq (0.65295Q_p^*/i_e^*)^{1.10812} && 2Q_p^* < i_e < 5Q_p^* \\
&\simeq (0.5Q_p^*/i_e^*) && 5Q_p^* < i_e < \infty
\end{aligned}
\qquad (4.19)
$$

Figure 4.5 shows this approximation. As it can be seen, it is very close to the original function, which is represented by the solid line. Consequently, the double integral given by Equation 4.17 is split up into a sum of four double integrals, whose integration limits are determined as follows:

1. $Q_p^* < i_e < 1.2Q_p^*$:

$$t_e^* = 2i_e^{*-0.4} (Q_p^*/i_e^*)^{3.1358} /0.871K_1$$

or solving for i_e:

$$i_{e_1} \equiv i_e = (2Q_p^{*3.1358} /0.871K_1t_e)^{1/3.5358} \qquad (4.20)$$

For $i_e = Q_p^*$, then $t_e^* = 2.2962Q_p^{*-0.4} /K_1$

For $i_e = 1.2Q_p^*$, then $t_e^* = 1.2051Q_p^{*-0.4} /K_1$

2. $1.2Q_p^* \leq i_e \leq 2Q_p^*$

$$t_e^* = 2i_e^{-0.4} \left(0.80482Q_p^*/i_e\right)^{1.36396}/0.871K_1$$

$$i_{e_2} \equiv i_e = \left[2\left(0.80482Q_p^*\right)^{1.36396}/0.871K_1 t_e\right]^{1/1.76396} \tag{4.21}$$

For $i_e = 1.2Q_p^*$, then $t_e^* = 1.238Q_p^{*-0.4}/K_1$

For $i_e = 2Q_p^*$, then $t_e^* = 0.5028Q_p^{*-0.4}/K_1$

3. $2Q_p^* \leq i_e \leq 5Q_p^*$:

$$t_e^* = 2i_e^{-0.4} \left(0.65295Q_p^*/i_e\right)^{1.10812}/0.871K_1$$

$$i_{e_3} \equiv i_e = \left[2\left(0.65295Q_p^*\right)^{1.10812}/0.871K_1 t_e\right]^{1/1.50812} \tag{4.22}$$

For $i_e = 2Q_p^*$, then $t_e^* = 0.50337Q_p^{*-0.4}/K_1$

For $i_e = 5Q_p^*$, then $t_e^* = 0.1264Q_p^{*-0.4}/K_1$

4. $5Q_p^* \leq i_e \leq \infty$

$$t_e^* = Q_p^* i_e^{-1.4}/0.871K_1$$

$$i_{e_4} \equiv i_e = \left(Q_p^*/0.871K_1 t_e\right)^{1/1.4} \tag{4.23}$$

For $i_e = 5Q_p^*$, then $t_e^* = 0.1206Q_p^{*-0.4}/K_1$

For $i_e = \infty$, then $t_e^* = 0.$

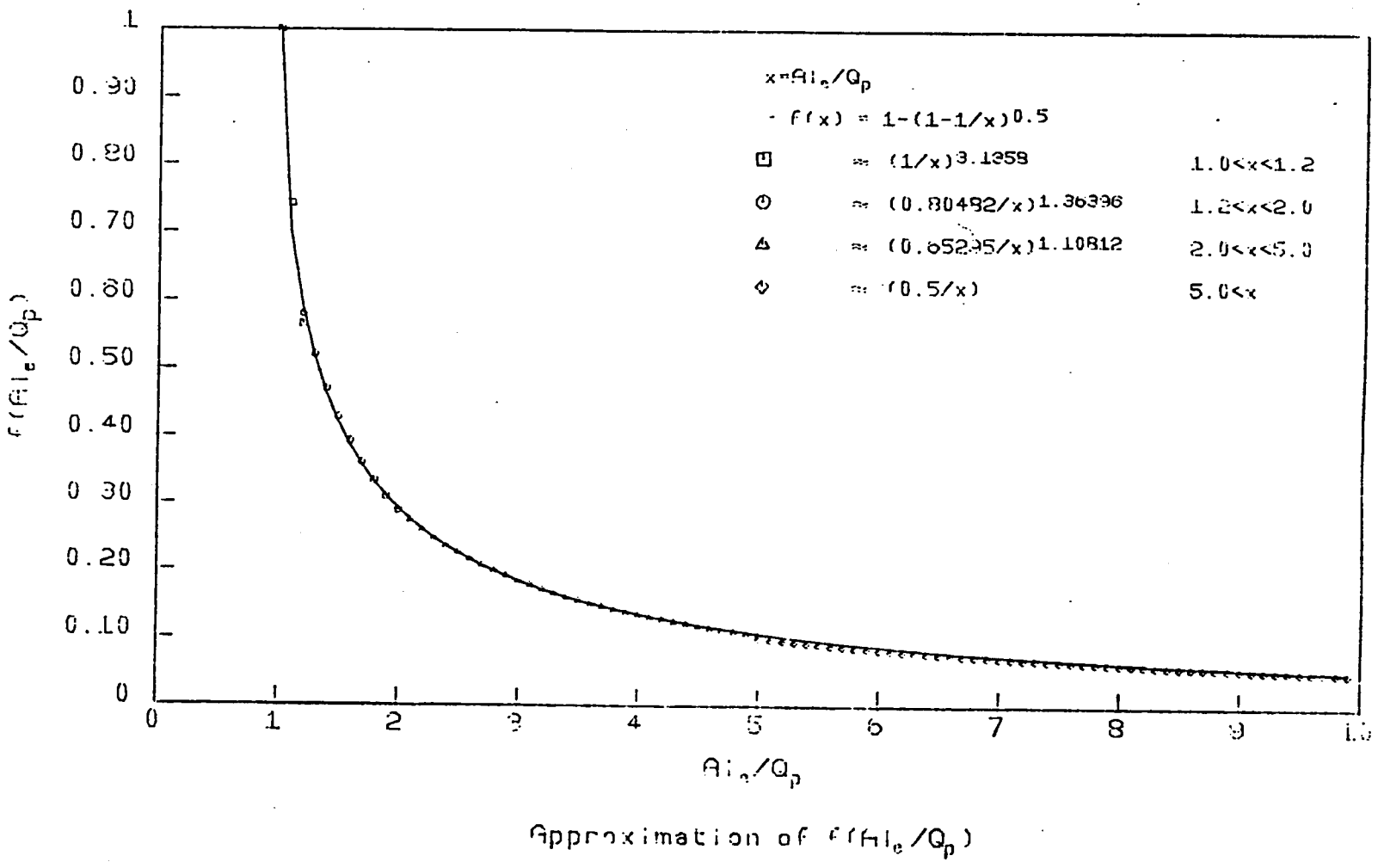

Approximation of $f(Ai_e/Q_p)$

Figure 4.5

As one can suspect, the fact that an explicit expression for i_e could be found will allow, for each split double integral, the interchange of the integration order and the analytical evaluation of the resulting inner integral.

Figure 4.6 shows the i_e-t_e plane, where the shaded area constitutes the integration region for the fourth term of Equation 4.15. Then, it follows that this term may be expressed as:

$$\int_{Q_p^*}^{\infty} \left[\int_o^{t_e^*} f_{I_e,T_e}(i_e,t_e)dt_e \right] di_e \approx$$

$$\int_0^{t_{e_4}} \left[\int_{Q_p^*}^{i_{e_4}} f_{I_e,T_e}(i_e,t_e)di_e \right] dt_e + \int_{t_{e_4}}^{t_{e_3}} \left[\int_{Q_p^*}^{i_{e_3}} f_{I_e,T_e}(i_e,t_e)di_e \right] dt_e$$

$$+ \int_{t_{e_3}}^{t_{e_2}} \left[\int_{Q_p^*}^{i_{e_2}} f_{I_e,T_e}(i_e,t_e)di_e \right] dt_e + \int_{t_{e_2}}^{t_{e_1}} \left[\int_{Q_p^*}^{i_{e_1}} f_{I_e,T_e}(i_e,t_e)di_e \right] dt_e \tag{4.24}$$

where the integral is given by Equation 3.32, i_{e_1}, i_{e_2}, i_{e_3} and i_{e_4} are given by Equations 4.20 to 4.23, and t_{e_1} to t_{e_4} are defined as

$$\begin{aligned} t_{e_1} &= 2.2962 Q_p^{*-0.4}/K_1 \\ t_{e_2} &= 1.2216 Q_p^{*-0.4}/K_1 \\ t_{e_3} &= 0.5033 Q_p^{*-0.4}/K_1 \\ t_{e_4} &= 0.1235 Q_p^{*-0.4}/K_1 \end{aligned} \tag{4.25}$$

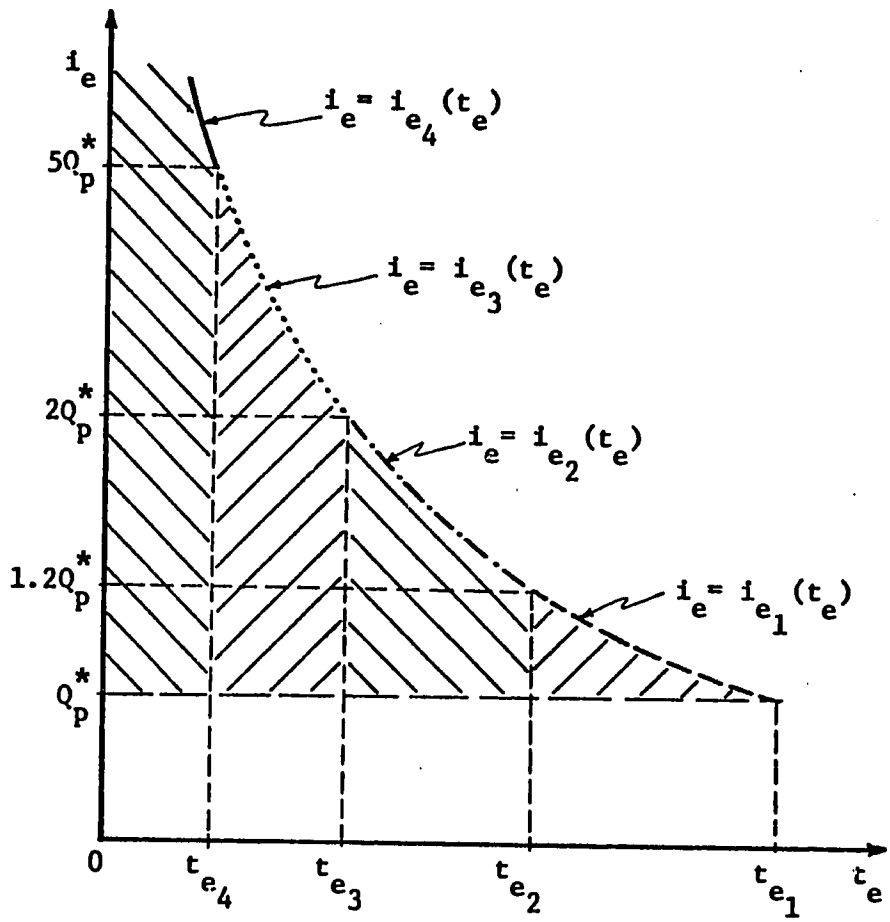

Integration region for evaluating the 4^{th} term of Equation 7.15

Figure 4.6

The inner integrals of Equation 4.24 can be evaluated analytically in a similar manner to that used to calculate the third term of Equation 4.15. As a result, each right hand side component of Equation 4.24 has the following form:

$$\delta\exp(-\beta a-s\sigma)\Gamma(\sigma+1)\sigma^{-\sigma}\left\{\int_{t_{e_{i+1}}}^{t_{e_i}} \exp-\left[\delta t_e + 1.4434\beta S_i^k\, t_e^j\, Q_p^{*\ell}\right]dt_e\right.$$

$$\left. - \int_{t_{e_{i+1}}}^{t_{e_i}} \exp-\left[\delta t_e + 1.4434\beta S_i^k\, t_e^j\, i_{e_i}^{\ell}\right]dt_e\right\} \qquad (4.26b)$$

where t_{e_i} is given by Equation 4.25, and i_{e_i} by Equations 4.20 to 4.23.

Replacing Equation 4.26 in Equation 4.24, adding Equation 4.16 and the spike at $Q_p=0$, and after some manipulations, the expression for the cumulative distribution of Q_p becomes:

$$F_Q(Q_p) = 1 - \delta\exp(\beta a-2\sigma)\Gamma(\sigma+1)\sigma^{-\sigma}\left\{I + \sum_{i=1}^{4} J_i\right\} \qquad (4.26b)$$

where

$$I = \int_{2.2962Q_p^{*-0.4/K_1}}^{\infty} \exp-\left\{\delta t_e + 1.4434\beta S_i^k\, t_e^j\, Q_p^{*\ell}\right\}dt_e \qquad (4.27)$$

and,

$$J_i = \int_{a_iQ_p^{*-0.4/K_1}}^{b_iQ_p^{*-0.4/K_1}} \exp-\left\{\delta t_e + 1.4434\beta S_i^k\, t_e^j\left[2(c_iQ_p^*)^{d_i}/0.871K_1t_e\right]^{\ell/e_i}\right\}dt_e \qquad (4.28)$$

where the coefficients a_i, b_i, c_i, d_i, and e_i are listed in Table 4.2.

Integrals I and J_i must be evaluated numerically. However, the asymptotic behavior of $F_Q(Q_p)$ when Q_p tends to infinity may be verified as follows: as $Q_p \to \infty$ the lower limit of I tends to zero as well as

TABLE 4.2

Coefficients of J_i

i	a_i	b_i	c_i	d_i	e_i
1	0	0.1235	0.5	1.0	1.4
2	0.1235	0.5033	0.6529	1.1081	1.5081
3	0.5033	1.2216	0.8048	1.3640	1.7640
4	1.2216	2.2962	1.0	3.1358	3.5358

the integrand, so that I tends to zero; in addition, as Q_p tends to infinity the lower and upper limits of J_i become the same, so that J_i tends also to zero. Therefore,

$$F_Q(Q_p) \to 1 \quad \text{as} \quad Q_p \to \infty$$

On the other extreme, when Q_p is equal to zero, J_i becomes zero and I transforms to:

$$\int_0^\infty e^{-\delta t_e} \, dt_e$$

and therefore,

$$F_Q(0) = 1 - \exp(-\beta a - 2\sigma)\Gamma(\sigma+1)\sigma^{-\sigma}$$

which is the value of the spike at (i_e, t_e) equal to $(0,0)$, in agreement with Equation 3.32.

It is important to note that the distribution just derived is conditional on the initial soil moisture concentration, since Philip's solution of the one-dimensional equation of the diffusion process is based on an initial condition given by a uniform soil moisture content (see Section 3.4.1).

Finally, the exceedance probability of floods, $F_Q(Q_p)$, may be related to the annual exceedance reccurrence interval through Equation 3.12. Appendix B contains the Fortran program to calculate it. Figures 4.7 to 4.11 present the derived flood frequency distributions for an hypothetical basin, whose relevant geomorphologic and climatic parameters are listed below:

A_Ω = 13Km^2

L_Ω = 8 Km

R_L = 2.70

m_i = 0.4 cm/hr

m_{t_r} = 3hr

m_ν = 50

The purpose of these figures is to show the effect of some variables in the resulting flood frequency distribution. It is assumed that the variability in time and space of soil moisture is such that it is best to parameterize basin response in terms of some average soil moisture concentration, s_o. In Figure 4.7, the number of independent rainfall events in the year m_ν varies between 40 and 60, showing an increment of the magnitude of floods as m_ν increases. Figure 4.8 presents the distribution for three values of α_Ω, namely 0.5, 1.0, and 1.5 $s^{-1}m^{-1/3}$, showing slight sensitivity to this parameter. In practice, this is advantageous since the estimation of α_Ω may involve the subjective estimation of Manning's n. Figure 4.9 compares the flood frequency distribution resulting from two different types of soils, which may represent the lumped soil characteristics of the basin. They are silty loam and clay loam, whose typical properties, taken from Eagleson (1978), are listed below:

Parameter	Silty Loam	Clay Loam
n	0.35	0.35
K(1)[cm/hr]	0.357	0.084
Ψ(1)[cm]	166	19
m	0.667	0.286

As it can be seen from the figure, the effect of the type of soil in the flood frequency distribution is very important: clay loam is more impervious than silty loam and can produce more surface runoff. In this example, the difference in flood magnitude for a given recurrence interval differ by a factor of two or three.

Figure 4.10 presents the flood frequency distribution when the climatic parameters, m_i, and m_{t_r}, change to 0.3 cm/hr and 4 hr, respectively, the soil is silty loam and the remaining parameters are the same as those given in the previous figure. This curve, compared with the corresponding one of Figure 4.9 gives lower values of the flood for a particular return interval. This means that for this specific case, the intensity is more important than the duration in relation with the magnitude of the floods.

In Figure 4.11, the sensitivity of the flood frequency distribution to the value of the average soil moisture is shown. As it is seen, its effect is appreciable with the obvious behavior: as s_o increases, more surface runoff is produced and therefore the magnitude of floods increases.

From the above analysis, soil parameters and soil moisture conditions must be secured in order to obtain the flood frequency distribution for a particular basin. Under the assumption that lumped soil parameters (effective porosity, saturated conductivity and pore disconnectedness index) may be determined from field samples, only soil moisture conditions need to be evaluated. If this is the case, one could, in principle, derive the PDF of uniform initial soil moisture for the storm events from physically based models of the infiltration and exfiltration processes (e.g., Eagleson 1978) and relevant climatic random variables with predefined probability distributions. However, given the Markovian nature involved

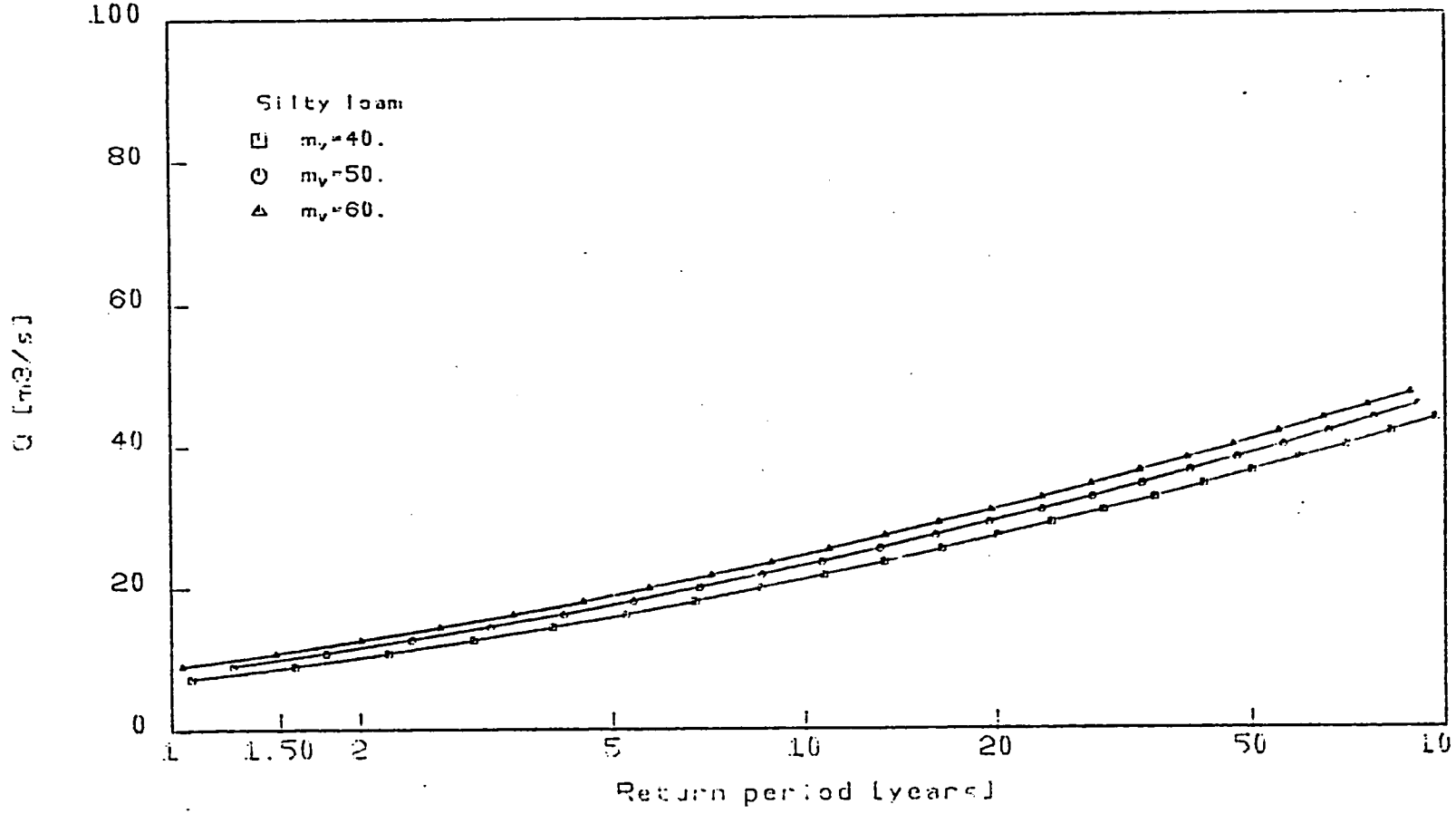

Flood frequency curve

i_p=0.4 cm/hr t_p=3.0 hr A=13.0 km² R_L=2.7 L=8.0 km α=1.00 $s^{-1}m^{1/3}$ c_v=0.40

Figure 4.7

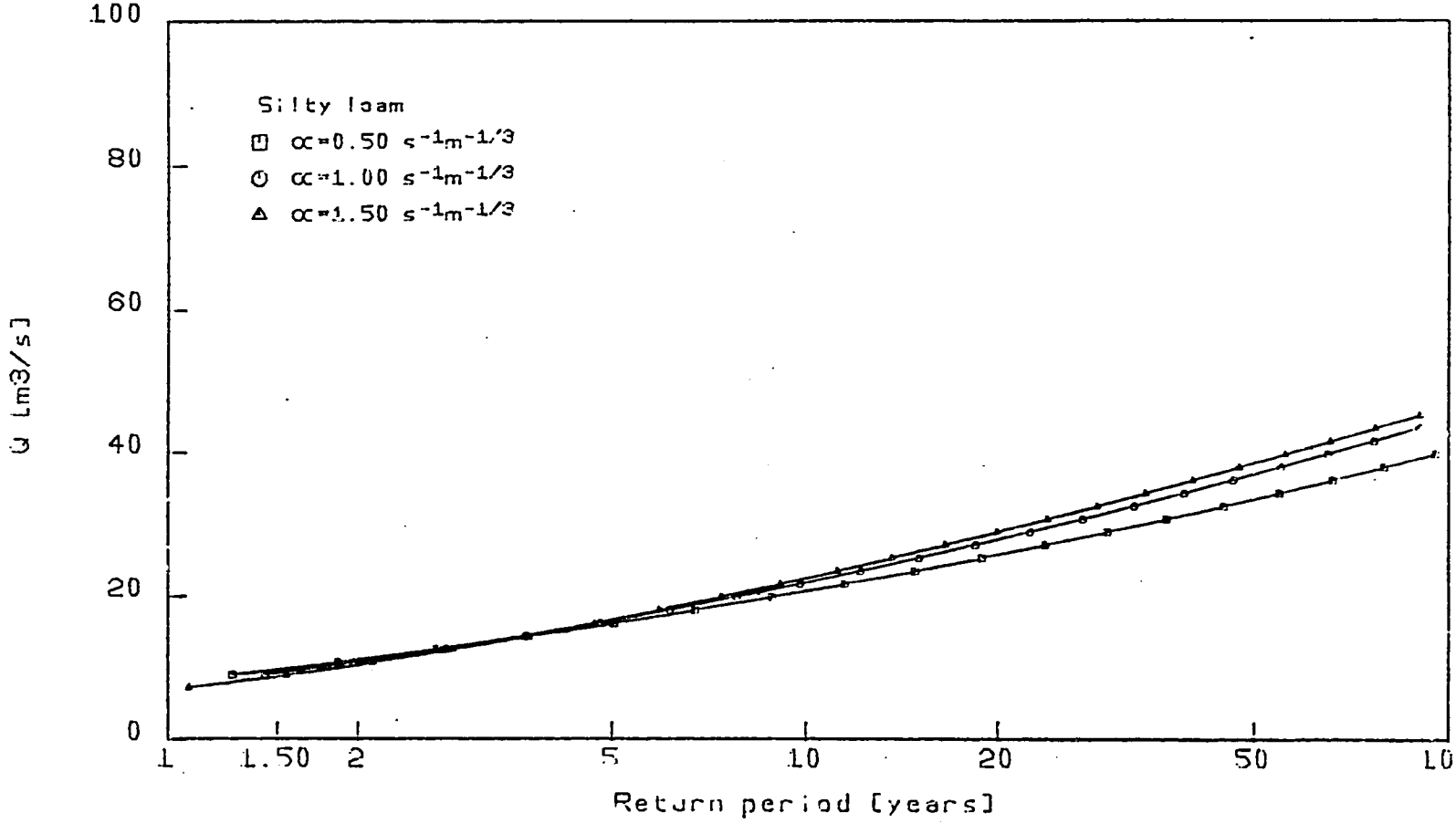

Flood frequency curve

i_r=0.4 cm/hr t_r=3.0 hr A=13.0 km² R_L=2.7 L=8.0 km s_0=0.35 m_y=50.

Figure 4.8

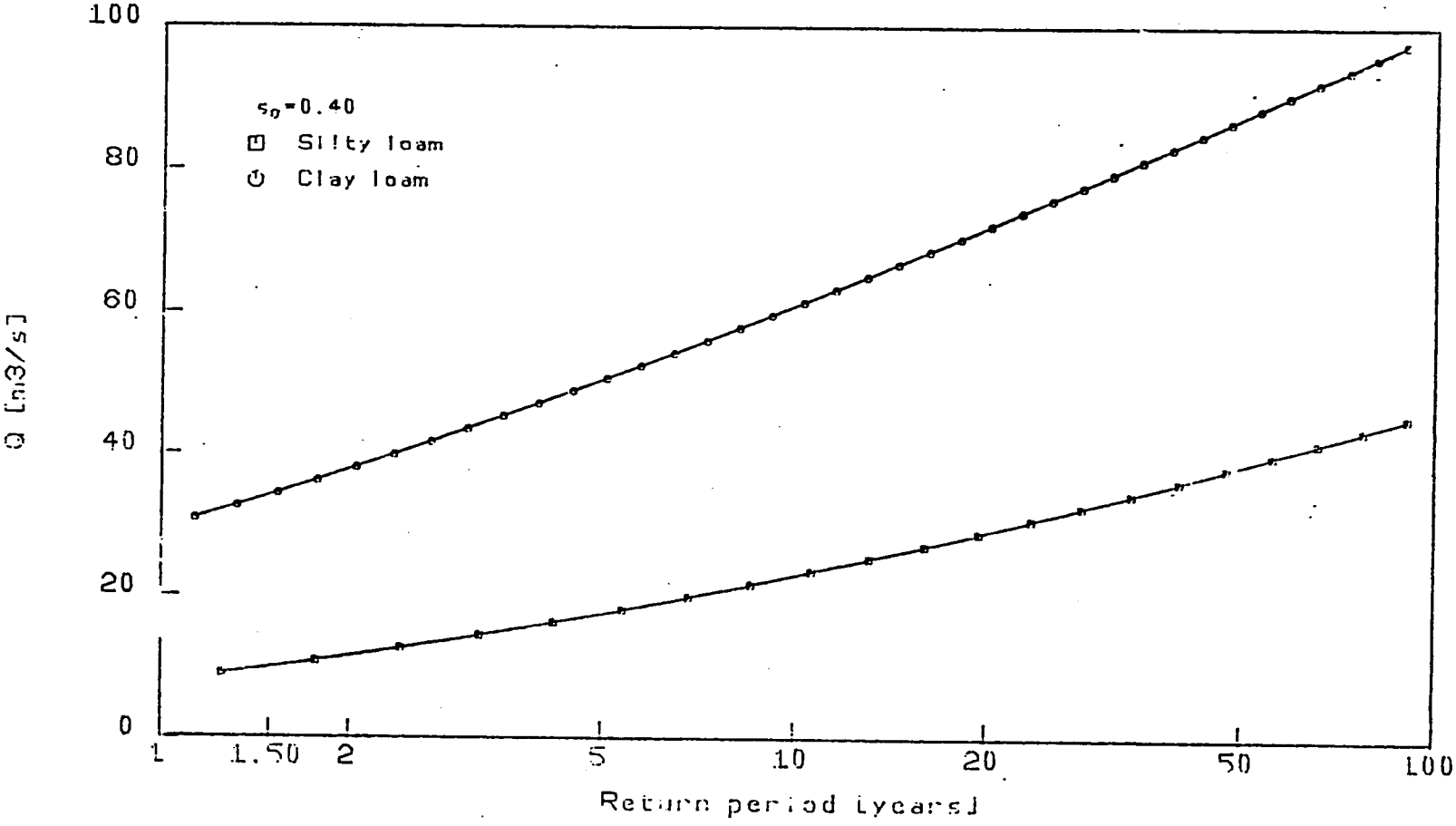

Flood frequency curve

i_p=0.4 cm/hr t_p=3.0 hr A=13.0 km² R_L=2.7 L=8.0 km α=1.00 $s^{-1}m^{-1/3}$ n_i=50.

Figure 4.9

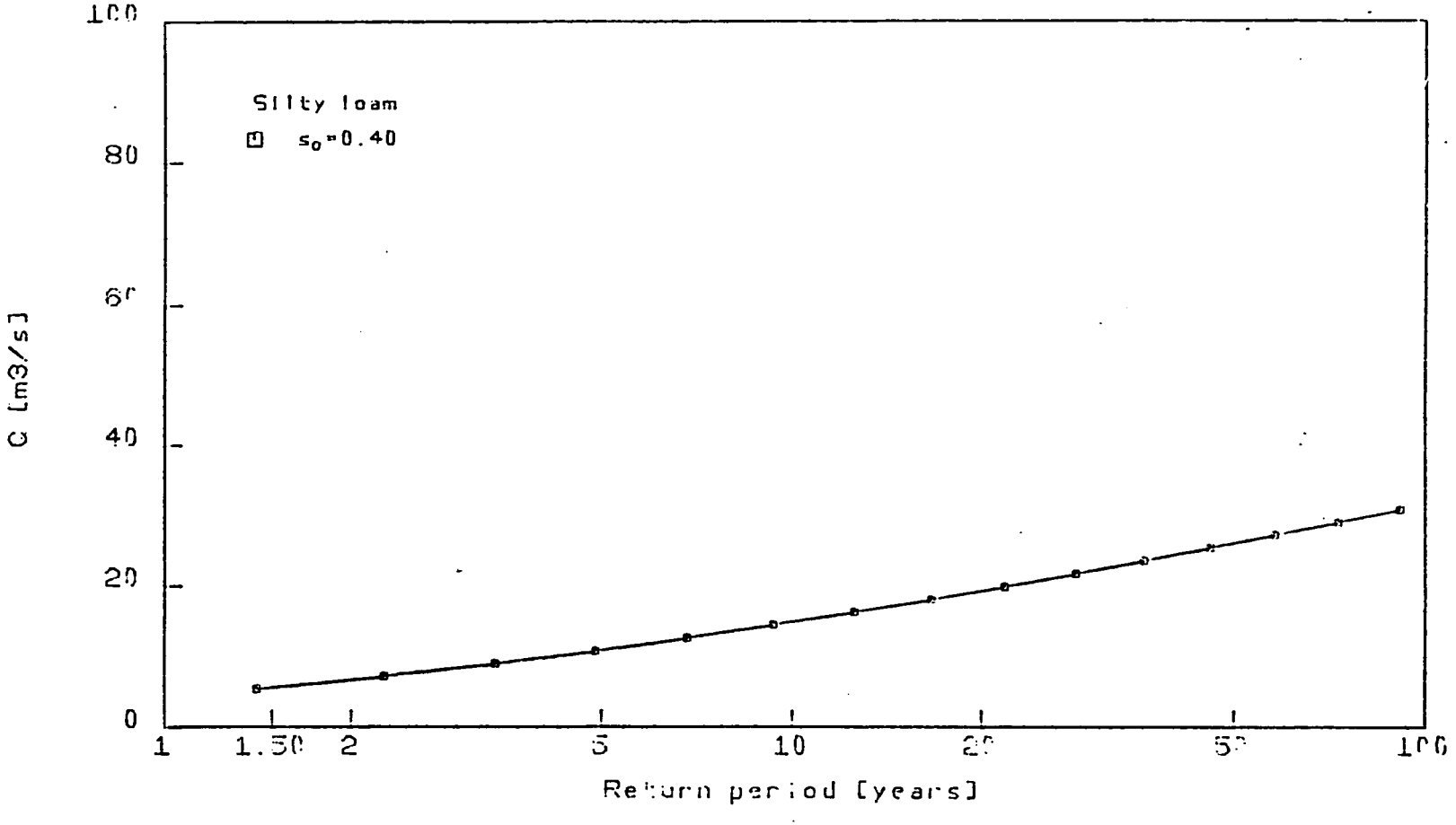

Flood frequency curve

i_p=0.3 cm/hr t_r=4.0 hr A=13.0 km^2 R_L=2.7 L=8.0 km α=1.00 s^{-1}m$^{-1/3}$ m_v=50.

Figure 4.10

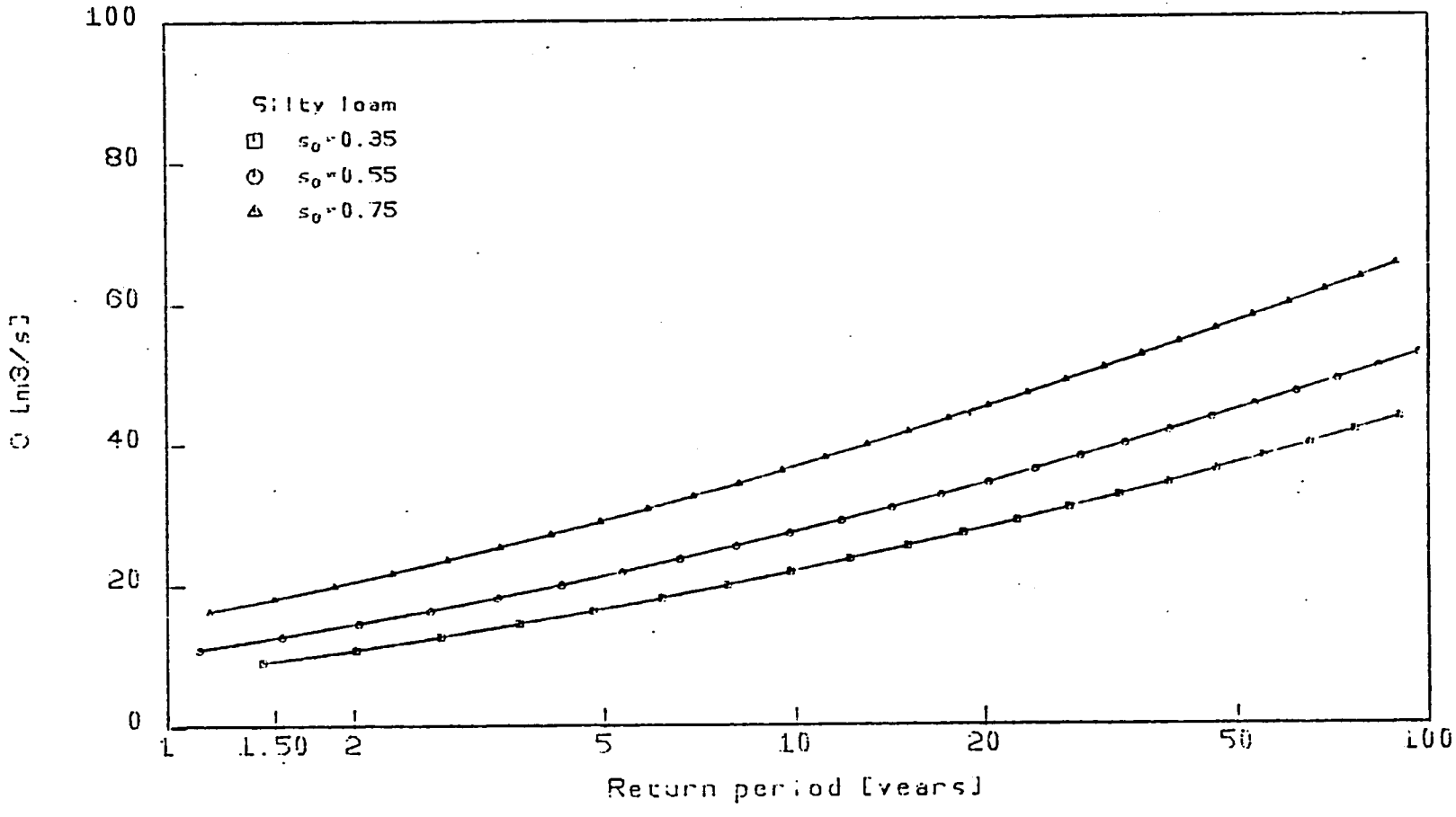

Flood frequency curve

i_p=0.4 cm/hr t_p=3.0 hr A=13.0 km² R_L=2.7 L=8.0 km α=1.00 $s^{-1}m^{-1/3}$ m_p=50.

Figure 4.11

in the infiltration-exfiltration chain, (Cordova and Bras, 1981) the soil moisture at the beginning of the rainfall event will be a function of the soil moisture at the beginning of the previous interstorm event, and viceversa; and therefore, the PDF of interest could be calculated only implicitly. To avoid the above difficulty, it is proposed here to fit, from the results of enough simulations of the infiltration-exfiltration events, a beta distribution as the PDF of the initial soil moisture concentration, in such a way that the two parameters of this distribution are function of climatic parameters and soil properties. This is done in Appendix A using Eagleson's infiltration and exfiltration models (1978) and the results of 50 simulations for a wide range of climates and several types of soil. The resulting fitted beta distribution is:

$$f_S(s_o) = \frac{1}{B} s_o^{r-1}(1-s_o)^{t-r-1} \qquad (4.29)$$

$$0 < s_o < 1; \quad r < t$$

where

$$t = \bar{s}_o(1-\bar{s}_o)/\sigma_s^2 - 1 \qquad (4.30)$$

$$r = \bar{s}_o(1-\bar{s}_o)/\sigma_s^2 - 1 \qquad (4.31)$$

$$B = \Gamma(r)\,\Gamma(t-r)/\Gamma(t)$$

and from the regression analysis of the results of the above simulations, the expressions for $\bar{s}_o$ and σ_s are:

$$\bar{s}_o = 0.2761\, m_{t_r}/m_{t_b} + 0.02628 \ln[m_i/(1-M+Mk_v)\bar{e}_p] + 0.3767[\Psi(1)n/m_{t_b}K(1)m]^{1/6} - 0.15 \qquad (4.32)$$

where

M = vegetation canopy density

k_ψ = ratio of potential rates of transpiration and soil surface evaporation

with a coefficient of determination R^2 equal to 0.94, and

$$\sigma_s = 0.0753m_i^{\frac{1}{2}} - 0.0094m_{t_r} + 0.0816m_{t_b}^{\frac{1}{2}} + 7.50\bar{e}_p - 0.0915n - 0.00095K(1) + 0.838/\ell n[\Psi(1)] + 0.0555m^{\frac{1}{2}} + 0.3858 \quad (4.33)$$

with R^2 equal to 0.61. This equation requires that time be given in hours and length in centimeters.

In the above equations, m_{t_b} is the mean time between storms and $\bar{e}_p$ is the average potential rate of evaporation from bare soil.

Now that a distribution of s_o has been defined, the marginal cumulative distribution of Q_p may be found by:

$$F_Q(Q_p) = \int_0^1 F_{Q|S}(Q_p, s_o) f_S(s_o) ds_o \quad (4.34)$$

where $F_{Q|S}(Q_p, s_o)$ is given by Equation 4.26. However, a first order approximation with $\bar{s}_o$, (Equation 4.32), as the representative initial soil moisture concentration, will be attempted. This will be done for two basins: Santa Paula Creek Basin in California and Nashua River Basin in Massachusetts, for which climatic and soil data were available from Eagleson (1978).

4.5.1 Santa Paula Creek and Nashua River Basins

Santa Paula Creek basin has an area of 103.6 km^2 and is located in Santa Paula Canyon in Ventura County, about 80 km northwest of Los Angeles. This is the representative arid climate catchment used by Eagleson (1978) to verify his model of the annual water balance. The climatic parameters of this basin are listed below:

m_i = 0.1 cm/hr

m_{t_r} = 34.3 hr

m_{t_r} = 250 hr

e_p = 0.0114 cm/hr

M = 0.40

k_v = 1.0

m_v = 15.7

The type of soil that gave the best fit of the frequency of annual basin yield was silty loam, whose properties have been presented before; therefore, this type of soil will be used here.

The above data allow the evaluation of $\bar{s}_o$ by means of Equation 4.32:

$$\bar{s}_o = 0.32$$

From topographic maps, the relevant geomorphologic parameters are evaluated:

$$R_L = 2.3$$

$$L_\Omega = 16.9 \text{ km}$$

Besides, it is assumed that α_Ω, the kinematic parameter is equal to 1 $sec^{-1}m^{-1/3}$. Figure 4.12 shows the resulting flood frequency distribu-

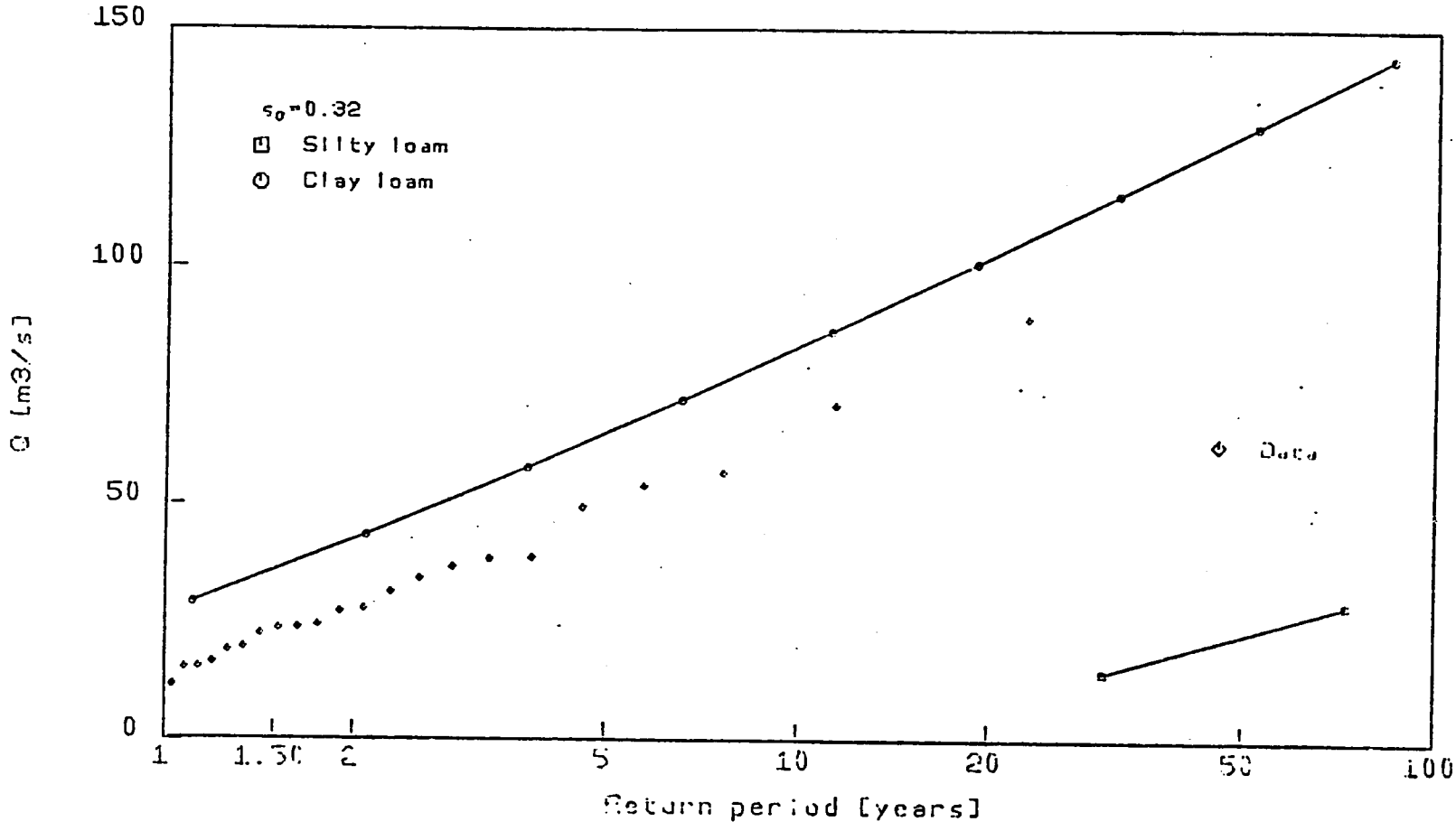

Flood frequency curve

i_r=0.1 cm/hr t_r=34.3hr A=103.6 km² R_L=2.3 L=16.9 km α=1.00 $s^{-1}m^{-1/3}$ m_v=16.

Santa Paula Creek

Figure 4.12

tion. As it can be seen, it is much lower than the observations (obtained from the U.S. Geological Survey, Water Supply Papers), indicating that the soil is so permeable that the produced surface runoff is not enough to match the historical flood peaks. In the same figure, the flood frequency distribution, using clay loam instead of silty loam is plotted, showing a better agreement with the observations. Sensitivity analysis of the soil parameters showed that the more important ones are the saturated permeability K(1) and the pore size distribution index m, which defines the asymptotic infiltration rate capacity, a, whose value is very important in the surface runoff generation (see Figure 3.2).

The wet basin of the Nashua River was the other climate adopted by Eagleson (1978) in his analysis. Specifically, he used the catchment corresponding to the Southern branch of the Nashua River, with an area of 280 km^2, located north of Worcester, Massachusetts. The climatic parameters of this catchment are:

m_i = 0.084 cm/hr

m_{t_r} = 7.7 hr

m_{t_b} = 72 hr

e_p = 0.0063 cm/hr

M ≃ 0.80

k_v = 1.00

m_v = 109

Clay loam was the soil which gave better agreement of the frequency of annual basin yield, and therefore, the long term average soil moisture concentration is calculated by Equation 4.32 as

$$\bar{s}_o = 0.42$$

Unfortunately, this branch of the Nashua River does not have flood records in order to compare the derived distribution. However, the northern branch does, with the characteristic that its area ($277km^2$) is almost the same that the one of the southern branch. To check the hydrologic homogeneity of the two branches, Table 4.3 lists the mean annual discharge for concurrent years. It can be seen that the values are very similar. Therefore, it is assumed that the results of Eagleson's analysis for the southern branch may be adopted in the northern one, whose catchment has the following geomorphologic parameters:

$$R_L = 3$$

$$L_\Omega = 22km$$

The value of α_Ω is assumed to be equal to 1.5 $sec^{-1}m^{-1/3}$.

Figure 4.13 plots the derived flood frequency distribution for the northern branch of the Nashua River. Also plotted are the observations obtained form the U.S. Geological Survey, Water Supply Papers. The derived distribution overestimates the floods for return periods less than ten years; otherwise, it underestimates the floods, but in general terms there is an acceptable agreement between the distribution and the data.

From the two derived frequency distributions, it seems that the results of the annual basin yield do not give the adequate soil parameters to reproduce the observed flood peaks. However, using ecological optimality concepts in the annual water balance, adequate soil parameters may be obtained. Given measures of soil porosity and vegetation canopy density, it is possible to determine the properities of the soil (i.e., hydraulic conductivity and connectivity) and the average soil moisture. This will be presented in the next sub-section.

TABLE 4.3

Mean Annual Discharge for the Sourthern and Northern Branches of the Nashua River (from U.S. Geological Survey, Water Supply Papers)

Year	Southern Branch	Northern Branch
1936	232	226
1937	210	213
1938	293	290
1939	227	214
1940	191	172
1941	113	111
1942	142	137
1943	184	185
1944	133	165
1945	194	201
1946	200	200
1947	155	158
1948	189	187
1950	131	140
1951	109	121
1961	207	209
1962	186	172
1963	177	189
1964	137	153
1965	90	81

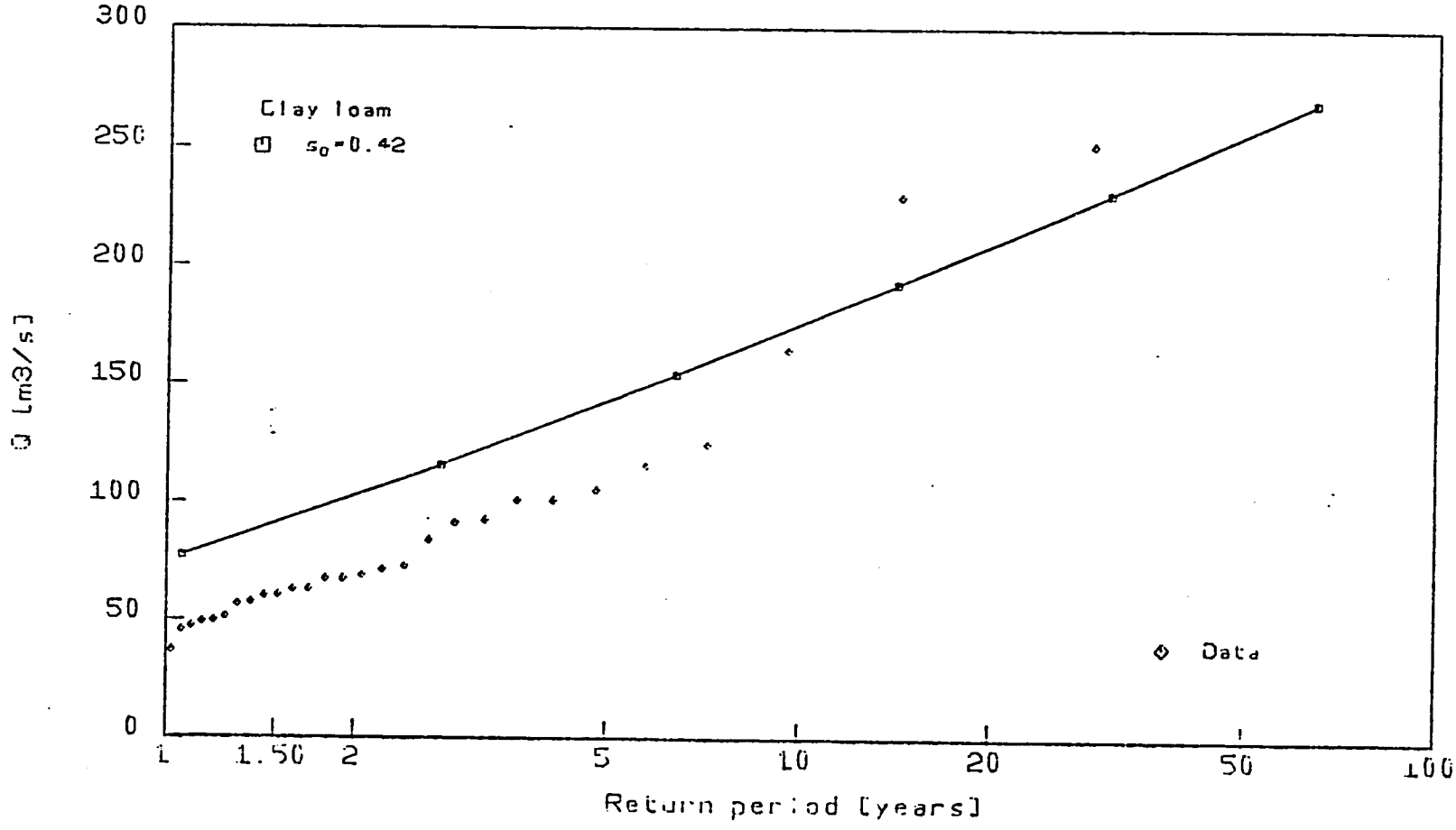

Flood frequency curve

i_p=0.1 cm/hr t_p=7.7 hr A=277.0 km² R_L=3.0 L=22.0 km α=1.50 $s^{-1}m^{1/3}$ m_y=109.

Nashua River Basin

Figure 4.13

4.5.2 Ecological Optimality in Water-Limited Natural Soil-Vegetation Systems

Eagleson (1982) uses his dynamic water balance model (1978) to quantify ecological optimality hypotheses of water-limited natural vegetation systems, concerning their equilibrium with respect to canopy M, species water use k_v, and hydraulic properties of the soil. Two different optimalities may be defined. If water is limiting, short-term ecological pressure will act to minimize water demand stress through adjustment of both canopy density and plant species so that the soil moisture is maximized. On the other hand, a natural soil-vegetation system will develop gradually and synergistically, through vegetation-induced changes in soil structure, toward a set of hydraulic soil properties for which minimum stress canopy density of a given species is maximum in a specified climate. Then, maximization of biomass productivity, $Mk_v \bar{e}_p$, will control the long-term joint development of soil and vegetation.

Combination of the above optimalities determines the climatic climax vegetation canopy density M_o^*, and the species water use coefficient k_v. Also obtained are the saturated permeability, pore disconnectedness index, and the average soil moisture concentration, as a function only of the climate characteristics and the effective porosity of the soil. This is very interesting in the context of the flood frequency distribution, since a prior calculation of the climatic climax parameters by means of the annual water balance model will give the required independent soil parameters [K(1) and c] along with the average initial soil moisture concentration. Eagleson and Tellers (1982) suggest a procedure to compute the climatic climax soil and vegetation properties. When M is known (e.g.,

by remote sensing) it is as follows:

1. Calculate the equilibrium plant coefficient, k_v, as:

$$k_{v_o} = -0.0018 + 2.26M - 6.73M^2 + 15.10M^3 \quad \text{if } M < 0.42 \tag{4.35}$$

$$k_{v_o} = 1 \quad \text{if } M \geq 0.42$$

2. Given the value of the effective porosity n, solve the water balance equation (see Appendix A of Eagleson, 1982) for $\bar{s}_o$ using the following empirical relations:

$$(c-3)\phi_i\ (c,\bar{s}_o) = 0.75 \tag{4.36}$$

$$\phi_i(c,\bar{s}_o) = 1/[5/3 + 0.5(c+1)(1+\bar{s}_o^{\,1.425 - 0.375(c+1)/2})] \tag{4.37}$$

$$k(1) = (0.058/\bar{s}_o)^{c+5} \tag{4.38}$$

where c is the soil pore disconnectedness index and k(1) is the saturated intrinsic permeability of the soil [cm^2]. With this value of $\bar{s}_o$, calculate c and K(1) from Equations 4.36 to 4.38 and evaluate the soil parameters used in Equation 4.26 of the derived flood frequency distribution:

$$m = 2/(c-3) \tag{4.39}$$

$$K(1) = 3x10^8 k(1) \tag{4.40}$$

$$\Psi(1) = 7.45x10^{-2}(n/k(1)\phi) \tag{4.41}$$

where

$$\log_{10}(\phi) = 0.150 + 0.065c + 0.035c^2$$

In the above equations, K(1) is given in cm/hr and $\Psi(1)$ in cm. Eagleson and Tellers (1982) give the climatic climax soil properties

TABLE 4.4

Climate Climax Soil Parameters for Santa Paula and Nashua Catchments:

Parameter	Santa Paula	Nashua
n	0.30	0.35
c	5.15	4.75
k(1), cm^2	14.9×10^{-11}	5.57×10^{-11}
$\bar{s}_o$	0.55	0.72
m	0.93	1.14
K(1), cm/hr	0.044	0.017
$\Psi(1)$, cm	650	1400

[K(1) and c] and the average soil moisture concentration for Santa Paula Creek and Nashua River catchments. The values are listed in Table 4.4, along with m, K(1) and $\Psi(1)$ calculated fro... ...uations 4.39 to 4.41.

4.5.3 Flood Frequency Distribution for Santa Paula and Nashua using Climatic Climax Soil Parameters

Values listed in Table 4.4 may be used to evaluate the flood frequency distributions for Santa Paula Creek and the northern branch of the Nashua River. Figure 4.14 plots the one corresponding to Santa Paula. As it can be seen, the agreement with the observations in remarkable. As an interesting comment, the value of $\bar{s}_o$, given by Equation 4.32 turns out to be 0.56, practically the same value obtained by the ecological optimality. Figure 4.15 shows the flood frequency distribution corresponding to the second river. The agreement is not as good but still satisfactory. Therefore, based on the above results, it is proposed here to evaluate the flood frequency distributions using the climatic climax parameters. The only parameters required, besides the climatic and geomorphologic characteristics, are the vegetation canopy density and the effective soil porosity.

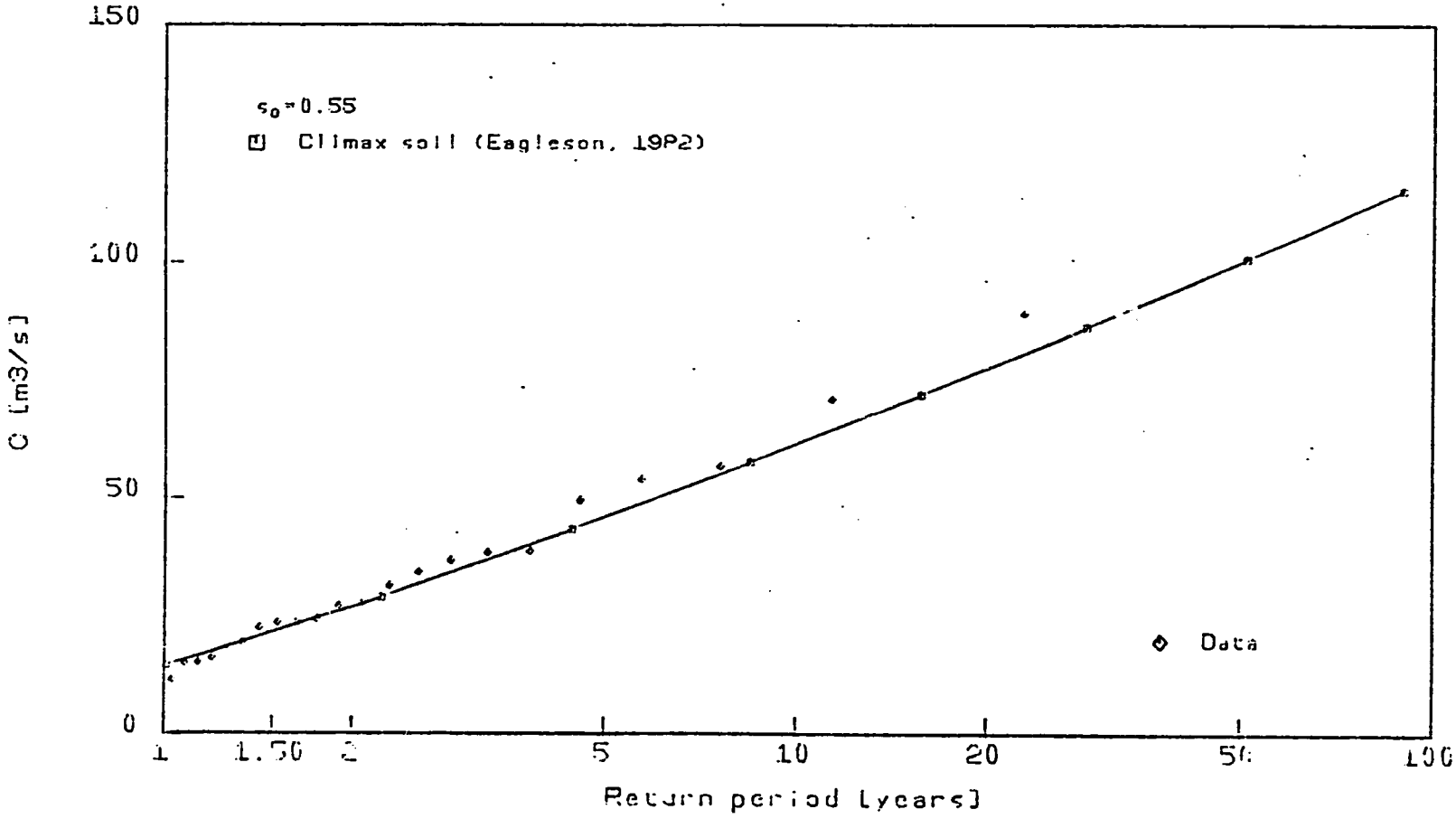

Flood frequency curve

i_p=0.1 cm/hr t_r=34.3hr A=103.6 km² R_L=2.3 L=16.0 km α=1.00 $s^{-1}m^{-1/3}$ n_r=16.

Santa Paula Creek

Figure 4.14

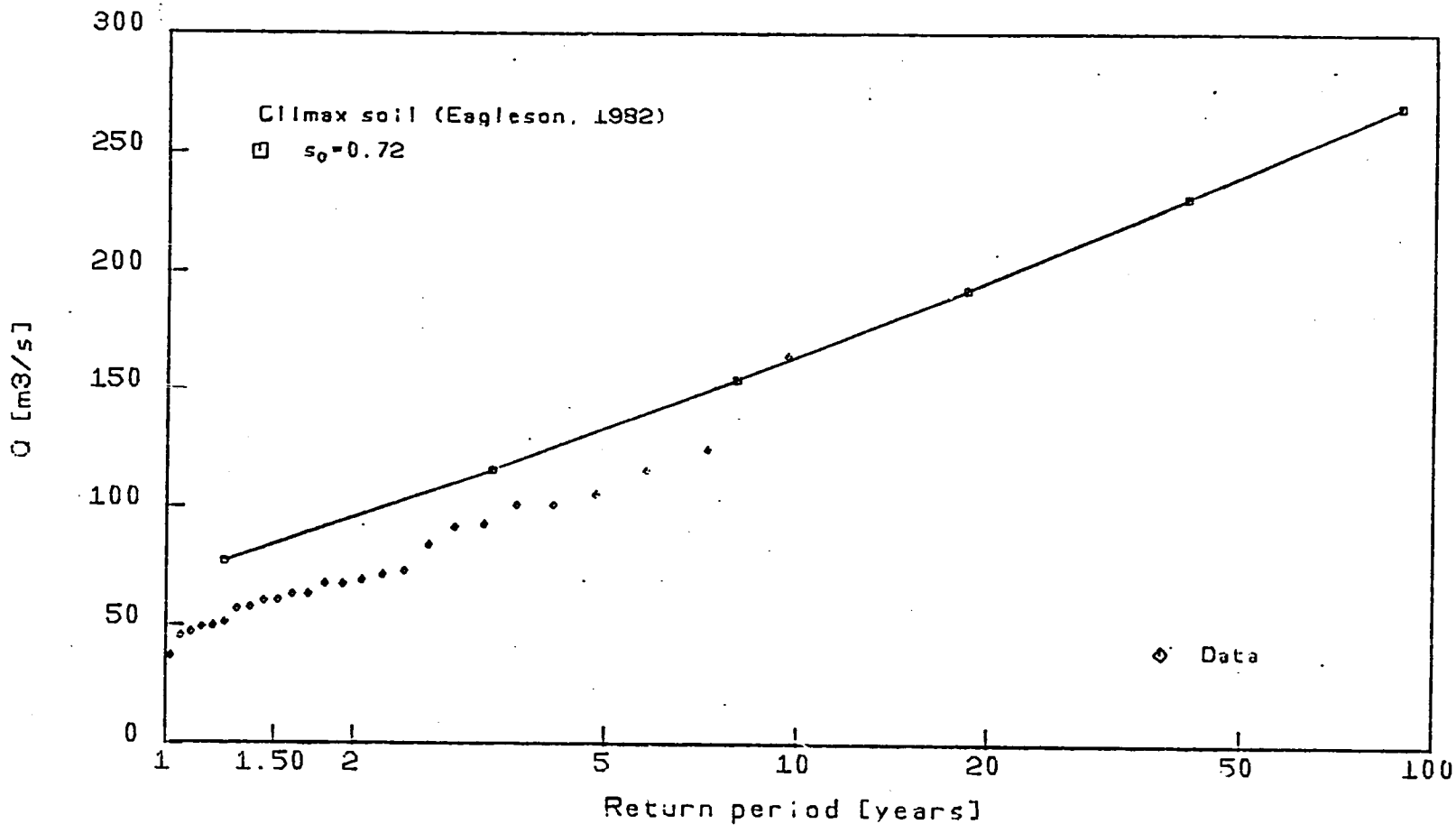

Flood frequency curve

i_r=0.1 cm/hr t_r=7.7 hr A=277.0 km² R_L=3.0 L=22.0 km α=1.50 $s^{-1}m^{-1/3}$ m_y=109.

Nashua River Basin

Figure 4.15

Chapter 5

SUMMARY AND CONCLUSIONS

5.1 Summary and Conclusions

In this work, two flood frequency distributions were derived, using the Geomorphoclimatic Instantaneous Unit Hydrograph as the basis for the rainfall-runoff relationship, along with the previously derived joint distributions of the intensity and duration of the effective rainfall. The first one corresponds to a conceptual model of the infiltration given by an average potential rate, whose determination usually involves information from other basins. The second one uses a physically based model of the infiltration process and it may be adequately calculated using climatic climax soil parameters resulting from ecological optimality concepts at an annual basis. This theoretical distribution, besides being based on physical grounds, may be evaluated for a particular basin with its own climatic and geomorphologic parameters as well as estimates of vegetative canopy density and effective soil porosity. This means that the distribution can be obtained with little or no on-site streamflow records, implying that in principle all regions of the world could be "hydrologically" mapped with reasonable efforts.

REFERENCES

Benjamin, J. R. and Cornell, C. A., Probability, Statistics, and Decision for Civil Engineers, McGraw-Hill Book Company, 1970.

Burkham, D. E., "Depletion of Streamflow by Infiltration in the Main Channels of the Tucson Basin, Southeastern Arizona," U.S. Geological Survey, Water-Supply Paper 1939-B, 1970a.

Burkham, D. E., "A Method for Relating Infiltration Rates to Streamflow Rates in Perched Streams," Geological Survey Research, U.S. Geological Survey, Prof. Paper 700-D, 1970b.

Chan, S. and R. L. Bras, "Derived Distribution of Water Volume Above a Given Threshold Discharge", Technical Report No. 234, Ralph M. Parsons for Water Resources and Hydrodynamics, Massachusetts Institute of Technology, 1978.

Chan, S. and R. L. Bras, "Urban Stormwater Management: Distribution of Flood Volumes," Water Resources Research, 15(2), pp. 371-382, 1979.

Cordova, J. R., and R. L. Bras, "Stochastic Control of Irrigation Systems," Technical Report No. 239, Ralph M. Parsons Laboratory for Water Resources and Hydrodynamics, Massachusetts Institute of Technology, 1979.

Cordova, J. R., and I. Rodriguez-Iturbe, "Geomorphologic Estimation of Extreme Flow Probabilities," accepted for publication Journal of Hydrology, 1982

Dahl, N. J., Non-steady Flow in Open Channels, Series Paper 10, The Royal Veterinary and Agricultural University, Copenhagen, 1981.

Doetsch, G., Introduction to the Theory and Application of the Laplace Transformation, New York, Springer-Verlag, 1961.

Eagleson, P. S., Dynamic Hydrology, McGraw-Hill, New York, 1970.

Eagleson, P. S., Dynamic of Flood Frequency," Water Resources Research 8(4), pp. 878-898, 1972.

Eagleson, P. S., "Climate, Soil and Vegetation 1. Introduction to Water Balance Dynamics," Water Resources Research, 14(5), pp. 705-712, 1978.

Eagleson, P. S., "Climate, Soil and Vegetation 2. The Distribution of Annual Precipitation Derived from Observed Storm Sequences," Water Resources Research, 14(5), pp. 713-721, 1978.

Eagleson, P. S., "Climate, Soil and Vegetation 3. A Simplified Model of Soil Moisture Movement in the Liquid Phase," Water Resources Research, 14(5), pp. 722-730, 1978.

Eagleson, P. S., "Climate, Soil and Vegetation 4. The Expected Value of Annual Evapotranspiration," Water Resources Research, 14(5), pp. 731-739. 1978.

Eagleson, P. S., "Climate, Soil and Vegetation 5. A Derived Distribution of Storm Surface Runoff," Water Resources Research, 14(5), pp. 740-748, 1978.

Eagleson, P. S., "Climate, Soil and Vegetation 6. Dynamics of the Annual Water Balance," Water Resources Research, 14(5), pp. 749-764, 1978.

Eagleson, P. S., "Climate, Soil and Vegetation 7. A Derived Distribution of Annual Water Yield," Water Resources Research, 14(5), pp. 765-776, 1978.

Eagleson, P. S., Water Balance Dynamics-Climate, Soil and Vegetation, MIT Press, in press, 1981.

Eagleson, P. S., "Ecological Optimality in Water-Limited natural soil-vegetation systems, 1. Theory and hypothesis," Water Resources Research, 18(2), pp. 325-340, 1982.

Eagleson, P. S. and T. E. Tellers, "Ecological Optimality in water-limited natural soil-vegetation systems, 2. Tests and Applications," Water Resources Research, 18(2), pp. 341-354, 1982.

Freeman, H., Introduction to Statistical Inference, Addison-Wesley Publishing Company, Incorporated, 1963.

Grace, R. A. and P. S. Eagleson, "The Synthesis of Short-time-increment rainfall sequences," Technical Report No. 91, Ralph M. Parsons Laboratory for Water Resources and Hydrodynamics, Massachusetts Institute of Technology, 1966.

Grayman, W. M. and P.S. Eagleson, "Streamflow Record length for Modelling Catchment Dynamics," Technical Report No. 114, Ralph M. Parsons Laboratory for Water Resources and Hydrodynamics, Massachusetts Institute of Technology, 1969.

Gupta, V. K., E. Waymire and C. T. Wang, "A Representation of an Instantaneous Unit Hydrograph from Geomorphology, "Water Resources Research, 16(5), pp. 855-862, 1980.

Harley, B. M., "Linear Routing in Uniform Open Channels," M. Eng. Science Thesis, Department of Civil Engineering, National University of Ireland, 1967.

Hebson, C. and E. Wood, "A Derived Flood Frequency Distribution, Water Resources Research, (18)5, pp. 1509-1518, 1982.

Henderson, F. M., "Some Properties of the Unit Hydrodraph," Journal of Geophys. Research, 68(16), pp. 4785-4793, 1963.

Horton, R. E., "Erosional Development of Streams and Their Drainage Basin, Hydrophysical Approach to Quantitative Morphology," Bulletin of the Geological Society of America, 56, pp. 275-370, 1945.

International Mathematical and Statistical Libraries, Incorporated, "IMSL Library," Edition 8, 1980.

Kirshen, D. M. and R. L. Bras, "The Linear Channel and Its Effect on the Geomorphologic IUH," Technical Report No. 277, Ralph M. Parsons Laboratory for Water Resources and Hydrodynamics, Massachusetts Institute of Technology, 1982.

Linsley, R. K., M. A. Kohler, and J. L. Paulhus, Hydrology for Engineers, Third ed., McGraw-Hill Book Company, 1982.

O'Meara, B. E., "Linear Routing of Lateral Inflow in Uniform Open Channels," M. Eng. Science Thesis, Department of Civil Engineering, National University of Ireland, 1968.

Philip, J. R., "General Method of Exact Solution of the Concentration Dependent diffusion Equation, "Aust. J. Phys., 13(1), pp. 1-12, 1960.

Pilgrim, P. H., "Isocrones of Travel Time and Distribution of Flood storage from a Tracer Study on a small watershed," Water Resources Research, 13(3), pp. 587-595, 1977.

Restrepo-Posada, P. J. and P. S. Eagleson, "Identification of Independent Rainstorms," Journal of Hydrology, Vol. 55, pp. 303-319, 1982.

Rodriguez-Iturbe., I., and J. B. Valdes, "The Geomorphologic Structure of Hydrologic Response," Water Resources Research, 15(5), pp. 1409- 1420, 1979.

Rodriguez-Iturbe, I., G. Devoto and J. B. Valdes, "Discharge Response Analysis and Hydrologic Similarity: The Interrelation Between the Geomorphologic IUH and the Storm characteristics," Water Resources Research, 15(6), pp. 1435-1444, 1979.

Rodriguez-Iturbe, I., M. Gonzalez and R. L. Bras, "A Geomorphoclimatic Theory of the Instantaneous Unit Hydrograph," Water Resources Research, 18(4), pp. 877-886, 1982.

Schumm, S. A., "Evolution of Drainage Systems and Slopes in Badlands at Perth Amboy, New Jersey, "Geol. Soc. Amer. Bull., 67, pp. 597-646, 1956.

Strahler, A. N., "Quantitative Analysis of Watershed Geomorphology," Transactions, American Geophysical Union, 38(6), pp. 913-920, 1957.

U. S. Weather Bureau, "Rainfall Intensity-Frequency Regime," 1-5, Tech. Pap. 29, Washington, D. C., 1957-60.

Valdes, J. B., Y. Fiallo, and I. Rodriguez-Iturbe, "Rainfall-Runoff Analysis of the Geomorphologic IUH," Water Resources Research, 15(6), pp. 1421-1434, 1979.

APPENDIX A

A FITTED PROBABILITY DENSITY FUNCTION FOR THE INITIAL SOIL MOISTURE CONCENTRATION

A.1 Conservation of Water Mass Equation

In the short term, the equation of conservation of water for an homogeneous soil, considering a layer of characteristic depth Z may be written as:

$$nZ \frac{\partial s}{\partial t} = i_r - e_T - r_s - p \tag{A.1}$$

where,

s = effective soil moisture saturation

n = effective soil porosity

e_T = actual rate of evapotranspiration

r_s = rate of surface runoff

p = rate of percolation

In general, the right hand side terms are function of time, and then,

$$\frac{ds}{dt} = \frac{1}{nZ} [i_r(t) - e_T(t) - r_s(t) - p(t)] \tag{A.2}$$

Integrating,

$$\int ds = \frac{1}{nZ} \int [i_r(t) - e_T(t) - r_s(t) - p(t)]dt \tag{A.3}$$

Therefore, in order to describe the soil moisture concentration, models for the different water balance components are needed. First, and recalling the representation of the rainfall event used in this work, the intensity is assumed to be constant during the duration of the storm. On the other hand, the infiltration and exfiltration models proposed by

Eagleson (1978) are adopted here to evaluate $e_T(t)$ and $r_s(t)$. Finally, percolation is assum' constant throughtout the duration of the event (infiltration or exfiltration), although its magnitude is determined by the initial soil moisture of the corresponding event.

A.2 Rainfall Event Case

The representation of the components of the water balance during a rainfall event are as follows:

Precipitation: rectangular pulse of constant intensity i_r and duration t_r.

Evapotranspiration: no evapotranspiration.

Surface runoff: defined as the substraction of the infiltration rate capacity from the rainfall intensity. The infiltration rate capacity is defined as (Eagleson, 1978)

$$f_1^*(t) = \frac{1}{2} S_i t^{-\frac{1}{2}} + a \qquad (A.4)$$

where

$$S_i = 2(1-s_o)\{[5nK(1)\Psi(1)\phi_i(d,s_o)]/3m\Pi\}$$

$$a = K(1)(1+s_o^c)/2 - w,$$

where all the above parameters have been described in Section 6.4 and s_o is the initial constant value of the degree of saturation for the infiltration process. Figure 3.1 illustrates this process.

Percolation: defined as $K(1)s_o^c$ according to Eagleson (1978).

After integration of Equation A.3, the following expression is obtained:

$$s_1^{(j)} = s_o^{(j)} + [i_r t_r - K(1)s_o^{(j)c} t_r]/nZ, \qquad 0 \leq t_r \leq t_o$$

$$s_1^{(j)} = s_o^{(j)} + [i_r t_o + S_i(t_r^{\frac{1}{2}} - t_o^{\frac{1}{2}}) + a\,(t_r - t_o) - K(1)s_o^{(j)c} t_r]/nZ \quad t_r > t_o \qquad (A.5)$$

where s_1 is the final value of the degree of saturation for the infiltration process, the superscript j is a relative index of the location of the event in time, and t_o is the time from the beginning of the storm when surface runoff begins to be produced, expressed as:

$$t_o = S_i^2/2(i_r-a)^2 \tag{A.6}$$

A.3 Exfiltration Event Case

The representation of the components of the water balance during an interstorm period are:

Precipitation: no precipitation

Evapotranspiration: the potential rate of evaporation $e_p(t)$ is replaced by its long-term average value $\bar{e}_p$. Extending the infiltration equation of Philip, Eagleson (1978) has represented the exfiltration rate capacity by

$$f_e^*(t) = \frac{1}{2} S_e t^{-\frac{1}{2}} + a_e \tag{A.7}$$

where

$$S_e = 2s_1^{1+d/2}[nK(1)\Psi(1)\phi_e(d)/m\Pi]^{\frac{1}{2}}$$

$$a_e = w - Mk_v \bar{e}_p$$

where S_e is the exfiltration desorptivity, a_e is the asymptotic exfiltration capacity, $\phi_e(d)$ is the dimensionless desorption diffusivity of soil, d is the diffusivity index of soil, M is the vegetated fraction of surface, k_v is the ratio of potential rate of transpiration and soil surface evaporation, and s_1 is the initial value of the degree of satura-

tion of the soil for the exfiltration process. When the exfiltration rate capacity is greater than $\bar{e}_p$, the rate of evapotranspiration is assumed to be equal to this limiting potential value; otherwise, it will be equal to the former. Figure A.1 illustrates the above process.

Surface Runoff: no surface runoff.

Percolation: defined in the same manner as for the rainfall event case.

After integration of Equation A.3, with the water balance components defined above, the final value of the degree of saturation for the exfiltration process is:

$$s_o^{(j+1)} = s_1^{(j)} - [\bar{e}_p t_b + K(1) s_1^{(j)c} t_b]/nZ, \qquad 0 \leq t_b \leq t_e$$

$$s_o^{(j+1)} = s_1^{(j)} - [\bar{e}_p t_b + S_e(t_b^{\frac{1}{2}} - t_e^{\frac{1}{2}}) + a_e(t_b - t_e) + K(1) s_1^{(j)c} t_b]/nZ, \qquad t_b > t_e \tag{A.8}$$

where S_e is a function of $s_1^{(j)}$, t_b is the duration of the interstorm period and t_e is the time from the beginning of this period when the soil begins to govern the exfiltration process, which may be expressed as:

$$t_e = \frac{S_e^2}{2\bar{e}_p^2(1+Mk_v-w/\bar{e}_p)}\left[1 - M + \frac{M^2k_v+(1-M)w/\bar{e}_p}{2(1+Mk_v-w/\bar{e}_p)}\right] \tag{A.9}$$

A.4 The Distribution of s_o

In Equation A.5 and A.8, the independent variables involved are i_r, t_r, and t_b. All these three variables may be represented adequately by exponential distributions, i.e.,

$$f_{I_r}(i_r) = \beta e^{-\beta i_r}, \qquad i_r > 0, \quad \beta > 0 \tag{A.10}$$

$$f_{T_r}(i_r) = \delta e^{-\delta t_r}, \qquad t_r > 0, \quad \delta > 0 \tag{A.11}$$

$$f_{T_b}(t_b) = \gamma e^{-\gamma t_b}, \qquad t_b > 0, \quad \gamma > 0 \tag{A.12}$$

Therefore, in principle, one could derive the PDFs of s_o and s_1 from the mentioned equations and the above distributions. However, the infiltration and exfiltration are interdependent Markov process which make the mathematics untractable.

A Monte Carlo approach is taken here. A distribution is fitted to the results of enough simulations experiments, based in Equations A.5 and A.8 for different combinations of climate and type of soil. The simulation procedure is as follows: given a climate and soil, (1) for j=1 assume an initial value of $s_o^{(j)}$; (2) generate, using an exponential pseudo-random number algorithm, a value of i_r and t_r; (3) using Equation A.5 calculate the soil saturation at the end of the storm event $s_1^{(j)}$;(4) generate a value of t_b with the previous pseudo-random number algorithm and calculate, by means of Equation A.8 and $s_1^{(j)}$ of step 3, the final value of the degree of saturation for the exfiltration process, which is equivalent to the initial value of soil moisture for the next infiltration event s_o^{j+1}, (5) go step 2 and continue until j=N, where N is defined a priori.

Before the distribution is chosen, it is required to specify the magnitude of Z, the depth of the layer of soil considered in the conservation of mass (see Equation A.1). In this work, it is assumed that Z is a measure of the penetration depth of the wet and dry fronts during

storm and interstorm periods respectively. This penetration depth has two components (Eagleson, 1978): a diffusive component z_1 given by

$$z_1 = 4(Dt)^{\frac{1}{2}}$$

and a gravitational seepage component z_2, given by the product of seepage velocity and time. The appropriate soil moisture saturation for the evaluation of this seepage velocity is that at the initial soil moisture saturation, s, i.e.,

$$z_2 = \frac{K(s)}{n}t \tag{A.13}$$

Consequently, Z is given by:

$$Z = z_1+z_2 = 4(Dt)^{\frac{1}{2}} + K(s)t/n \tag{A.13}$$

where n is the effective soil porosity. For a storm event, the characteristic time is the storm duration t_r and $D=D_i$, the sorption diffusitivity. In the case of an interstorm period, the characteristic time becomes the interstorm duration t_b and $D=D_e$, the desorption diffusivity. Since t_r and t_b are random variables, Z is also a random variable, whose distribution can be derived using the procedure explained in Section 5.2. However, the interest here is not its PDF but a representative value to perform the simulations, and the most adequate is its expected value, which turns to be for infiltration:

$$Z_i = E[z_1+z_2] = 4\Gamma(1.5)(\bar{D}_i/\beta)^{\frac{1}{2}} + K(\bar{s}_o)/\beta n \tag{A.14}$$

and

$$Z_e = E[z_1+z_2] = 4\Gamma(1.5)(\bar{D}_e/\delta)^{\frac{1}{2}} + K(\bar{s}_o)/\delta n \tag{A.15}$$

where $\bar{D}_i$ and $\bar{D}_e$ are the sorption and desorption diffusivities evaluated at the mean value of the soil moisture concentration $\bar{s}_o$:

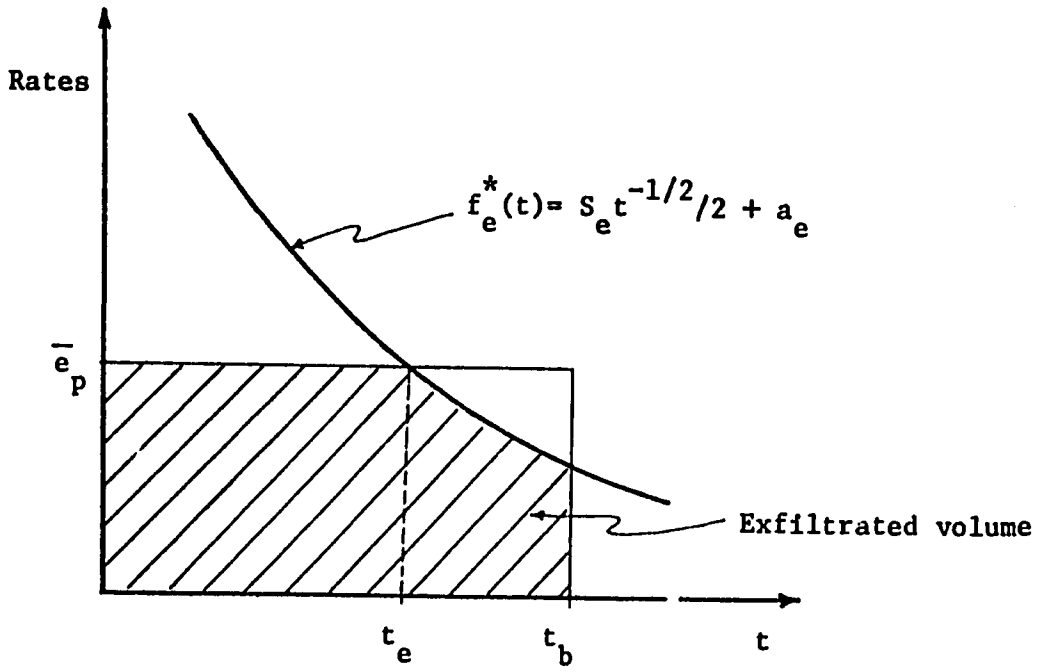

Representation of the exfiltration process

Figure A.1

$$\bar{D}_i = 5K(1)\Psi(1)\phi_i(d,\bar{s}_o)/3mn$$

$$\bar{D}_e = K(1)\Psi(1)s_o^d\,\phi_e(d)/mn$$

The value of Z used in Equations A.5 and A.8 will be the biggest between Z_i and Z_e, which can be evaluated only if $\bar{s}_o$ is known before the simulation. However, it is not, and therefore a trial and error simulation procedure is required: (1) pick a value of $\bar{s}_o$; (2) evaluate Z_i and Z_e using Equations A.14 and A.15 and choose $Z = \max\{Z_i, Z_e\}$; (3) perform the simulation according to the procedure outlined before and compute $\bar{s}_o$; (4) compare this value with the one used in step 2; if they are different, modify $\bar{s}_o$ properly and go to step 2, otherwise terminate the procedure keeping the simulated values of $s_o^{(j)}$.

For the present case, the best distribution to be fitted is a beta distribution, since it is simple and very flexible, and is limited in its basic form for values between 0 and 1, the same range over which soil moisture concentration may vary. This distribution is defined as:

$$f_S(s_o) = \frac{1}{B}\, s_o^{r-1}(1-s_o)^{t-r-1}$$
$$0 \leq s_o \leq 1\,, \quad r < t \tag{A.16}$$

where

$$t = \bar{s}_o(1-\bar{s}_o)/\sigma_s^2 - 1 \tag{A.17}$$

$$r = \bar{s}_o^{-2}(1-\bar{s}_o)/\sigma_s^2 - 1 \tag{A.18}$$

$$B = \frac{\Gamma(\Gamma)\Gamma(t-r)}{\Gamma(t)} \tag{A.19}$$

in which $\bar{s}_o$ is the mean of the initial soil moisture concentration and σ_s is its variance.

Figure A.2 presents the distribution of the initial soil moisture concentration resulting from the simulations and the corresponding fitted beta distribution. For each case all the climatic and soil characteristics information is given, as well as the values of Z, $\bar{s}_o$, σ_s, t and r. The number of generated values of s_o in each simulation was 2000, and basically, the results are independent of the initial value of $s_o^{(1)}$. The units used here are hours for time and centimeters for length. The simulations cover a wide range of climates: from the wet tropical climate of Santa Rita, Colombia, to the arid climates of Santa Paula, California, and Sudan; they include also typical climates for the northeastern region of the United States. These climates were combined with different types of soil (Eagleson, 1978), i.e., silty loam, clay loam, sandy loam and clay, with the purpose of obtaining "general" expressions for $\bar{s}_o$ and σ_s from regression analyses, which are:

$$\bar{s}_o = 0.2761\ \bar{t}_r/\bar{t}_b + 0.02628\ln[\bar{i}_r/(1-M+Mk_v)\bar{e}_p] + 0.3767[\Psi(1)n/\bar{t}_b K(1)m]^{1/6} - 0.15 \qquad (A.19)$$

with a coefficient of determination R^2 of 0.94, and,

$$\sigma_s = 0.0753\bar{i}_r^{\frac{1}{2}} - 0.0094\bar{t}_r + 0.0816\bar{t}_b^{-\frac{1}{2}} + 7.50\bar{e}_p - 0.0915n - 0.00095K(1) + 0.838/\ln[\Psi(1)] + 0.0555m^{\frac{1}{2}} + 0.3858 \qquad (A.20)$$

with R^2 equal to 0.61.

Using the above two equations, the parameters of the beta distribution can be fitted by means of Equations A.17 and A.18.

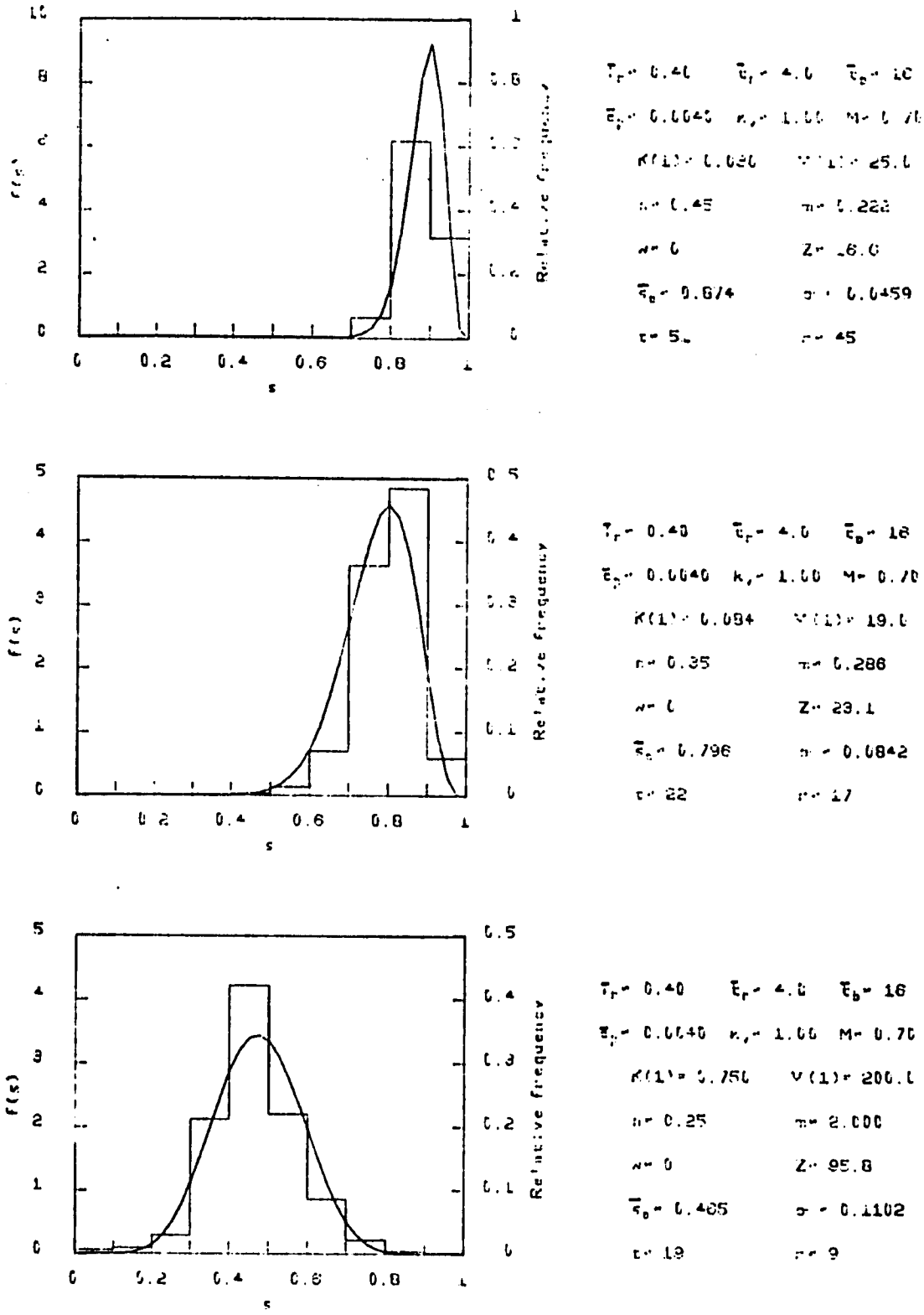

Figure A.2 Initial soil moisture distribution from simulation

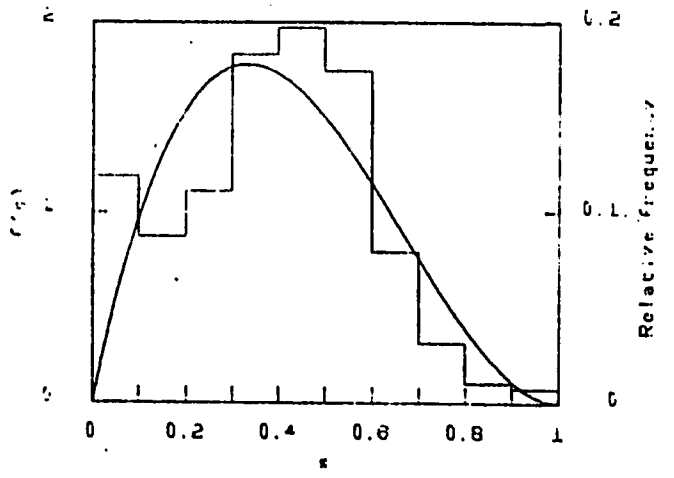

$\bar{T}_r$ = 0.10 $\bar{t}_r$ = 34.3 $\bar{t}_b$ = 250

$\bar{\varepsilon}_p$ = 0.0111 k_r = 1.00 M = 0.70

K(1) = 0.094 V(1) = 19.0

n = 0.35 m = 0.298

w = 0 Z = 49.1

$\bar{\varepsilon}_o$ = 0.383 σ = 0.2037

c = 5 r = 2

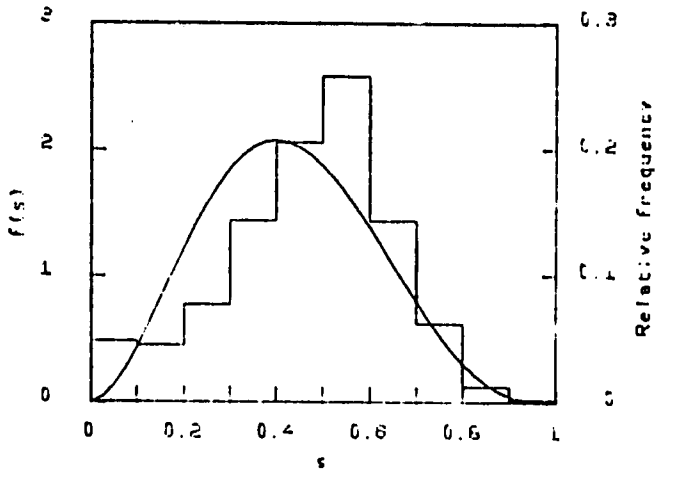

$\bar{T}_r$ = 0.10 $\bar{t}_r$ = 34.3 $\bar{t}_b$ = 250

$\bar{\varepsilon}_p$ = 0.0110 k_r = 1.00 M = 0.70

K(1) = 0.030 V(1) = 25.0

n = 0.45 m = 0.222

w = 0 Z = 33.7

$\bar{\varepsilon}_o$ = 0.464 σ = 0.1804

c = 7 r = 3

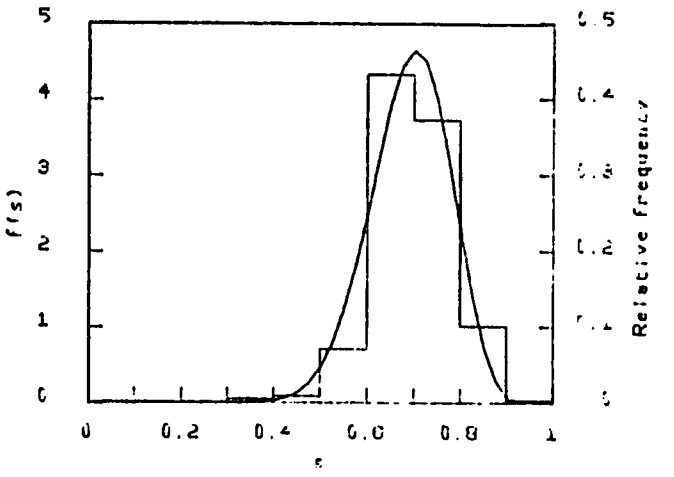

$\bar{T}_r$ = 0.40 $\bar{t}_r$ = 4.0 $\bar{t}_b$ = 16

$\bar{\varepsilon}_p$ = 0.0040 k_r = 1.00 M = 0.70

K(1) = 0.360 V(1) = 166.0

n = 0.35 m = 0.687

w = 0 Z = 93.8

$\bar{\varepsilon}_o$ = 0.696 σ = 0.0892

c = 20 r = 20

Figure A.2 (Continuation)

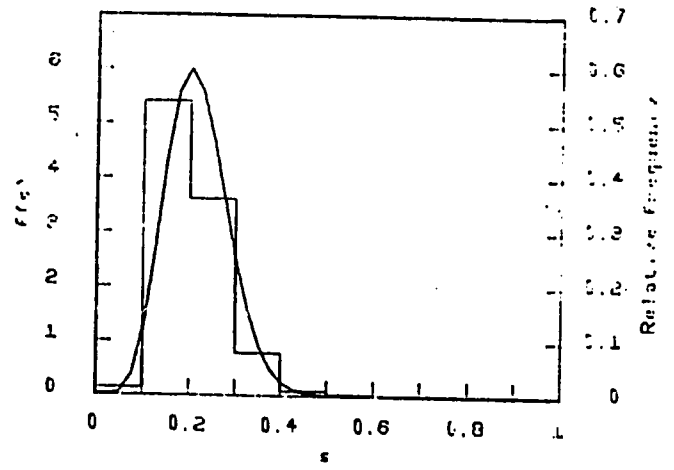

$\bar{T}_r$= 0.09 $\bar{t}_r$= 7.7 $\bar{t}_s$= 72

$\bar{t}_p$= 0.0500 κ_r= 1.00 M= 0.70

K(1)= 0.750 V(1)= 200.0

n= 0.25 m= 2.000

w= 0 Z= 116.6

$\bar{s}_o$= 0.202 σ = 0.0650

c= 37 r= 8

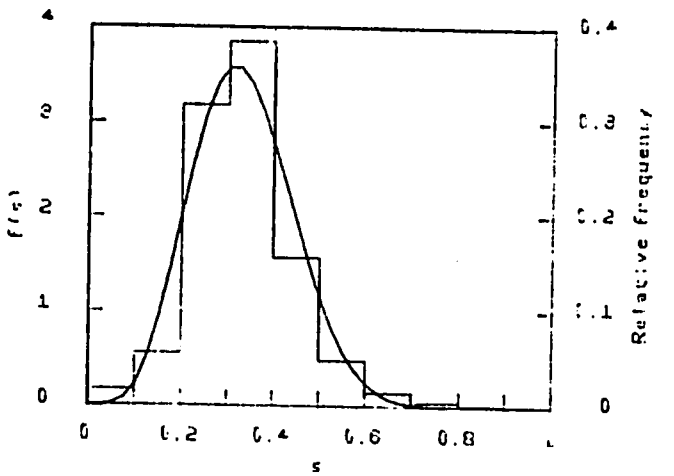

$\bar{T}_r$= 0.10 $\bar{t}_r$= 34.3 $\bar{t}_s$= 250

$\bar{t}_p$= 0.0110 κ_r= 1.00 M= 0.70

K(1)= 0.360 V(1)= 166.5

n= 0.35 m= 0.667

w= 0 Z= 219.2

$\bar{s}_o$= 0.332 σ = 0.1326

c= 19 r= 6

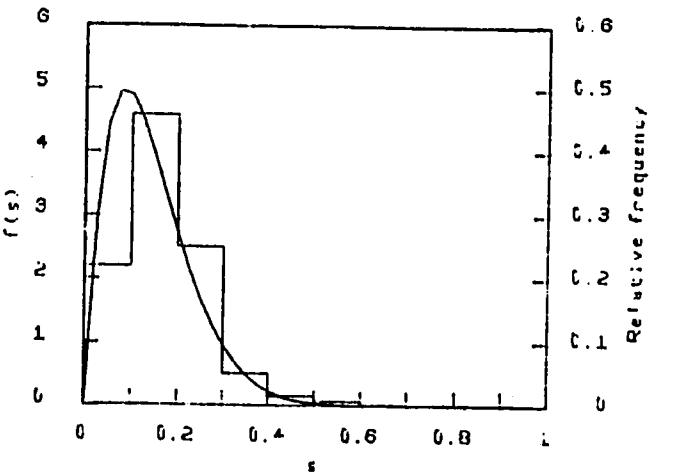

$\bar{T}_r$= 0.10 $\bar{t}_r$= 34.2 $\bar{t}_s$= 250

$\bar{t}_p$= 0.0110 κ_r= 1.00 M= 0.70

K(1)= 0.750 V(1)= 200.0

n= 0.25 m= 2.000

w= 0 Z= 243.4

$\bar{s}_o$= 0.169 σ = 0.0955

c= 14 r= 2

Figure A.2 (Continuation)

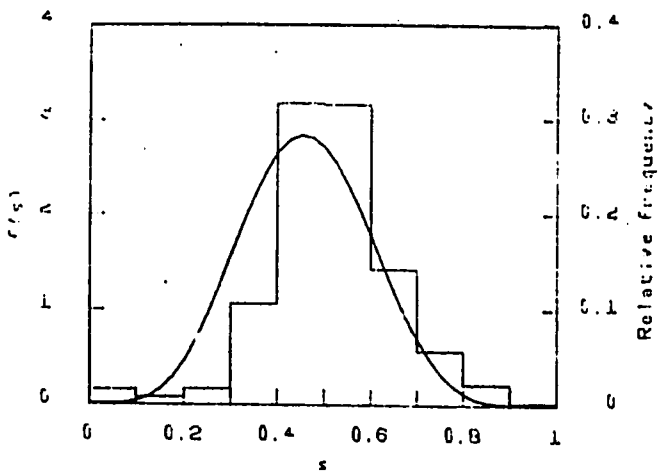

$\bar{T}_p$= 0.01 $\bar{t}_r$= 7.7 $\bar{t}_b$= 72

$\bar{\varepsilon}_p$= 0.0060 κ_1= 1.00 M= 0.70

K(1)= 0.384 V(1)= 19.0

n= 0.35 m= 0.258

w= 0 Z= 25.2

$\bar{s}_0$= 0.512 σ = 0.1357

t= 13 r= 6

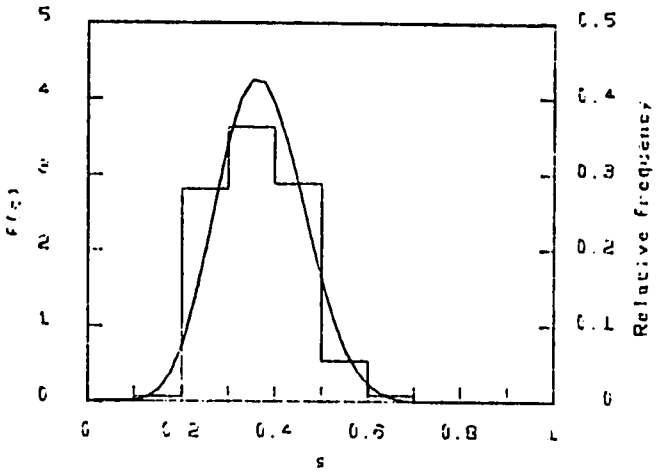

$\bar{T}_p$= 0.09 $\bar{t}_r$= 7.7 $\bar{t}_b$= 72

$\bar{\varepsilon}_p$= 0.0060 κ_1= 1.00 M= 0.70

K(1)= 0.360 V(1)= 186.0

n= 0.35 m= 0.607

w= 0 Z= 106.1

$\bar{s}_0$= 0.363 σ = 0.0904

t= 27 r= 10

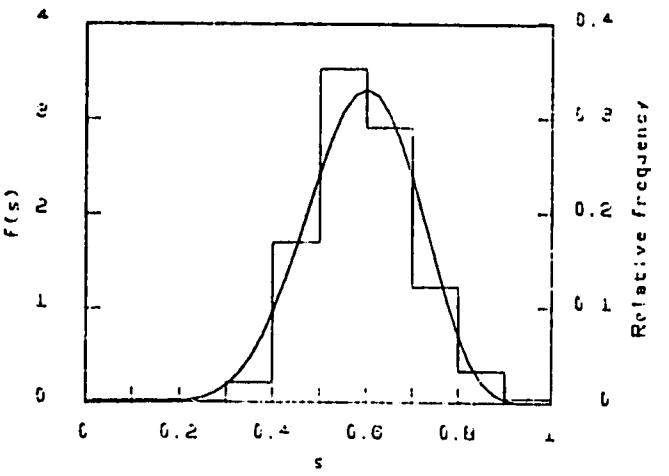

$\bar{T}_p$= 0.09 $\bar{t}_r$= 7.7 $\bar{t}_b$= 72

$\bar{\varepsilon}_p$= 0.0060 κ_1= 1.00 M= 0.70

K(1)= 0.630 V(1)= 25.0

n= 0.45 m= 0.222

w= 0 Z= 17.7

$\bar{s}_0$= 0.591 σ = 0.1149

t= 17 r= 10

Figure A.2 (Continuation)

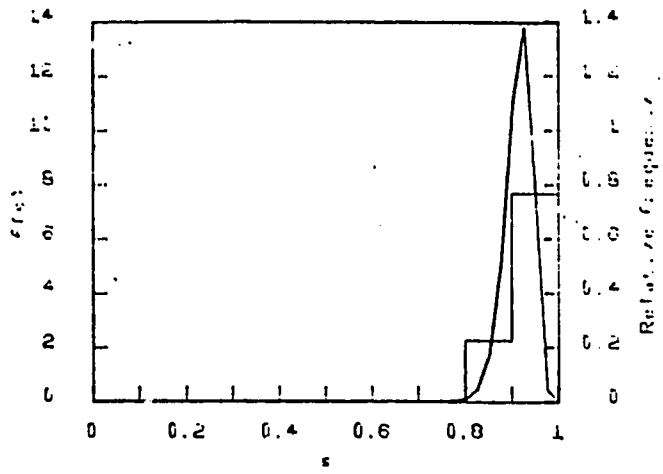

$\bar{T}_p$= 1.00 $\bar{t}_r$= 2.1 $\bar{t}_b$= 8

$\bar{\varepsilon}_p$= 0.0051 κ_1= 1.11 M= 0.71

K(1)= 0.030 V(1)= 25.0

κ= 0.45 m= 0.222

w= 0 Z= 12.5

$\bar{s}_g$= 0.919 σ = 0.0286

t= 91 r= 63

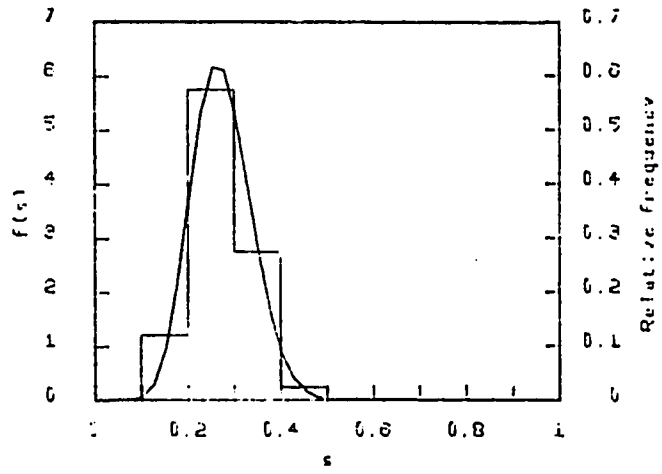

$\bar{T}_p$= 0.20 $\bar{t}_r$= 0.8 $\bar{t}_b$= 12

$\bar{\varepsilon}_p$= 0.0050 κ_1= 1.20 M= 0.70

K(1)= 0.750 V(1)= 200.0

κ= 0.25 m= 2.000

w= 0 Z= 36.6

$\bar{s}_g$= 0.274 σ = 0.0637

t= 48 r= 13

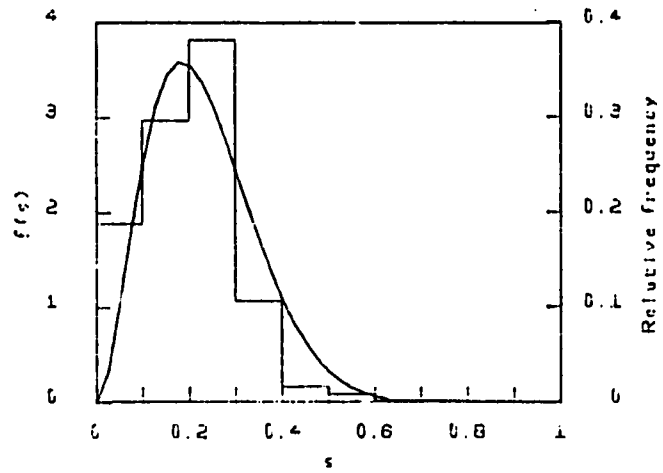

$\bar{T}_p$= 1.00 $\bar{t}_r$= 1.5 $\bar{t}_b$= 15

$\bar{\varepsilon}_p$= 0.0050 κ_1= 1.00 M= 0.70

K(1)= 10.000 V(1)= 25.0

κ= 0.27 m= 1.500

w= 0 Z= 72.7

$\bar{s}_g$= 0.195 σ = 0.1062

t= 13 r= 3

Figure A.2 (Continuation)

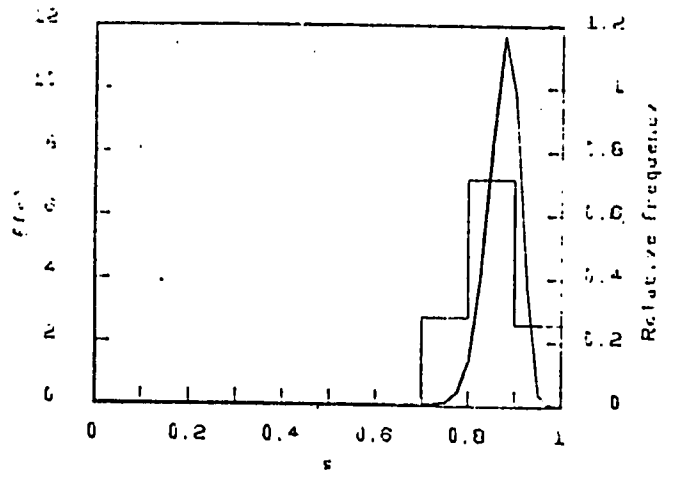

$\bar{T}_r$= 3.00 $\bar{t}_r$= 2.0 $\bar{t}_b$= 3

$\bar{\epsilon}_p$= 0.0050 K_t= 1.10 M= 0.70

K(1)= 0.260 V(1)= 160.0

n= 0.25 m= 0.667

w= 0 Z= 75.1

$\bar{s}_s$= 0.875 σ = 0.0340

t= 94 r= 82

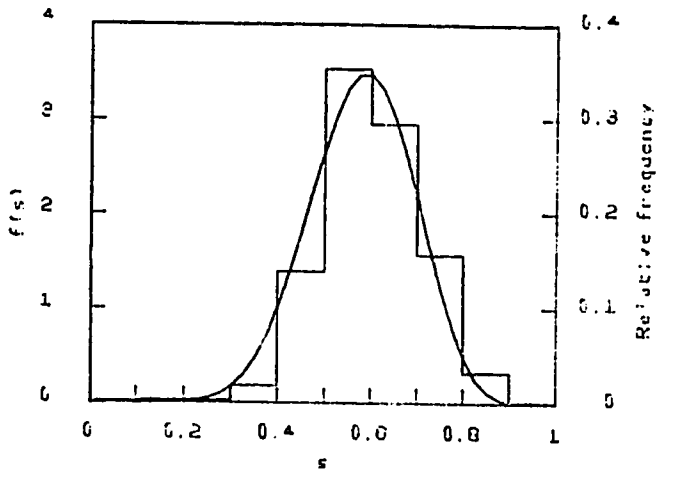

$\bar{T}_r$= 1.00 $\bar{t}_r$= 2.0 $\bar{t}_b$= 6

$\bar{\epsilon}_p$= 0.0050 K_t= 1.00 M= 0.70

K(1)= 0.750 V(1)= 200.0

n= 0.25 m= 2.000

w= 0 Z= 72.4

$\bar{s}_s$= 0.801 σ = 0.1098

t= 19 r= 11

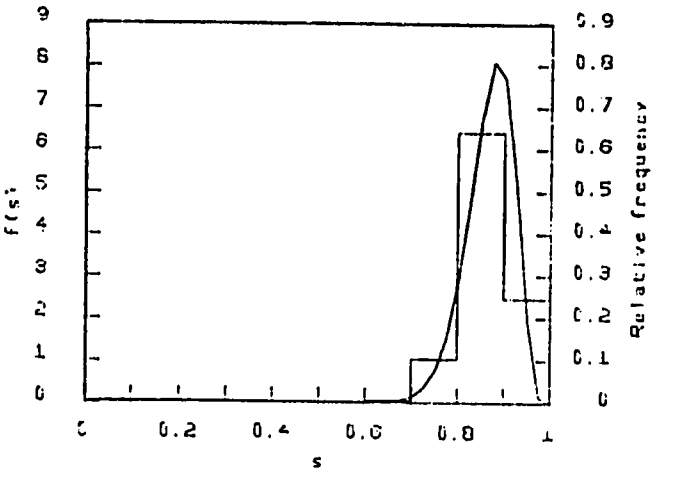

$\bar{T}_r$= 1.00 $\bar{t}_r$= 2.0 $\bar{t}_b$= 6

$\bar{\epsilon}_p$= 0.0050 K_t= 1.00 M= 0.70

K(1)= 0.683 V(1)= 19.0

n= 0.35 m= 0.286

w= 0 Z= 17.5

$\bar{s}_s$= 0.863 σ = 0.0508

t= 45 r= 39

Figure A.2 (Continuation)

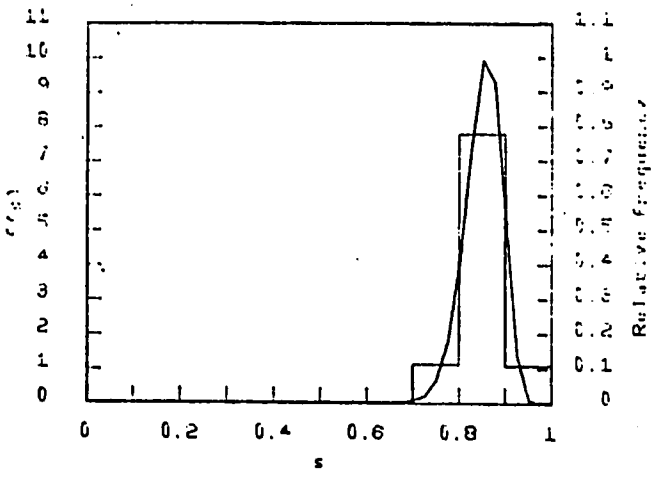

$\bar{T}_r$= 1.00 $\bar{t}_r$= 1.0 $\bar{t}_b$= 5

$\bar{a}_p$= 0.0020 k_v= 1.00 M= 0.70

K(1)= 0.360 V(1)= 166.0

n= 0.35 m= 1.200

w= 0 Z= 73.8

$\bar{s}_b$= 0.649 σ = 0.0398

t= 90 r= 68

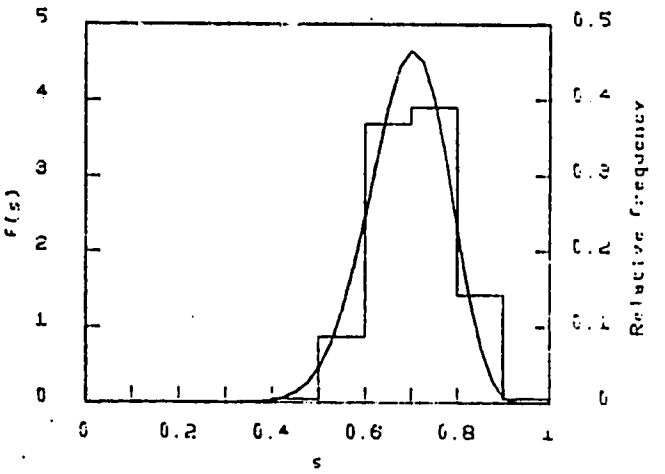

$\bar{T}_r$= 1.00 $\bar{t}_r$= 1.0 $\bar{t}_b$= 5

$\bar{a}_p$= 0.0030 k_v= 1.00 M= 0.70

K(1)= 0.360 V(1)= 166.0

n= 0.35 m= 1.200

w= 0 Z= 96.2

$\bar{s}_b$= 0.710 σ = 0.0833

t= 29 r= 20

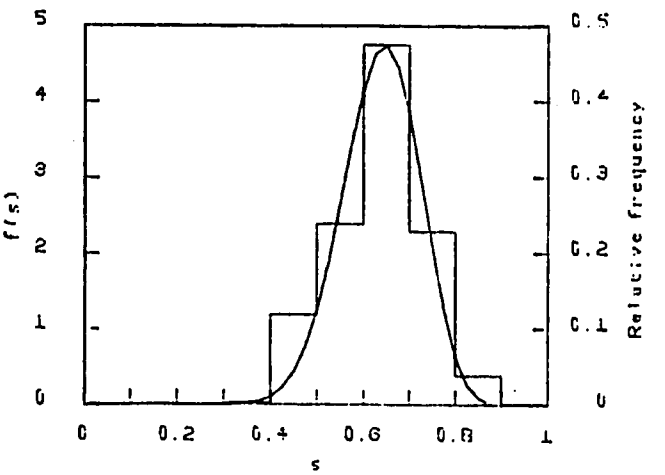

$\bar{T}_r$= 1.00 $\bar{t}_r$= 1.0 $\bar{t}_b$= 12

$\bar{a}_p$= 0.0050 k_v= 1.10 M= 0.70

K(1)= 0.360 V(1)= 166.0

n= 0.35 m= 0.667

w= 0 Z= 45.6

$\bar{s}_b$= 0.653 σ = 0.0822

t= 33 r= 21

Figure A.2 (Continuation)

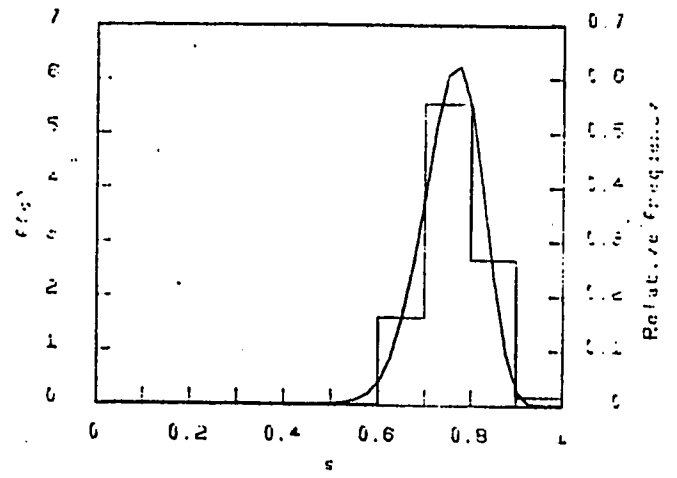

$\bar{T}_r$= 1.00 $\bar{t}_r$= 1.0 $\bar{t}_b$= 5

$\bar{e}_p$= 0.0035 k_y= 1.00 M= 0.7[illegible]

K(1)= 0.400 Y(1)= 100.0

n= 0.35 m= 0.667

w= 0 Z= 51.7

$\bar{s}_b$= 0.762 σ = 0.0820

t= 45 r= 34

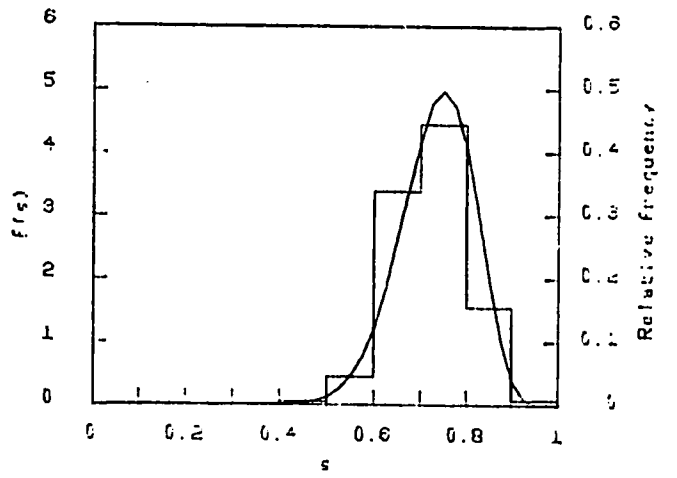

$\bar{T}_r$= 1.00 $\bar{t}_r$= 1.0 $\bar{t}_b$= 5

$\bar{e}_p$= 0.0030 k_y= 1.00 M= 0.70

K(1)= 0.360 Y(1)= 50.0

n= 0.35 m= 0.667

w= 0 Z= 28.4

$\bar{s}_b$= 0.721 σ = 0.0803

t= 30 r= 22

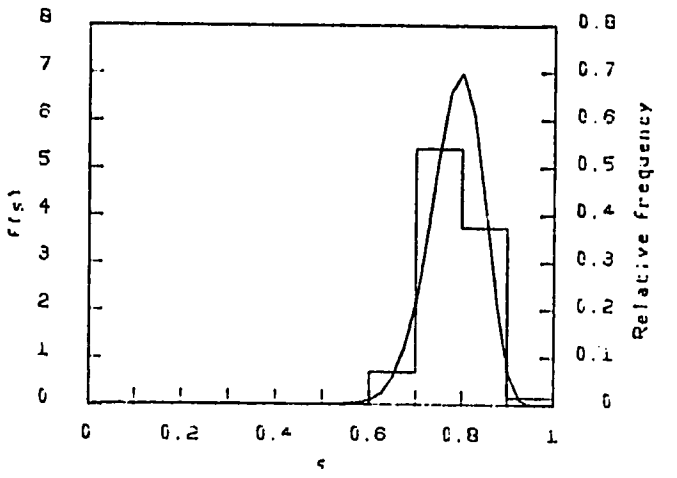

$\bar{T}_r$= 1.00 $\bar{t}_r$= 1.0 $\bar{t}_b$= 5

$\bar{e}_p$= 0.0030 k_y= 1.00 M= 0.70

K(1)= 0.360 Y(1)= 250.0

n= 0.35 m= 0.667

w= 0 Z= 60.5

$\bar{s}_b$= 0.791 σ = 0.0573

t= 51 r= 40

Figure A.2 (Continuation)

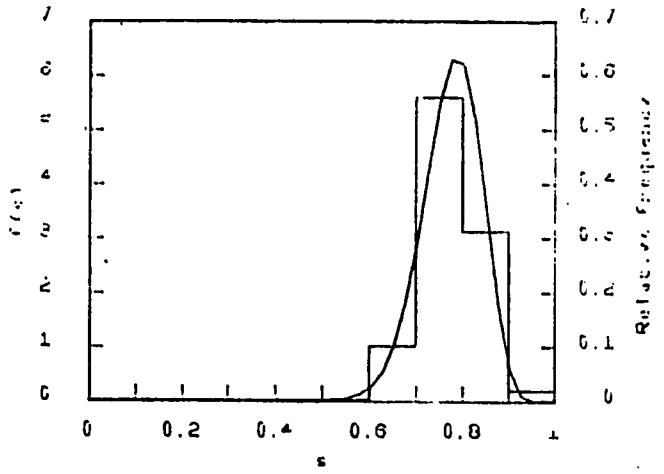

$\bar{T}_r$= 1.00 $\bar{t}_r$= 1.0 $\bar{t}_b$= 5

$\bar{a}_p$= 0.0030 K_y= 1.00 M= 0.70

K(1)= 0.360 V(1)= 100.0

n= 0.45 n_r= 0.667

w= 0 Z= 43.2

$\bar{s}_o$= 0.774 σ = 0.0626

t= 44 r= 34

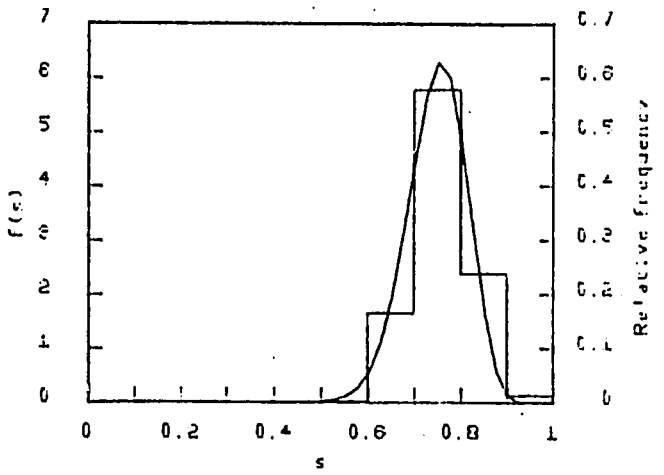

$\bar{T}_r$= 1.00 $\bar{t}_r$= 1.0 $\bar{t}_b$= 5

$\bar{a}_p$= 0.0030 K_y= 1.00 M= 0.70

K(1)= 0.360 V(1)= 166.0

n= 0.36 n_r= 0.667

w= 0 Z= 52.6

$\bar{s}_o$= 0.759 σ = 0.0618

t= 47 r= 35

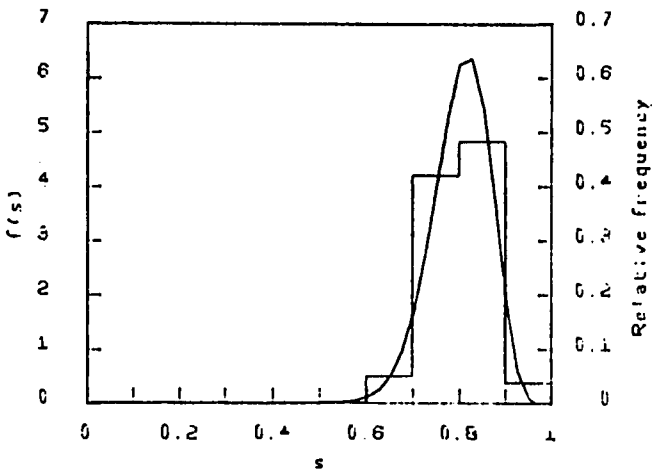

$\bar{T}_r$= 1.00 $\bar{t}_r$= 1.0 $\bar{t}_b$= 5

$\bar{a}_p$= 0.0030 K_y= 1.00 M= 0.70

K(1)= 0.250 V(1)= 166.0

n= 0.33 n_r= 0.667

w= 0 Z= 41.6

$\bar{s}_o$= 0.801 σ = 0.0625

t= 40 r= 32

Figure A.2 (Continuation)

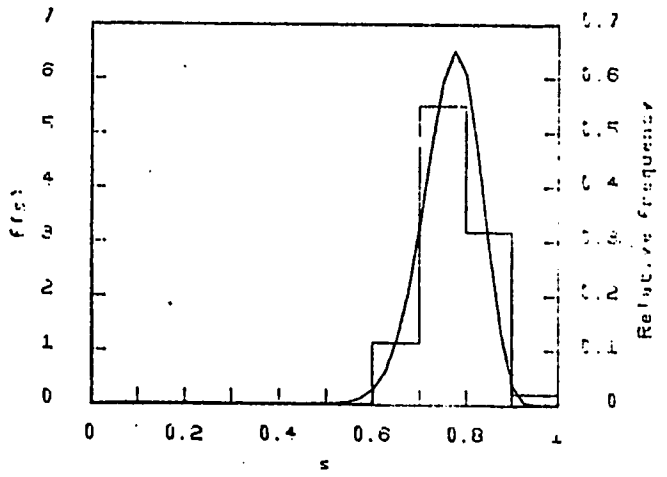

$\bar{T}_r$= 1.00 $\bar{t}_r$= 1.0 $\bar{t}_b$= 5

$\bar{e}_p$= 0.0030 κ_r= 1.20 M= 0.50

K(1)= 0.360 V(1)= 166.0

n= 0.35 m= 0.667

w= 0 Z= 49.0

$\bar{e}_a$= 0.773 σ= 0.0605

t= 47 r= 36

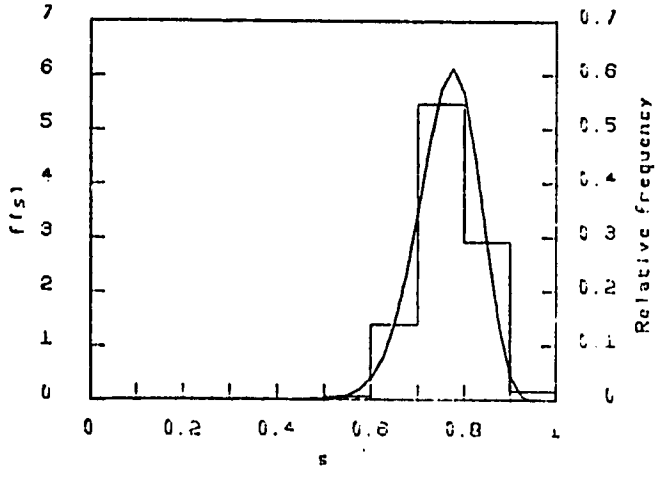

$\bar{T}_r$= 1.00 $\bar{t}_r$= 1.0 $\bar{t}_b$= 5

$\bar{e}_p$= 0.0030 κ_r= 1.20 M= 0.30

K(1)= 0.360 V(1)= 166.0

n= 0.35 m= 0.667

w= 0 Z= 49.0

$\bar{e}_a$= 0.766 σ= 0.0643

t= 42 r= 32

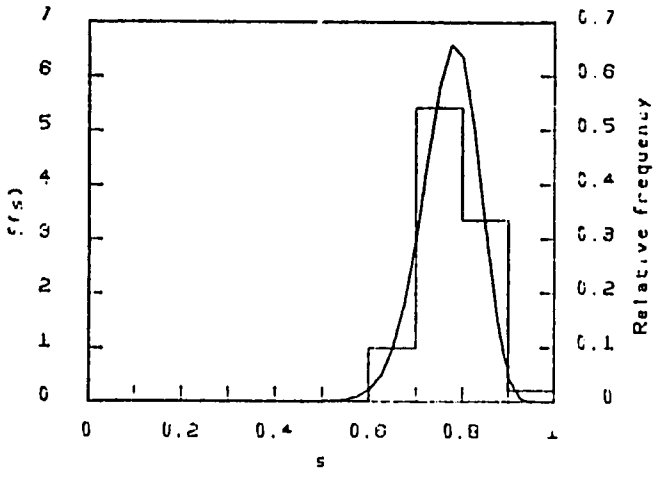

$\bar{T}_r$= 1.00 $\bar{t}_r$= 1.0 $\bar{t}_b$= 5

$\bar{e}_p$= 0.0030 κ_r= 1.00 M= 0.70

K(1)= 0.360 V(1)= 166.0

n= 0.40 m= 0.667

w= 0 Z= 45.8

$\bar{e}_a$= 0.777 σ= 0.0596

t= 49 r= 37

Figure A.2 (Continuation)

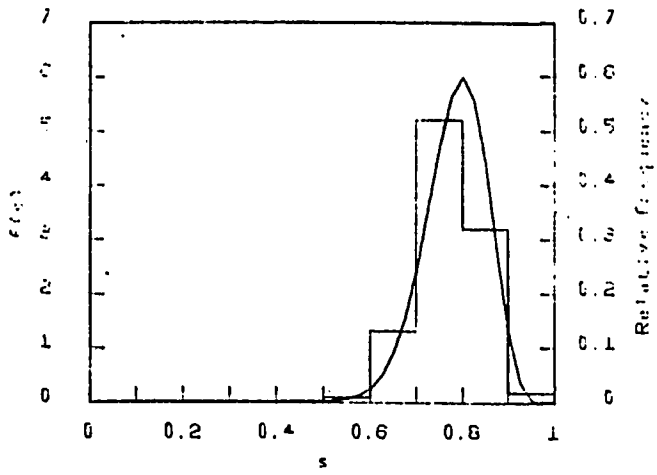

$\bar{T}_p$= 1.00 $\bar{t}_r$= 1.0 $\bar{t}_b$= 5

$\bar{a}_p$= 0.0030 k_r= 1.00 M= 0.50

K(1)= 0.360 V(1)= 166.0

n= 0.35 m= 0.667

w= 0 Z= 49.0

$\bar{s}_n$= 0.764 σ= 0.0659

t= 41 r= 31

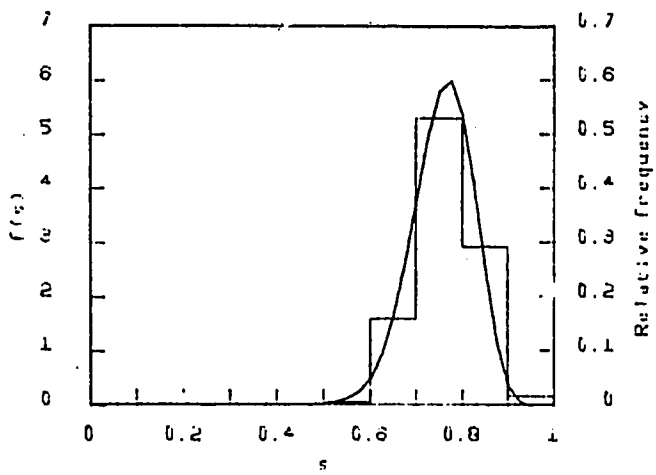

$\bar{T}_p$= 1.00 $\bar{t}_r$= 1.0 $\bar{t}_b$= 5

$\bar{a}_p$= 0.0030 k_r= 1.00 M= 0.50

K(1)= 0.360 V(1)= 166.0

n= 0.35 m= 0.667

w= 0 Z= 49.0

$\bar{s}_n$= 0.772 σ= 0.0661

t= 39 r= 30

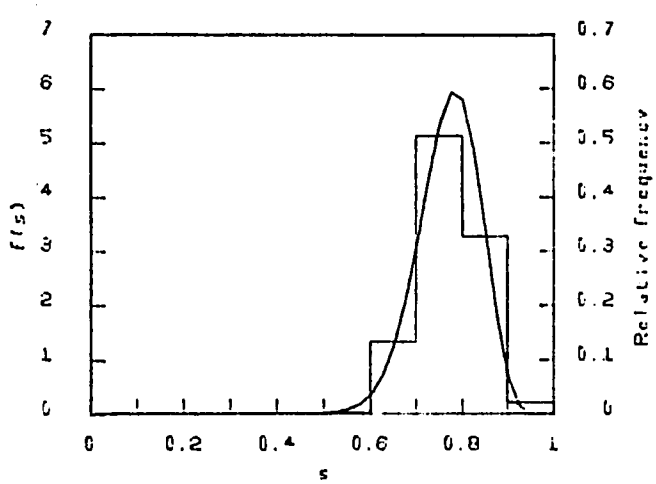

Figure A.2 (Continuation)

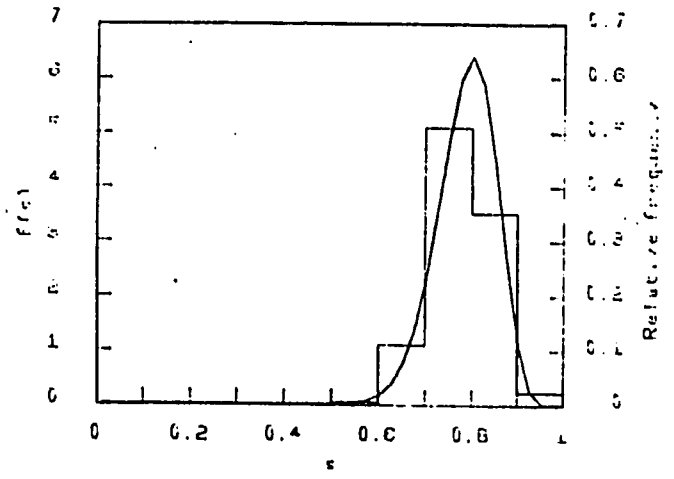

$\bar{T}_r$= 1.00 $\bar{t}_r$= 1.0 $\bar{t}_b$= 5

$\bar{\epsilon}_p$= 0.0028 k_v= 1.00 M= 0.70

K(1)= 0.360 V(1)= 166.0

n= 0.35 m= 0.667

w= 0 Z= 49.3

$\bar{s}_p$= 0.777 σ = 0.0631

t= 42 r= 33

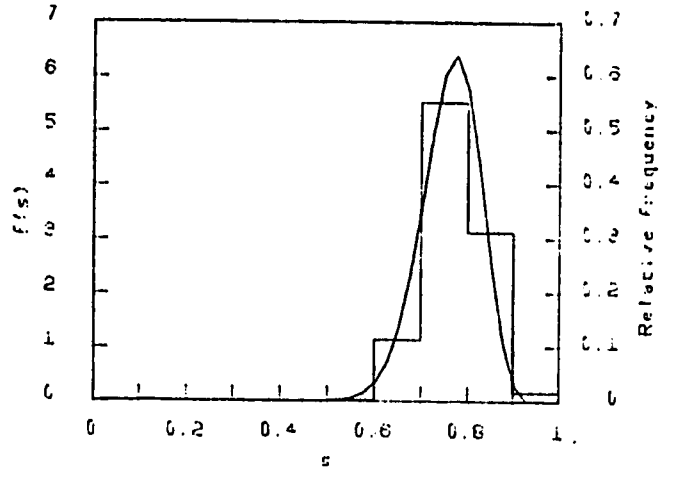

$\bar{T}_r$= 1.00 $\bar{t}_r$= 1.0 $\bar{t}_b$= 5

$\bar{\epsilon}_p$= 0.0030 k_v= 1.00 M= 0.70

K(1)= 0.360 V(1)= 166.0

n= 0.35 m= 0.667

w= 0 Z= 49.0

$\bar{s}_p$= 0.772 σ = 0.0618

t= 46 r= 35

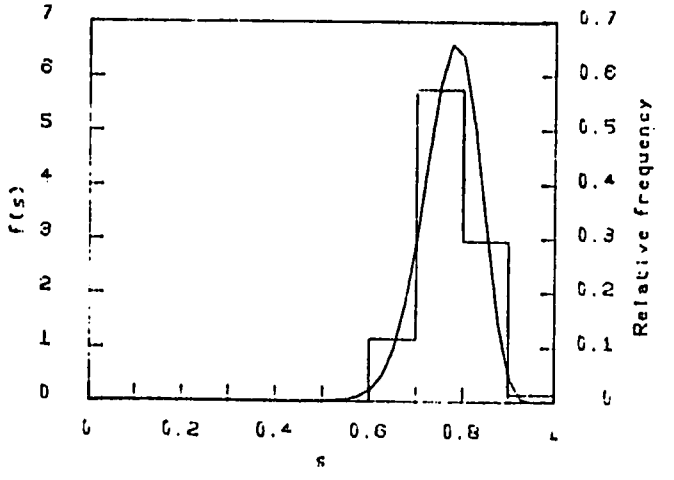

$\bar{T}_r$= 1.00 $\bar{t}_r$= 1.0 $\bar{t}_b$= 5

$\bar{\epsilon}_p$= 0.0030 k_v= 1.25 M= 0.70

K(1)= 0.360 V(1)= 166.0

n= 0.35 m= 0.667

w= 0 Z= 49.0

$\bar{s}_p$= 0.769 σ = 0.0602

t= 48 r= 37

Figure A.2 (Continuation)

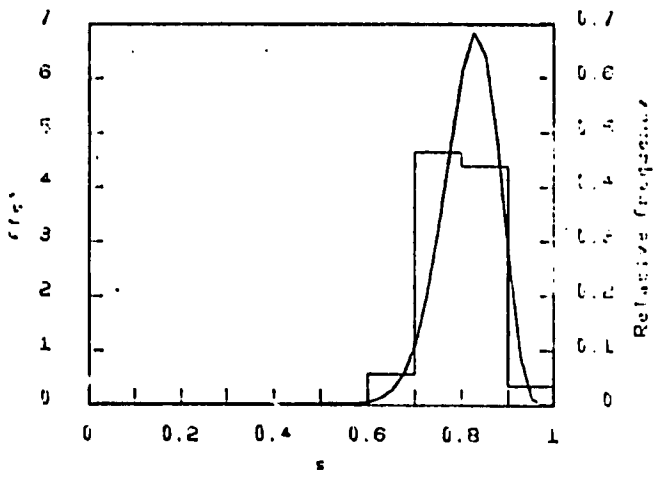

$\bar{T}_p$= 1.00 $\bar{T}_r$= 1.5 $\bar{T}_b$= 5

$\bar{T}_p$= 0.0050 k_v= 1.00 M= 0.70

K(1)= 0.360 V(1)= 166.6

n= 0.35 m= 0.667

w= 0 Z= 61.3

$\bar{s}_o$= 0.794 σ = 0.0600

t= 43 r= 35

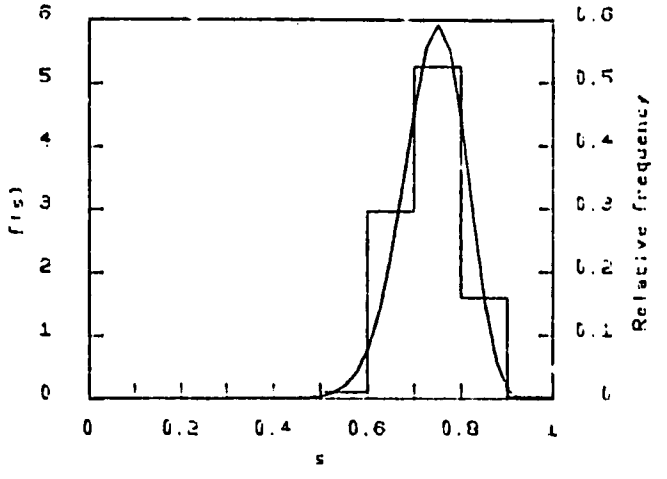

$\bar{T}_p$= 1.00 $\bar{T}_r$= 0.8 $\bar{T}_b$= 5

$\bar{T}_p$= 0.0050 k_v= 1.00 M= 0.70

K(1)= 0.360 V(1)= 166.6

n= 0.35 m= 0.667

w= 0 Z= 41.6

$\bar{s}_o$= 0.794 σ = 0.0671

t= 42 r= 31

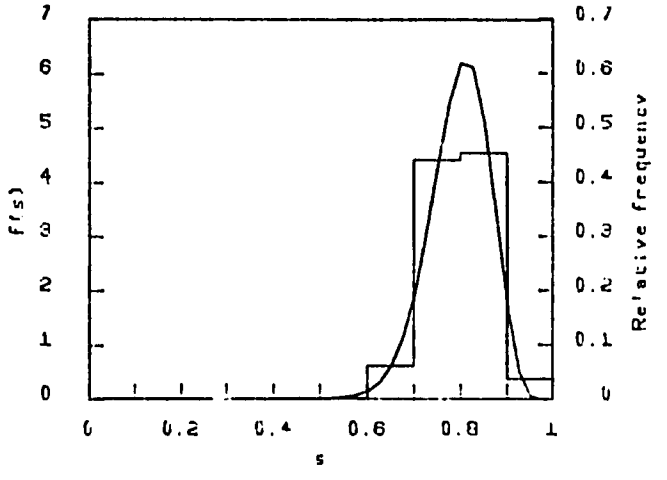

$\bar{T}_p$= 2.00 $\bar{T}_r$= 1.0 $\bar{T}_b$= 5

$\bar{T}_p$= 0.0050 k_v= 1.00 M= 0.70

K(1)= 0.360 V(1)= 166.6

n= 0.35 m= 0.667

w= 0 Z= 50.0

$\bar{s}_o$= 0.797 σ = 0.0637

t= 39 r= 31

Figure A.2 (Continuation)

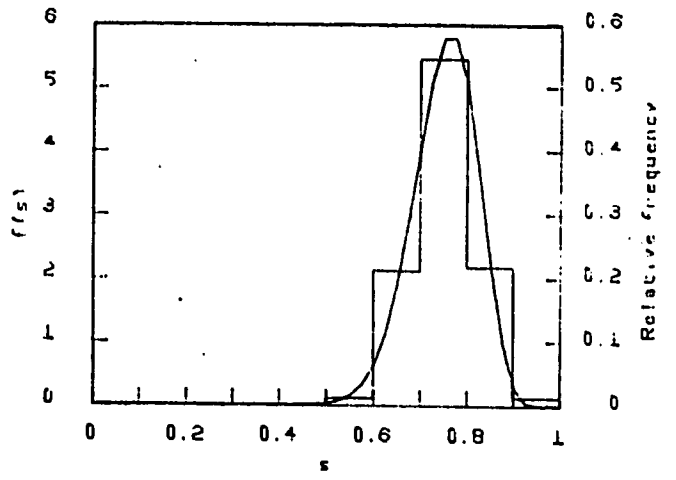

$\bar{T}_r$ = 0.75 $\bar{t}_r$ = 1.0 $\bar{t}_b$ = 5

$\bar{\epsilon}_p$ = 0.0050 κ_1 = 1.00 M = 0.70

K(1) = 0.360 V(1) = 166.0

n = 0.35 m = 0.667

w = 0 Z = 48.4

$\bar{\epsilon}_0$ = 0.750 σ = 0.0679

t = 46 r = 30

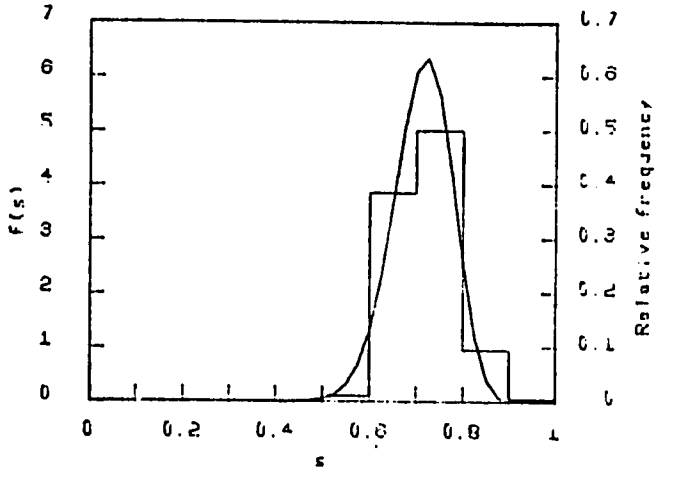

$\bar{T}_r$ = 0.50 $\bar{t}_r$ = 1.0 $\bar{t}_b$ = 5

$\bar{\epsilon}_p$ = 0.0050 κ_1 = 1.00 M = 0.70

K(1) = 0.360 V(1) = 166.0

n = 0.35 m = 0.667

w = 0 Z = 47.4

$\bar{\epsilon}_0$ = 0.718 σ = 0.0620

t = 52 r = 37

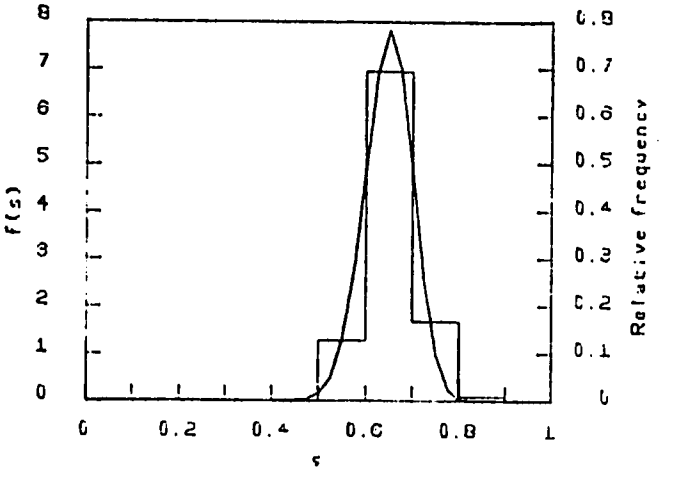

$\bar{T}_r$ = 0.25 $\bar{t}_r$ = 1.0 $\bar{t}_b$ = 5

$\bar{\epsilon}_p$ = 0.0050 κ_1 = 1.00 M = 0.70

K(1) = 0.360 V(1) = 166.0

n = 0.35 m = 0.667

w = 0 Z = 45.6

$\bar{\epsilon}_0$ = 0.654 σ = 0.0505

t = 88 r = 57

Figure A.2 (Continuation)

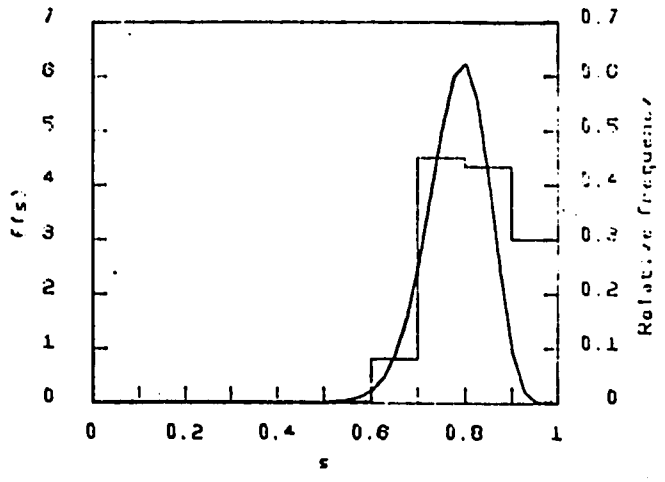

$\bar{T}_p$= 1.00 $\bar{t}_r$= 1.0 $\bar{t}_a$= 4

$\bar{e}_p$= 0.0050 k_v= 1.00 M= 0.70

K(1)= 0.360 Y(1)= 166.0

n= 0.35 m= 0.667

w= 0 Z= 50.0

$\bar{s}_a$= 0.791 σ = 0.0827

t= 41 r= 32

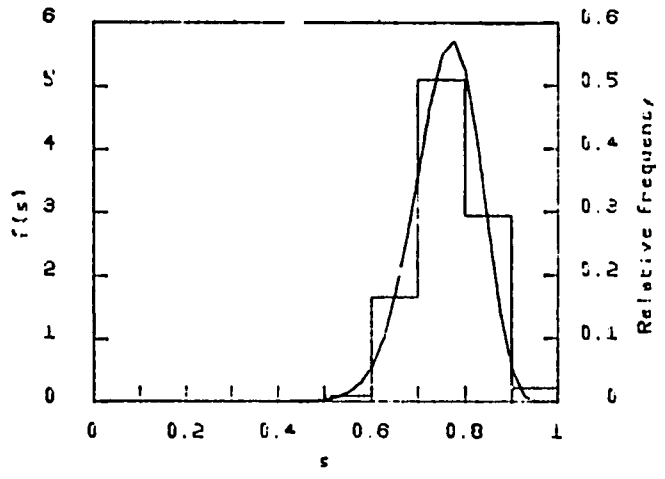

$\bar{T}_r$= 1.00 $\bar{t}_r$= 1.0 $\bar{t}_b$= 5

$\bar{e}_p$= 0.0050 k_v= 1.00 M= 0.70

K(1)= 0.360 Y(1)= 166.0

n= 0.35 m= 0.667

w= 0 Z= 48.6

$\bar{s}_a$= 0.765 σ = 0.0685

t= 37 r= 28

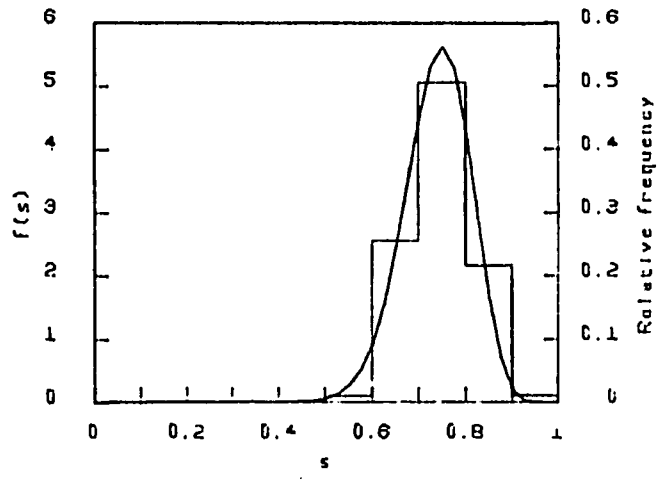

$\bar{T}_r$= 1.00 $\bar{t}_r$= 1.0 $\bar{t}_b$= 6

$\bar{e}_p$= 0.0050 k_v= 1.00 M= 0.70

K(1)= 0.360 Y(1)= 166.0

n= 0.35 m= 0.667

w= 0 Z= 48.0

$\bar{s}_a$= 0.745 σ = 0.0697

t= 38 r= 28

Figure A.2 (Continuation)

APPENDIX B

COMPUTER PROGRAM

```
C
C
C  ***************************************************
C
C
C       THIS PROGRAM CALCULATES THE FLOOD FREQUENCY CURVE
C       FOR A GIVEN BASIN USING THE GEOMORPHOCLIMATIC IUH
C       AND THE INFILTRATION LOSSES REPRESENTED BY
C       EAGLESON (1972 AND 1978).
C
C       PROGRAM WRITTEN BY MARIO A. DIAZ-GRANADOS, AT THE
C       PARSONS LABORATORY FOR WATER RESOURCES AND
C       HYDRODYNAMICS, M.I.T., CAMBRIDGE, MASS. 02139.
C
C
C  ***************************************************
C
C
      EXTERNAL F1,F2,F
      DIMENSION Q(200,3),FQ(200,3),T(200,3),AI(4),BI(4),
      DIMENSION X10(200),Y10(200),B12(3),NCAR(3),VA(3)
      DIMENSION CI(4),DI(4),NPUN(3),EI(4)
      DIMENSION THI(28),QHI(28)
      CHARACTER *40 B12
      REAL K1,MNU
      COMMON/XIOMA/BSTAR,DELTA,QP,XK1,S
      COMMON/XIOMA2/II
      DATA AI/0.0001,0.1235,0.5033,1.2216/
      DATA BI/0.1235,0.5033,1.2216,2.2962/
      PRINT,'PRINT NUMBER OF CURVES'
      READ(5,*)NCUR
      PRINT,'PRINT 1 IF EAGLESON 72, PRINT 2 IF EAGLESON 78'
      READ(5,*)NEAG
      GO TO(16,17),NEAG
      PRINT,'IF CHANGE S0, PRINT 1; IF ALPHA, PRINT 2;
     & IF MNU, PRINT 3; IF SOIL, PRINT 4'
      READ(5,*)NCON
      PRINT,'PRINT MIR(CM/HR), MTR(HR), AREA(KM2), RL, XL(KM)
     &,ALFA(1/(S.M**(1/3))), DELTAI(CM/HR), MNU'
      READ(5,*)BETA1,DELTA1,A,RL,XL,ALFA,DELTAI,MNU
      PRINT,'PRINT S0, N(POROSITY), K1(CM/HR), PHI1(CM),
     & XM(PORE SIZE), W(CM/HR)'
      READ(5,*)S0,XN,K1,PHI1,XM,W
      PI=3.14159
      GO TO 80
16    PRINT,'PRINT MIR(CM/HR),MTR(HR),AREA(KM2),RL,XL(KM),
     &ALFA(1/S.M(1/3))),PHI(CM/HR),DELTAI(CM/HR),MNU'
      READ(5,*)BETA1,DELTA1,A,RL,XL,ALFA,PHI,DELTAI,MNU
      PRINT,'PRINT 1 IF ALFA, 2 IF MNU, 3 IF PHI'
      READ(5,*)MCON
```

```
80      DO 99 I=1,NCUR
        GO TO(81,82),NEAG
81      GO TO(91,92,94),MCON
82      GO TO(90,91,92,93),NCON
90      PRINT,'PRINT S0'
        IF(I.EQ.1)VA(1)=S0
        IF(I.EQ.1)GO TO 2
        READ(5,*)S0
        VA(I)=S0
        GO TO 2
91      PRINT,'PRINT ALFA'
        IF(I.EQ.1)VA(1)=ALFA
        IF(I.EQ.1)GO TO 2
        READ(5,*)ALFA
        VA(I)=ALFA
        GO TO 2
92      PRINT,'PRINT MNU'
        IF(I.EQ.1)VA(1)=MNU
        IF(I.EQ.1)GO TO 2
        READ(5,*)MNU
        VA(I)=MNU
        GO TO 2
93      IF(I.EQ.1)GO TO 2
        PRINT,'PRINT N,K1,PHI1,XM'
        READ(5,*)XN,K1,PHI1,XM
        PRINT,'PRINT TYPE OF SOIL'
        READ(5,310)B12(I)
        PRINT,'PRINT NUMBER OF CHARACTERS IN THE PREVIOUS LINE'
        READ(5,*)NCAR(I)
        GO TO 2
94      PRINT,'PRINT PHI'
        IF(I.EQ.1)VA(1)=PHI
        IF(I.EQ.1)GO TO 2
        READ(5,*)PHI
        VA(I)=PHI
2       BETA=1./BETA1
        DELTA=1./DELTA1
        XK1=(A*RL)**0.4*ALFA**0.6/XL
        XK=1.-EXP(-1.1*DELTA**-0.25)
        XK=XK+EXP(-1.1*DELTA**-0.25-0.003861*A)
        BSTAR=BETA/XK
        GO TO(84,83),NEAG
83      C=(2.+3.*XM)/XM
        D=C-1./XM-1.
        CALL SOIL(S0,C,D,FII)
        S=2.*(1.-S0)*(5.*XN*K1*PHI1*FII/(3.*XM*PI))**0.5
        A0=K1*(1.+S0**C)*0.5-W
        SIGMA=DELTA*(S*BSTAR/(2.8284*DELTA))**(2./3.)
        GA=GAMMA(SIGMA+1.)
        CONST=DELTA*EXP(-BSTAR*A0)*EXP(-2.*SIGMA)*GA/SIGMA**SIGMA
```

```
      CONST1=CONST/DELTA
      SPIKE=1.-CONST1
      AERR=0.0
      RERR=0.001
      NN=0
      DEL=0.0
1     DEL=DEL+DELTAI
      NN=NN+1
      QP=DEL
      XINF=2.2962*QP**-0.4/XK1
      AREA=0.0
      NV=0
5     XSUP=XINF+15.
      EDEL=0.001
      ARE=TEGRAL(F1,XINF,XSUP,EDEL)
      NV=NV+1
      AREA=AREA+ARE
      IF(NV.EQ.1)GO TO 10
      IF(ABS((AREA-ARE1)/AREA).LE.0.001)GO TO 20
10    ARE1=AREA
      XINF=XSUP
      GO TO 5
20    AREA1=0.
      DO 30 II=1,4
      XINF=AI(II)*QP**-0.4/XK1
      XSUP=BI(II)*QP**-0.4/XK1
      EDEL=0.001
      ARE=TEGRAL(F2,XINF,XSUP,EDEL)
      AREA1=AREA1+ARE
30    CONTINUE
      AREAT=AREA+AREA1
      FQ(NN,I)=1.-CONST*AREAT
      Q(NN,I)=QP*A/0.36
      T(NN,I)=1./(MNU*(1.-FQ(NN,I)))
      IF(T(NN,I).GT.100.)GO TO 35
      IF(T(NN,I).GE.1.01)GO TO 1
      NN=NN-1
      GO TO 1
35    NN=NN-1
      NPUN(I)=NN
      DO 40 J=1,NN
      T(J,I)=1.522*(ALOG(T(J,I))-ALOG(1.01))
40    CONTINUE
      GO TO 99
84    AERR=0.0
      RERR=0.001
      NN=0
      DEL=0.
401   DEL=DEL+DELTAI
      NN=NN+1
```

```
      QP=DEL
      XINF=QP
      AREA=0.
      NV=0
405   XSUP=XINF+1.
      EDEL=0.001
      ARE=TEGRAL(F,XINF,XSUP,EDEL)
      NV=NV+1
      AREA=AREA+ARE
      IF(NV.EQ.1)GO TO 410
      IF(ABS((AREA-ARE1)/AREA).LE.0.001)GO TO 420
410   ARE1=AREA
      XINF=XSUP
      GO TO 405
420   FQ(NN,I)=1.-BSTAR*EXP(-BSTAR*PHI)*AREA
      Q(NN,I)=QP*A/0.36
      T(NN,I)=1./(MNU*(1.-FQ(NN,I)))
      IF(T(NN,I).GT.100.)GO TO 435
      IF(T(NN,I).GE.1.01)GO TO 401
      NN=NN-1
      GO TO 401
435   NN=NN-1
      NPUN(I)=NN
      DO 440 J=1,NN
      T(J,I)=1.522*(ALOG(T(J,I))-ALOG(1.01))
440   CONTINUE
99    CONTINUE
      QMAX=0.
      QMIN=9999.
      DO 105 J=1,NCUR
      NN=NPUN(J)
      DO 104 I=1,NN
      IF(Q(I,J).GT.QMAX)QMAX=Q(I,J)
      IF(Q(I,J).LT.QMIN)QMIN=Q(I,J)
104   CONTINUE
105   CONTINUE
      PRINT,'PRINT 1 IF COMPARISON WITH OBSERVATIONS'
      READ(5,*)MCOM
      IF(MCOM.NE.1)GO TO 222
      PRINT,'PRINT FILE NUMBER OF HISTORICAL DATA'
      READ(5,*)NFILO
      READ(NFILO,*)NPOINTS
      READ(NFILO,*)(QHI(I),I=1,NPOINTS)
      XNPON=NPOINTS
      DO 226 I=1,NPOINTS
      THI(I)=(XNPON+1.)/(XNPON+1.-I)
      THI(I)=1.522*(ALOG(THI(I))-ALOG(1.01))
226   CONTINUE
      IF(QHI(NPOINTS).GT.QMAX)QMAX=QHI(NPOINTS)
222   CONTINUE
```

```
      PRINT,'QMIN=',QMIN,'QMAX=',QMAX
      PRINT,'PRINT QMIN,QMAX,QDELTA'
      READ(5,*)QMIN,QMAX,QDELTA
      PRINT,'PRINT BASIN NAME'
      READ(5,310)B12(1)
      XDEL1=1.
      YDEL1=(QMAX-QMIN)/4.
      DO 800 J=1,NCUR
      IJ=J-1
      NNPU=NPUN(J)
      DO 700 I=1,NNPU
      X10(I)=T(I,J)
700   Y10(I)=Q(I,J)
C
C
C
C           THE FOLLOWING SUBROUTINE PLOTS EACH FLOOD FREQUENCY
C           DISTRIBUTION. THIS SUBROUTINE IS NOT SELF CONTAINED
C           IN THIS PROGRAM, AND THEREFORE AN APPROPIATE ONE
C           MUST BE USED.
C
C
      CALL SCLGPH(X10,Y10,NNPU,0.04,IJ,0.01,XDEL1,QMIN,YDEL1)
800   CONTINUE
      IF(MCOM.NE.1)GO TO 900
      CALL SCLGPH(THI,QHI,-NPOINTS,0.04,5,0.01,XDEL1,QMIN,YDEL1)
900   CONTINUE
      STOP
      END
C
C
C
C
      REAL FUNCTION F1(X)
      REAL X
      COMMON/XIOMA/BSTAR,DELTA,QP,XK1,S
      F1=0.0
      ARG=DELTA*X+1.4434*BSTAR*S**0.1558*X**-0.0779*QP**0.8442
      IF(ARG.GT.-88.)F1=EXP(-ARG)
      RETURN
      END
C
C
C
C
      REAL FUNCTION F2(X)
      REAL X
      DIMENSION CI(4),DI(4),EI(4)
      COMMON/XIOMA/BSTAR,DELTA,QP,XK1,S
      COMMON/XIOMA2/II
```

```
      DATA CI/0.5,0.65295,0.80482,1.0/
      DATA DI/1.0,1.10812,1.36396,3.1358/
      DATA EI/1.4,1.50812,1.76396,3.5358/
      F2=0.0
      C=CI(II)
      D=DI(II)
      E=EI(II)
      ARG=DELTA*X+1.4434*BSTAR*S**0.1558*X**-0.0779
      ARG=ARG*(2.*(C*QP)**D/(0.871*XK1*X))**(0.8442/E)
      IF(ARG.GT.-88.)F2=EXP(-ARG)
      RETURN
      END
C
C
C
      REAL FUNCTION F(X)
      REAL X
      COMMON/XIOMA/BSTAR,DELTA,QP,XK1,S
      F=0.0
      ARG=BSTAR*X+2.*DELTA*(1.-SQRT(1.-QP/X))/(0.871*XK1*X**0.4)
      IF(ARG.GT.-88)F=EXP(-ARG)
      RETURN
      END
C
C
C
C
C
      REAL FUNCTION TEGRAL(FI,A,B,EDEL)
C
C
C     THIS FUNCTION USES THE ROMBERG INTEGRATION METHOD TO
C     INTEGRATE FI FROM A TO B
C
C
      EXTERNAL FI
      DIMENSION T(30,30)
      T(1,1)=(B-A)*(FI(A)+FI(B))/2
      T(1,2)=T(1,1)/2+(B-A)*FI((A+B)/2)/2
      T(2,1)=(4*T(1,2)-T(1,1))/3
      J=3
5     DX=(B-A)/2**(J-1)
      X=A-DX
      N=2**(J-2)
      SUM=0.
      DO 10 I=1,N
      X=X+2.*DX
      SUM=SUM+FI(X)
10    CONTINUE
      T(1,J)=T(1,J-1)/2+DX*SUM
```

```
      DO 20 L=2,J
      K=J+1-L
      T(L,K)=(4**(L-1)*T(L-1,K+1)-T(L-1,K))/(4**(L-1)-1)
20    CONTINUE
      TT=ABS((T(J,1)-T(J-1,1))/T(J,1))
      IF(TT.LE.EDEL)GO TO 30
      J=J+1
      IF(J.GT.30)PRINT,'WARNING TEGRAL: MATRIX DIMENSION > 30'
      GO TO 5
30    TEGRAL=T(J,1)
      RETURN
      END
C
C
      SUBROUTINE SOIL(S0,C,D,FII)
C
C
C         THIS SUBROUTINE CALCULATES THE DIMENSIONLESS
C         INFILTRATION DIFFUSIVITY.
C
C
      N=D
      L=N+1
      A=0.
      DO 10 I=1,N
      CALL BINOM(N,I,B)
      A=A+(1./(N+5./3.-I))*B*(S0/(1.-S0))**I
10    CONTINUE
      FINF=(1.-S0)**N*(1./(N+5./3.)+A)
      A=0.
      DO 11 I=1,L
      CALL BINOM(L,I,B)
      A=A+(1./(L+5./3.-I))*B*(S0/(1.-S0))**I
11    CONTINUE
      FISUP=(1.-S0)**L*(1./(L+5./3.)+A)
      TA=N
      TB=L
      Q=(ALOG(D)-ALOG(TA))/(ALOG(TB)-ALOG(TA))
      FII=EXP(ALOG(FINF)+(ALOG(FISUP)-ALOG(FINF))*Q)
      RETURN
      END
C
C
C
C
      SUBROUTINE BINOM(NI,N,B)
C
C
C     THIS SUBROUTINE EVALUATES THE BINOMIAL COEFFICIENT.
C
```

```
C
      J=1
      DO 1 I=1,NI
1     J=J*I
      K=1
      KK=NI-N
      DO 2 I=1,KK
      K=K*I
2     CONTINUE
      L=1
      DO 3 I=1,N
3     L=L*I
      A=J
      C=K
      D=L
      B=A/(C*D)
      RETURN
      END
C
C
C
```